SNS-101060100-TR0006-R00

# Status Report on Mercury Target Development and Related Issues

**Date: July 2002**

SNS-101060100-TR0006-R00

# Status Report on Mercury Target Development and Related Issues

**July 31, 2002**

Date Published: July 2002

Prepared for the
U.S. Department of Energy
Office of Science

UT-BATTELLE, LLC
managing the
Spallation Neutron Source Activities at the
Argonne National Laboratory
Brookhaven National Laboratory
Thomas Jefferson National Accelerator Facility
Lawrence Berkeley National Laboratory
Los Alamos National Laboratory
Oak Ridge National Laboratory
under contract DE-AC05-00OR22725
for the
U.S. DEPARTMENT OF ENERGY

## TABLE OF CONTENTS

## LIST OF TABLES

## LIST OF FIGURES

## EXECUTIVE SUMMARY

This report summarizes the status of present R&D efforts to quantify, understand and mitigate the effects of cavitation induced erosion in the SNS liquid mercury target. The phenomenon, which is essentially the only remaining R&D issue for Target Systems, may be understood in the following way. When short pulses of protons strike the target volume the rapid heating produces pressure waves, rising to values of more than 20 MPa in the case of SNS. These waves are propagated in the target volume and reflected as rarefaction waves of similar magnitude. The rarefaction phase causes the liquid to form bubbles or cavitate. Subsequent bubble collapse near the container wall is usually asymmetric giving rise to impulsive liquid jets and shock waves, which erode or 'pit' the surface. This 'pitting' or erosion of the mercury container may limit the lifetime of the target. It should be understood however that no safety hazard is involved, since multiple barriers ensure mercury containment.

Although cavitation induced erosion in mercury targets was only recently observed, it is well known in water systems, such as circulatory pumps or ship propellers. A certain amount of expertise exists in the US and methods for reducing erosion damage have been developed. A group of US experts in cavitation erosion met at SNS in May to advise on the R&D program being followed by Target Systems. The report of this meeting (Appendix B) concluded that the very thorough investigations carried out at SNS provided an accurate assessment of the problem and validated the approach to finding a practical solution.

Efforts are being concentrated on three areas, each of which should lead to reduction of the erosion damage:

1. Evaluation of cavitation resistant materials and coatings.
2. Modification of the target geometry in order to disperse the pressure waves.
3. Investigation of mitigation techniques such as introduction of non-dissolvable bubbles into the system.

The above parameters are being assessed in two different groups of experiments:

- In beam tests carried out mainly at LANL's WNR facility at prototypical SNS energy densities.
- Out of beam mechanical tests, which have demonstrated the capability to produce damage similar to that observed in WNR tests and can achieve large numbers of cycles.

Proton beam tests evaluating various target geometries and surfaces have been carried out at WNR using mercury filled containers, irradiated with up to 1000 pulses of 800 MeV protons at beam intensities comparable to SNS operation at almost 3 MW (the level 0 baseline for SNS requires > 1 MW). Three separate test campaigns were performed in July 2001, December 2001 and June 2002. The samples from the most recent test campaign have not yet been evaluated.

All specimens, except one, showed evidence of cavitation erosion. The undamaged surface was a 20% cold worked SS316 steel, which had been surface hardened by a propriety process called Kolsterizing. Generally two types of pits are observed. Large pits, observable by eye, and which occur in localized areas, and smaller (5–15 μm) randomly distributed pits. The large pits must be eliminated to ensure reasonable target lifetimes. The effects of changing the geometry of the target to eliminate this severe damage was addressed in the December WNR tests. Results are expected in August 2002. The damage due to smaller pits covers more extensive regions of the surface and may be reduced by surface hardening.

Although linear extrapolations of the erosion damage, based on the regions of small pits after 200 pulses, indicate that reasonable lifetimes may be achieved, the time evolution of the erosion due to cavitation in this system is not known and cannot be compared to data in water.

The out of beam mechanical tests are designed to address the question of time evolution and pulse frequency. Reasonable target lifetimes imply that the target should withstand approximately $10^8$ pulses at a frequency of 60 Hz. Four test devices have been developed, one in collaboration with the Japanese Spallation Source project, which will allow erosion profiles to be determined up to $10^7$ cycles and 20 Hz. Results of these tests are expected in September 2002.

The SNS has made basic design studies of an alternative solid target, which could replace the liquid mercury target. The neutron performance of a solid target can be equivalent to mercury at 1 MW though evolution to higher powers can only be envisaged for mercury. Evaluation of the cost and schedule impact on the project of changing to a solid target led to a decision date of October 15, 2002. The SNS Experimental Facilities Advisory Committee endorsed the decision criteria, which should be met to continue with a mercury target after October:

- Testing of a target geometry and material combination at WNR that has pitting damage, which can be scaled to 14 days of operation at SNS at 1 MW proton beam power.
- Demonstration of high cycling scaling behavior of 'high pressure pulse' pitting damage up to one million cycles for materials similar to those successfully tested at WNR.
- No obvious fabricability, radiation damage or engineering problems with selected geometry or materials.

It should be emphasized that, during the first two years of operation of SNS, the proton beam power levels on the target are not expected to exceed 300 kW, allowing ample time to evaluate the full-scale performance of the target. A detailed analysis of time that would be required to exchange a mercury target for a solid version, after this low level of operation, implies a facility shutdown of at least 23 months.

Both the Japanese (JNS) and the European (ESS) spallation source projects plan to use liquid mercury targets since it is the only known way of going to higher beam power. The R&D efforts at SNS have been carried out within the framework of an international collaboration and, with suitable support, we have a major role to play in the future development of high power targets within this collaboration.

Overall, high confidence still exists internationally that a solution to the cavitation issue can be found using a combination of materials, dispersive target geometries, and mitigation techniques. A significant R&D effort is being carried out worldwide which is expected to furnish relevant results within the time frame required for SNS to make an informed decision to continue with the mercury target.

.

## 1.0 BACKGROUND/INTRODUCTION

The mercury target development program for the Spallation Neutron Source (SNS) has successfully addressed most of the critical issues previously identified with this new concept, including:

- The ability of the mercury to adequately cool the reference target container material in the baseline coolant passage,
- Capability of the flowing mercury to transport the time-averaged power away from the target region to the process bay,
- Performance of the double-walled heat exchanger in transferring the heat from the primary mercury loop to a secondary water loop,
- Performance of other mercury process equipment, such as the centrifugal pump, flow control valves and orifices, and instrumentation and controls in a full-scale fashion,
- Radiation damage to the target container material,
- Fatigue lifetime limits in air and mercury under an extensive range of conditions,
- Compatibility of the target container material with liquid mercury, and
- Validation of computational fluid mechanics tools that can be used to perform design basis calculations.

The remaining major concern is the so-called cavitation erosion issue.

The process leading to pitting begins with the rapid pressure increase resulting from the intense heating of the liquid metal from a single pulse of protons. This heating occurs essentially instantaneously compared to acoustic wave time scales; therefore, the mercury undergoes a large pressure increase. Prior to 2001, the SNS R&D program efforts on this issue had focused on studying the effects that these pressure spikes have on the structural integrity of the mercury target container. For example, in-beam tests with mercury targets concentrated on measuring the vessel strain using an array of target shapes, diagnostics, and instruments.

During 2000, a team of researchers at the Japan Atomic Energy Research Institute (JAERI) observed pitting of stainless steel surfaces that were in contact with mercury subjected to large mechanically induced pressure pulses of the same magnitude as those expected for full power (2 MW) pulses in SNS. The question then became, “Do the inner surfaces of liquid mercury target containers with comparable beam-induced pressure pulses also pit?” Post-irradiation examinations of targets previously used in pulsed proton beam tests at LANL’s WNR facility

were unable to resolve this question because no pre-test inspections had been performed and the roughness of the surfaces was too great to distinguish between beam-induced pits and other imperfections in the surface of the materials.

Because of the urgency associated with completing the SNS target design, two test campaigns were conducted in 2001 to study the pitting issue; the first in July and the second in December. Large pits, visible to the naked eye, were found near the center of most of the specimens tested in July and December of 2001. Microscopy revealed that small, randomly distributed pits were present on all of the test specimens except one, which had been treated with a surface hardening process.

In addition to summarizing the status of pitting erosion testing including recent progress on in-beam and off-line tests, this report discusses the implications of switching from a mercury target to a water-cooled solid target after some initial period of operation. This information is intended to provide decision makers with a rough estimate of the schedule associated with design, licensing, fabrication, decontamination, installation and start-up efforts. The implications of starting SNS operations with a water-cooled solid target and then switching to a mercury target have not yet been addressed in any detail, but some preliminary comments are provided.

A more detailed discussion of the underlying physical mechanisms involved in pitting was compiled in a report released in April 2002 [1]. This report is attached as Appendix A.

## 2.0 UPDATE ON TARGET PITTING TESTS

### 2.1 Summary of WNR 2001 Test Results

#### 2.1.1 Pitting Measurements

Two test campaigns were conducted at the LANSCE – WNR during 2001 to investigate cavitation damage in mercury spallation targets. The WNR beam parameters are summarized in Table 2.1. Although total energy per pulse was substantially lower than the SNS target, by tailoring the beam size, the maximum energy density in test targets was comparable to that in SNS. Using a test target size that was roughly ½ scale of SNS, the proportion of the beam cross-sectional area to the target cross-sectional area was also comparable.

Table 2.1 WNR Beam Parameters for Cavitation Damage Tests

| | SNS (@ 2 MW) | WNR |
|---|---|---|
| Proton Energy [GeV] | 1 | 0.8 |
| Protons per pulse | $2 \times 10^{14}$ | $2.8 \times 10^{13}$ |
| Beam size [mm] | Elliptic, ~ 70x200 | Circular, $\sigma \sim 10$ |
| Energy deposited in mercury target [kJ] | 20 | 2.2 |
| Maximum energy deposition density [$MJ/m^3$] | 13 | 19 |

Test targets consisted of sealed stainless steel containers filled with mercury. Beam entrance and exit windows were machined flat and highly polished to assist in the identification of any features larger than a few microns that may have been introduced by the test. Scanning electron microscopy (SEM), optical microscopy, and laser profilometry were used to conduct detailed examination of the flange surfaces before and after irradiation. The polished surfaces were inspected for evidence of cavitation-induced erosion. The initiation of surface erosion was observed in the form of individual hemispherical depressions presumably formed by the collapse of cavitation bubbles near the surface. Irregular craters, formed by dislodged material, were also observed in many of these depressions (see Figs. 2.1–2.5 for examples of pitting). The relative degree of pitting was used as a measure of the importance of parameters, which were varied in the tests.

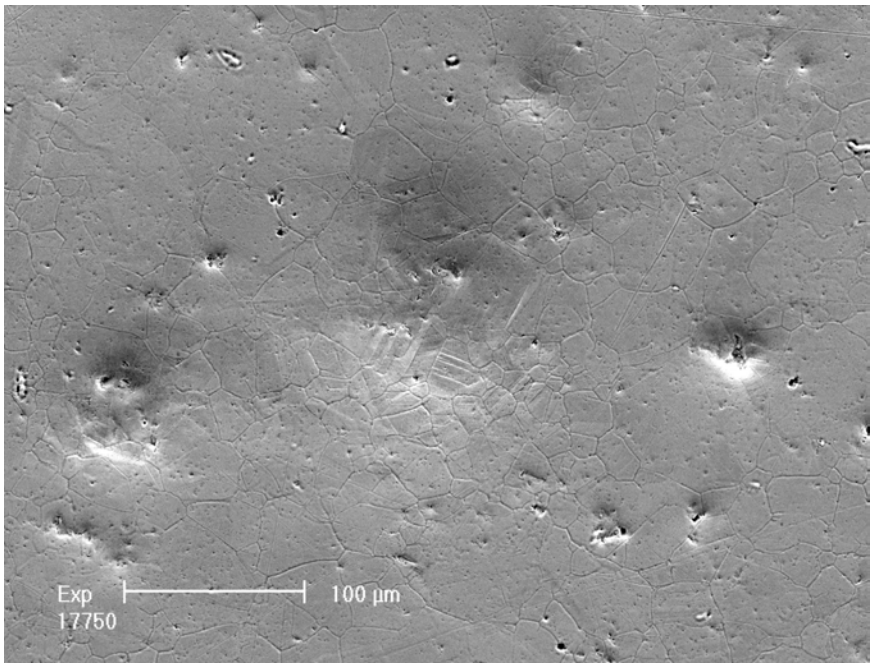


Fig. 2.1. Hemispherical depression in surface, slip lines verify deformation

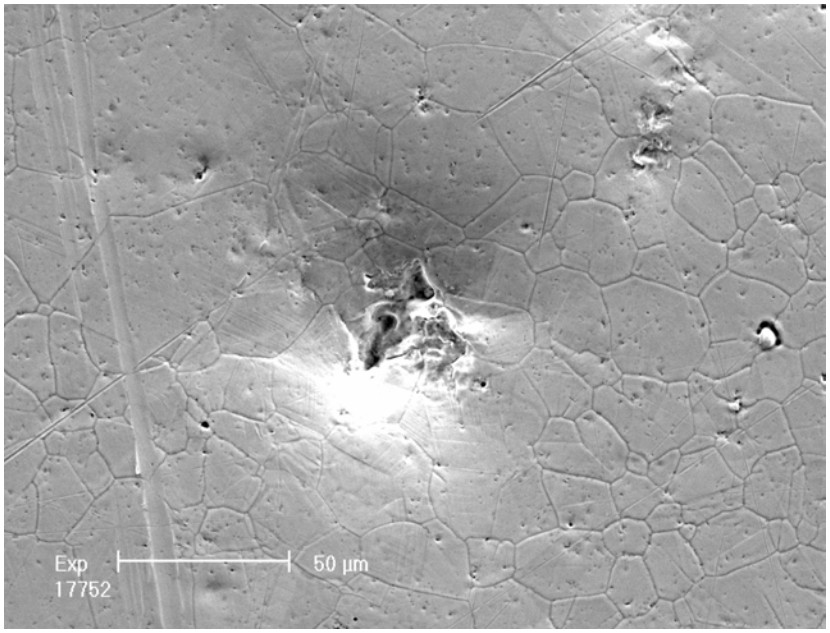


Fig. 2.2. Irregularly shaped crater at the bottom of a pit.

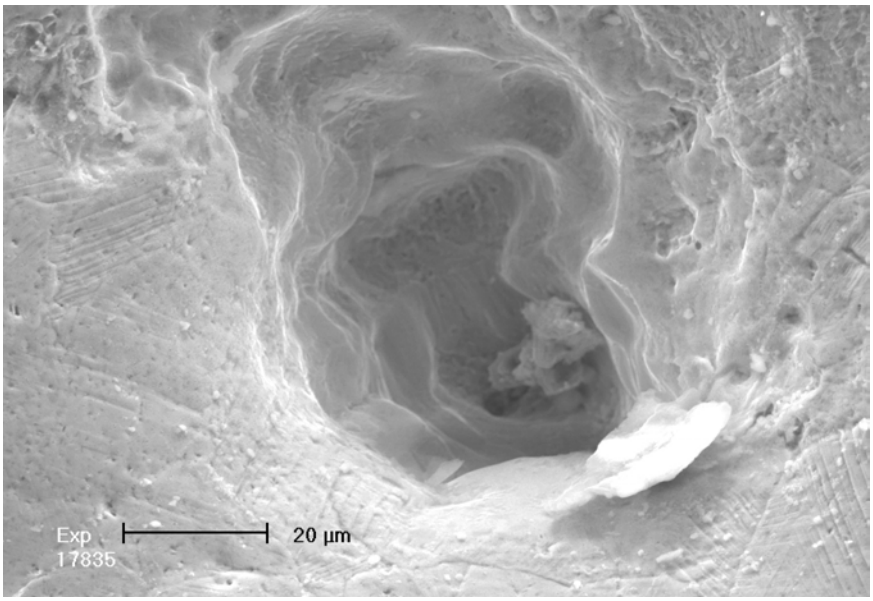


Fig. 2.3 Close up of crater caused by forceful removal of material.

Details and images of the examinations of specimen surfaces from the two test targets irradiated in July 2001 can be found in Section 3.1.3 of Appendix A. Several conclusions and additional questions were formed from this initial round of irradiations. The irradiation conditions listed in Table 2.1 were sufficient to produce observable pitting. This pitting showed some indication of a relationship to the geometry of the test target. A proprietary surface hardening treatment called Kolsterizing showed particular promise in mitigating the observed pitting.

For the December 2001 round of irradiations, the number of mercury targets increased to six and a larger array of variables was investigated. Several different specimen materials were tested, including Stellite 6B and Nitronic 60, which were specifically chosen due to their known cavitation damage resistance in water. Soft, annealed 316LN stainless steel was the most susceptible to pitting. The Kolsterized surface, which was 6 times harder than annealed 316LN, showed no pits larger than the 1 μm resolution limit of the pre-inspection. The so-called cavitation damage resistant materials showed pitting similar to that observed in 316LN stainless steel. At this initial stage of erosion, where deformation occurred in individual isolated pits, any improvements in the response of these cavitation-resistant materials to deformation induced fatigue cracking could not be measured. However, the observation of craters within individual

pits shows that, for the impact parameters, which occur with the collapse of cavities in these targets, fatigue crack growth is not the only mechanism that can lead to material loss.

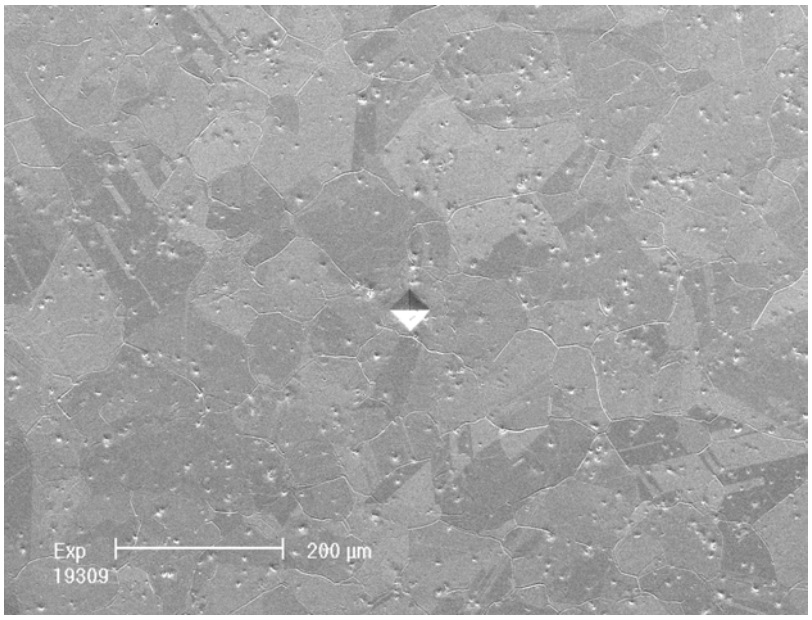


Fig. 2.4 Cavitation-induced pitting of annealed 316LN stainless steel

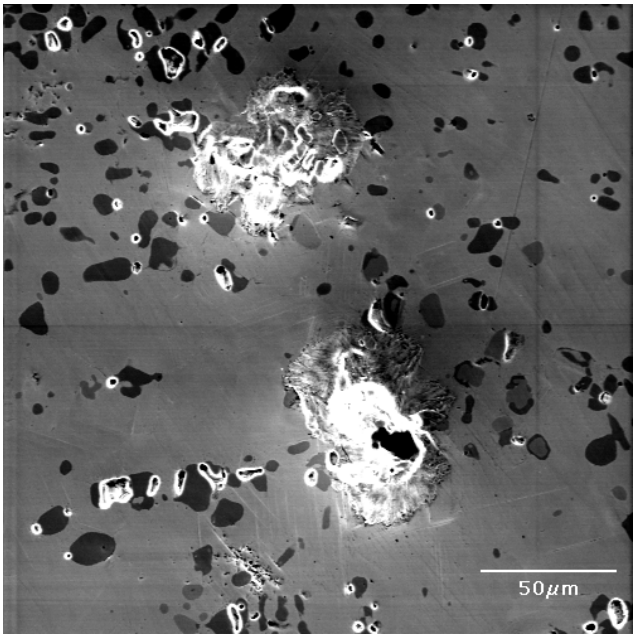


Fig. 2.5 Two large pits with craters in Stellite.

A cylindrical target with a conical offset and a six way cylindrical cross showed similar pitting to that observed in the simple cylindrical targets.

A rectangular target was irradiated to investigate the question of whether the high-density cluster of large pits observed on each specimen from the cylindrical targets was a result of geometrical focusing of the pressure pulse. This test also included a dual front window with a narrow mercury gap, prototypical of the double walled SNS target design. Because of the change in acoustic impedance with this arrangement, a firm conclusion as to the focusing effect of the cylindrical shape could not be made. Enhanced pitting was observed on the boundary surfaces of the narrow mercury filled gap. Craters on these surfaces were different from previously observed craters, exhibiting a shallower profile (see Figs. 2.6–2.7). The surface facing the bulk mercury behind the slot showed only a small degree of pitting. It is not clear whether this is due to the elimination of radial focusing or simply a result of protection by the narrow mercury layer.

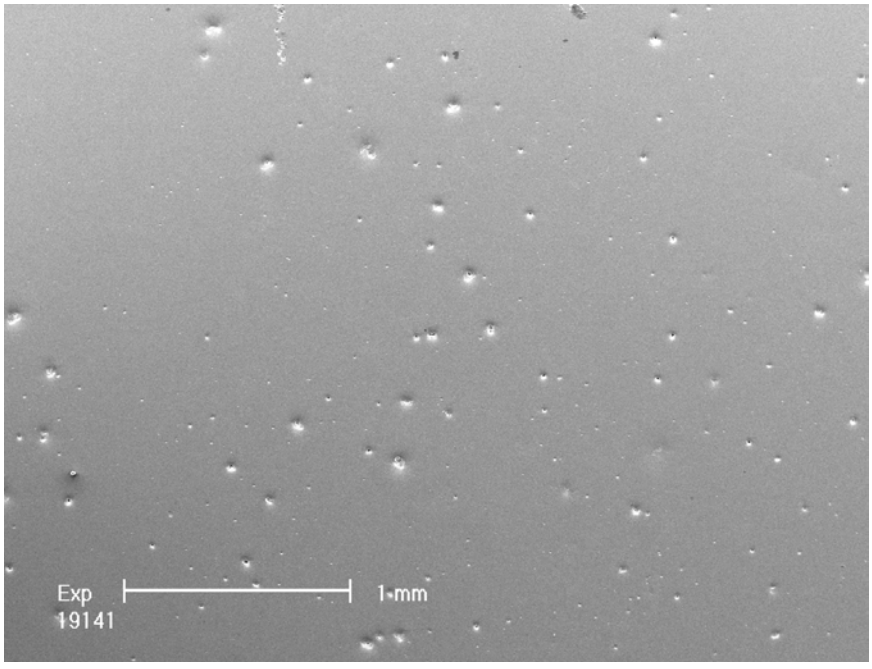


Fig. 2.6 Heavy pitting was evident on the surfaces bounding the narrow mercury layer.

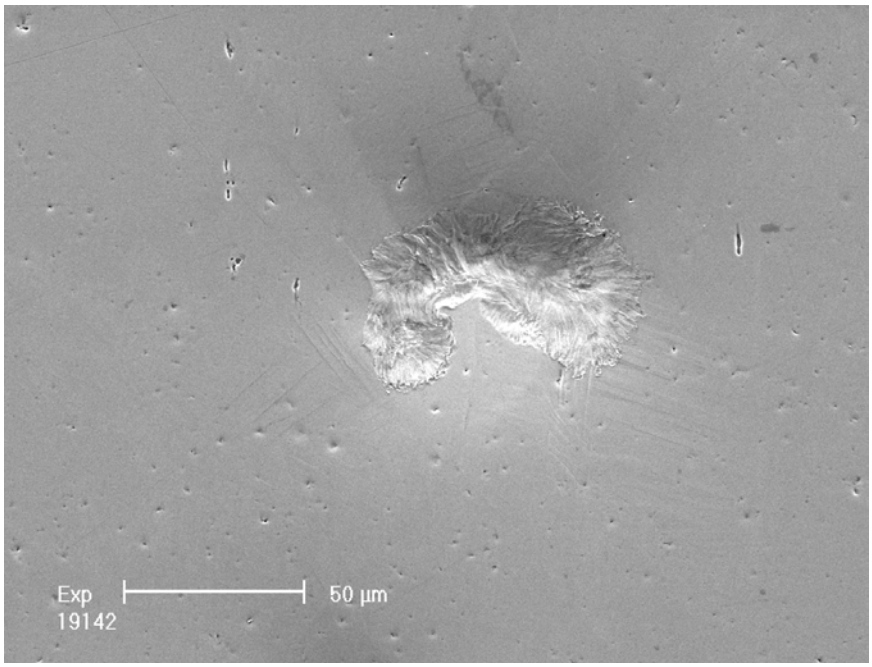


Fig. 2.7 Crater on surface bounding the narrow mercury layer.

### 2.1.2 Interpretation of Test Results

The pulsed proton beam tests performed to date have shown that surface damage occurs for all materials tested so far except one (no observable damage of a thick, cold worked 316 SS specimen with a Kolsterizing treatment). Using the data from the 200 pulse tests performed in 2001 to estimate the SNS target lifetime requires an enormous extrapolation. The nominal target lifetime based on embrittlement due to irradiation damage is set at 1250 hours for a pulse repetition rate of 60 Hz and time averaged power of 2 MW (corresponds to 5 dpa in 316SS). This goal represents $2.7 \times 10^8$ pulses, or more than a factor of a million more pulses than obtained in the tests.

The pitting damage that occurred in targets tested in 2001 is summarized in Table 2.2. This table shows the fraction of the surface that is pitted and the nominal depth of pits in the worst region of each specimen. Using the simple linear extrapolation described in Appendix A, the estimated lifetimes for two of the specimens are shown in Fig. 2.8. These results show that some materials could nearly achieve the desired lifetime; however, there is no reason to believe that the linear extrapolation is valid. It should also be noted that the thick, cold-worked 316SS specimen that had a Kolsterizing treatment had an unlimited lifetime using this simple approach whereas in reality 200 pulses with this material might be within an incubation period prior to the onset of pitting damage. Also, any beneficial effect of Kolsterizing may be removed by irradiation.

Based on the above discussion, it is clear that developing a method to extrapolate the limited pulsed beam data to the range of desired target lifetimes is needed. To facilitate this extrapolation, off-line tests that simulate pitting up to a large number of pulses are being fabricated and tests have been initiated on several devices. These off-line tests, which are discussed in Section 2.3 of this report, are considered to be an important part of the near term efforts aimed at making a decision on whether or not to continue with mercury as the initial SNS target material.

Table 2.2 Summary of WNR pitting tests conducted in 2001

| Target Shape | Position | Front diaphrgam material/ Thick or Thin | Large Pits?* | f | h | |
|---|---|---|---|---|---|---|
| Cylindrical | Front | Stellite 6B/Thick | Yes | 0.3 | 100 | |
| | Rear | Nitronic 60-20% CW/Thick | Yes | 0.4 | 25 | |
| Cylindrical | Front | **Kolsterised 316SS-50% CW/Thick** | **No** | **0** | **0** | |
| | Rear | 316SS - Annealed/Thick | Yes | 0.15 | 25 | |
| Cylindrical | Front | 316SS - Annealed/Thin | Yes | 0.4 | 50 | From July 2001 tests |
| | Rear | Kolsterised 316SS - Annealed/Thin | Yes | 0.3 | 15 | |
| Rectangular | Front of Small Hg Layer (Surface 1) | Nitronic -60, 25% CW | Yes | 0.05 | 25 | |
| | Rear of Small Hg Layer (Surface 2) | Nitronic -60, 25% CW | Yes | 0.04 | 25 | |
| | Front of Bulk Hg Region (Surface 3) | Nitronic -60, 25% CW | No | 0.02 | 5 | |
| | Rear of Bulk Hg Region (Surface 4) | Nitronic -60, 25% CW | No | 0.0005 | 2.5 | |

Large Pit Clusters = Visible to the naked eye
f = fraction of surface pitted (results shown for worst region)
h = nominal depth of pits (microns)

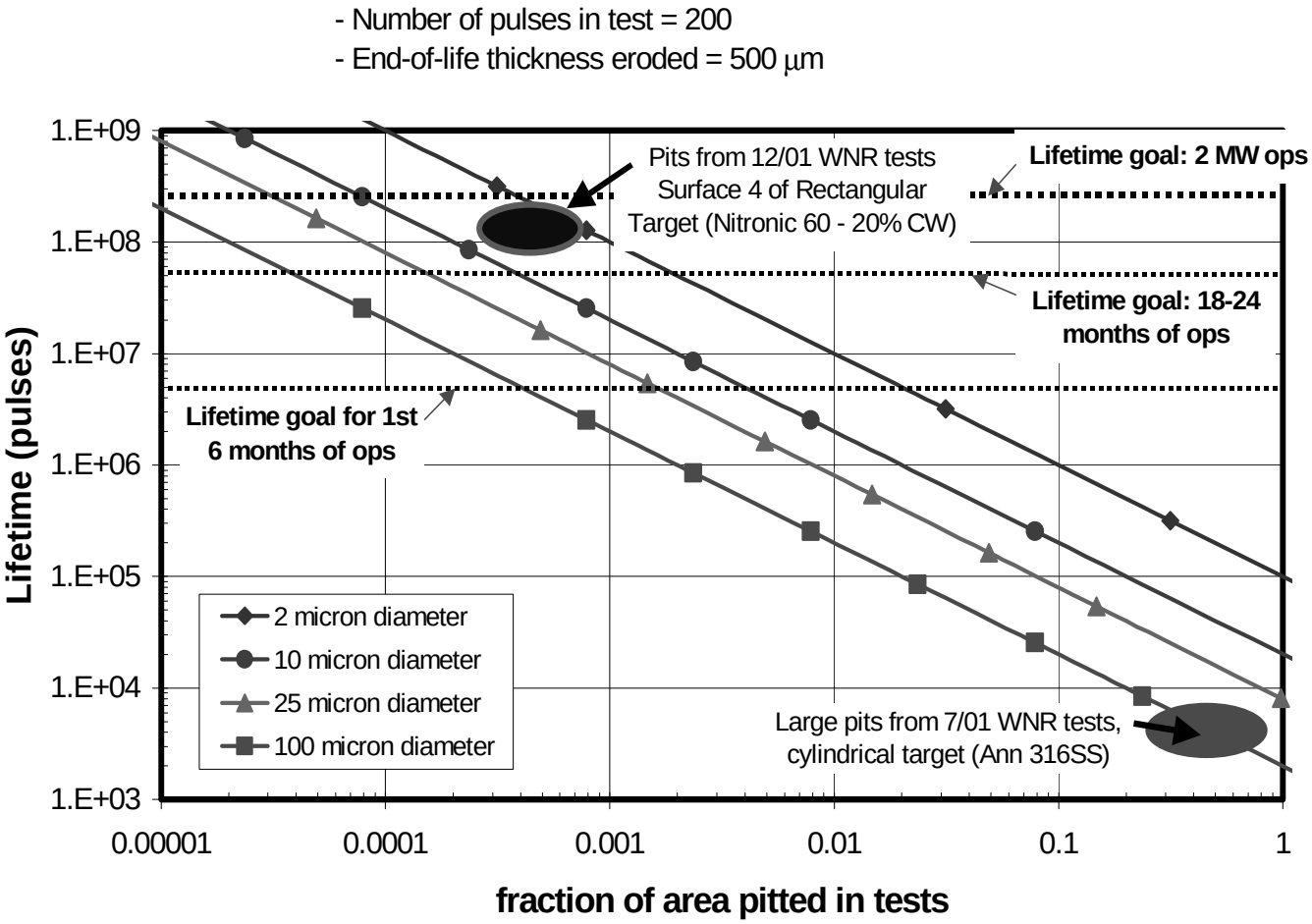


Fig. 2.8 Pitting erosion lifetimes estimated by linearly extrapolating from pulsed beam tests.

### 2.1.3 Limitations/shortcomings of WNR tests

The total number of pulses on WNR test targets has been limited to 200 (prior to June 2002, when one target was exposed to 1,000 pulses). This is six orders of magnitude lower than the anticipated SNS dpa limited lifetime, and the test targets incur negligible radiation damage dose compared to SNS. Significantly more test pulses are not feasible because of facility constraints and difficulties handling higher activation levels. Extrapolating the test results to the SNS dpa lifetime is highly uncertain. The WNR pulse repetition rate is limited to 0.03 Hz (2 per minute) vs. 60 Hz for SNS, and the beam size and total energy are smaller than for SNS. This leads to the need to perform scaled experiments, which is problematic since the underlying physical processes are not well understood.

Furthermore, WNR targets used for cavitation tests are not prototypic of SNS. They are short, closed volumes without mercury flow. Increasing the length or including flow may be

possible but at considerable increase in test complexity and cost. Polished, flat surfaces were used, in lieu of prototypical surface finishes and shapes, to facilitate pre- and post-test examinations.

### 2.2 June 2002 Pitting Tests

Tests for studying beam induced cavitation damage were conducted in June 2002 at the WNR using a total of 21 targets. The test plan was established based on (1) information needs for the October decision, (2) results from previous experiments, and (3) recommendations from the cavitation damage experts review (May 2002) as well as from the Experimental Facilities Advisory Committee. Rectangular target geometry, employed for most tests, avoided potential effects of radial wave focusing. Figure 2.9 shows a typical target with its front test plate removed. Vessel temperature and strain were monitored during these tests. Evaluation of the test surfaces will begin in August after shipment back to ORNL and decontamination.

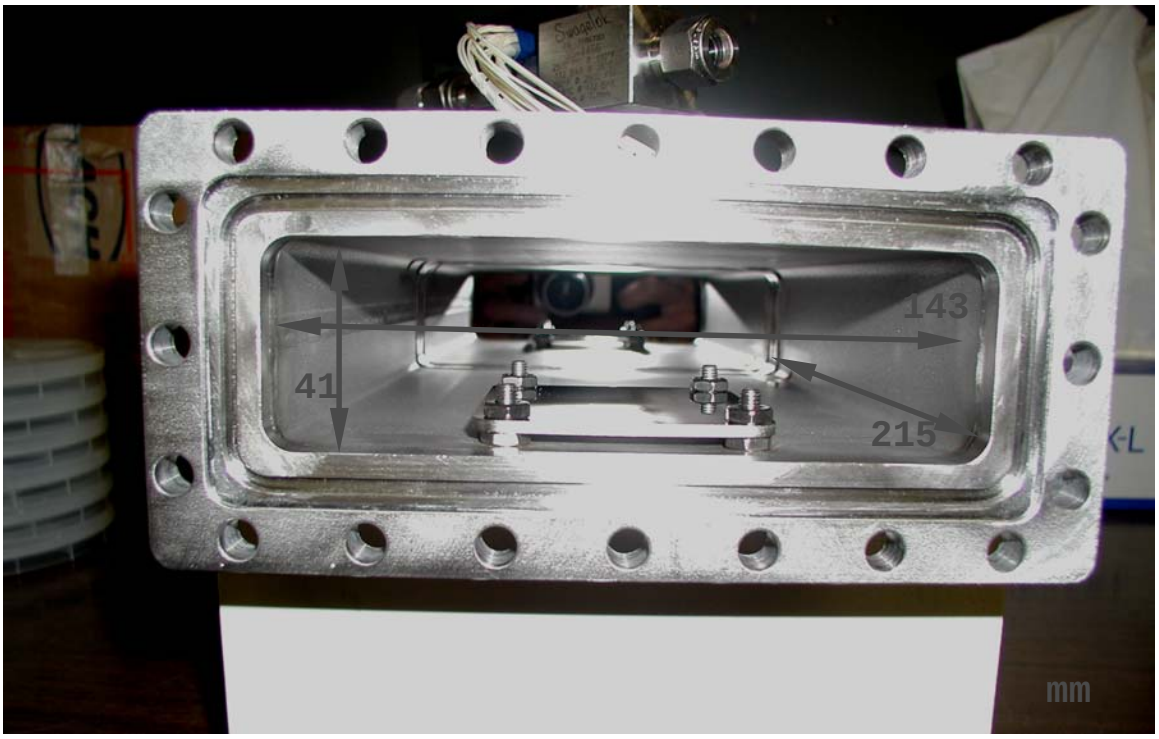


Fig. 2.9 Rectangular test target geometry used for most of the June 2002 tests. Front beam window is removed.

The 21-targets tested in June 2002 are listed in Table 4.1. A top priority test examined beam intensity as a parameter. Using cold worked, 316LN type stainless steel for the test surfaces, three beam intensity values equivalent to SNS at 0.4, 1.0 and 3.0 MW operating conditions were applied to three individual targets for 100 pulses each. This test attempts to determine if a threshold exists for cavitation damage. A threshold of a few hundred kilowatts would be encouraging for the early years of SNS operation, since this would allow more time for developing a solution for full power SNS operation.

Table 2.3 List of 21 targets used during June 2002 WNR pitting tests

- **Most targets have rectangular cross-section.**
- **Many have plates at top or bottom to simulate slot in duplex structure.**
- **Base case uses CW 316SS test surfaces and 100 pulses.**

- **Power dependence**
  - High-Power (Base Case).
  - Medium Power.
  - Low Power.
- **Bubble/gas layer tests**
  - Three thin targets in series (study effect of length and bubbles).
  - Protective gas layer flowing along the beam window.
  - Small, stagnant gas layer at top of target.
- **Geometry effects**
  - Double-wall: "Water-Cooled" Container.
  - Double wall: "Hg Cooled" Container.
  - Curved nose effect.
  - "L" shape with 45° reflection on rear and free surface on top to simulate long target.
- **Material variations**
  - Kolsterized, CW 316SS test surfaces.
  - Electro-polished surface.
  - Nitronic-60 instead of 316SS.
- **Bubble diagnostic target**
- **1,000 pulses instead of 100**
- **Three Cylindrical targets fabricated by FzJ (material/coating variations)**
  - Martensitic steel from ESS.
  - CrN coating from JAERI.
  - Annealed 316LN.
- **PbBi filled cylindrical target**
  - Repeat of previous test, but with target completely filled.

Gas bubble injection, an approach being investigated by the ESS project as a means to reduce target vessel strains from pressure pulses, was also studied in the June 2002 tests. It is hoped that the gas bubbles will also mitigate cavitation damage. An ESS researcher joined the SNS experiment at the WNR (as well as a JNS researcher). The bubble creation technology needed for the experiment is in its infancy for liquid metals, and there was little time to develop this test target. The experiment may not be representative of the potential of this approach. Figure 2.10 shows this target in preparation.

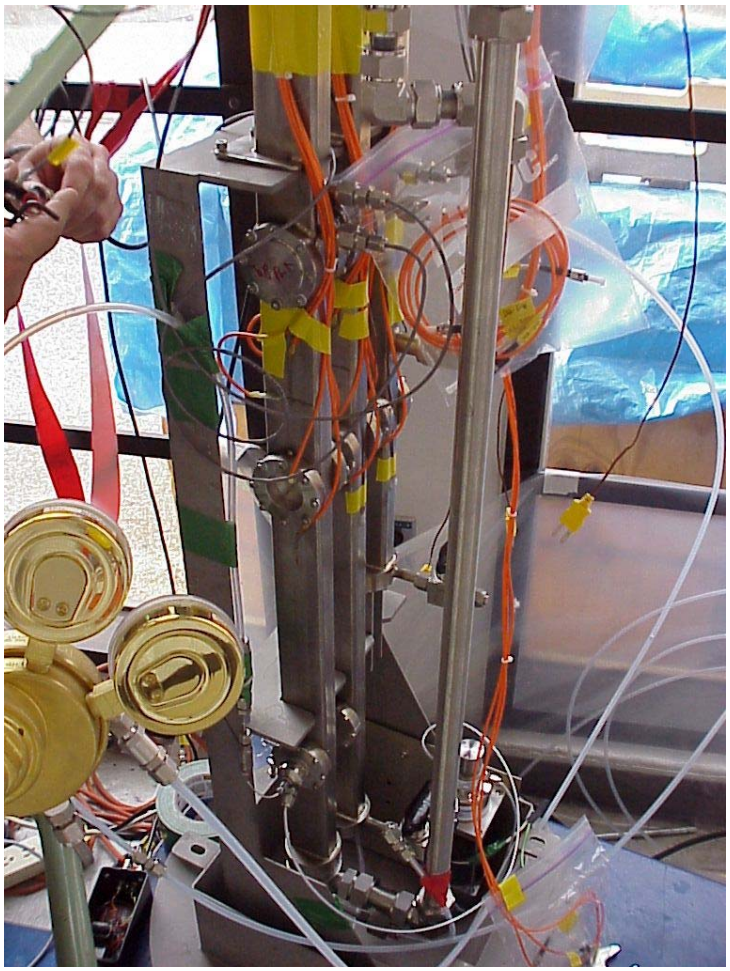

Fig. 2.10 Bubble mitigation target in preparation. The three vertical targets are in the center.

Results from the December 2001 WNR test on a rectangular, double-walled target suggested acoustic wave propagation was an important mechanism leading to cavitation damage. As a result, the June 2002 experiment included two targets with a double beam window. One employed mercury in the inter-wall space, while the second used water. The different acoustic impedance in this space may protect target surfaces facing the bulk mercury region, and SNS target design could be adapted to use water in the inter-wall space. Also included in the testing was a simulation of the double wall structure on the bottom surface of the target to see if it was vulnerable to damage similar to the front double wall window.

A noted shortcoming of previous targets was the fact that the real SNS target has no wall opposite the beam window. Pressure waves originating in the front end of the target will propagate down the mercury piping and not reflect off a wall as they do in test targets. To approximate this lack of a reflecting wall, one test target was designed with an angled rear wall,

which directs waves into an energy dissipating volume. This should determine whether the reflections off this end are contributing to the damage. A picture is shown in Fig. 2.11.

One recommendation of the cavitation damage experts group was to test a technique used to acoustically hide naval vessels. A substantial wall of gas bubbles is created around the hull of a ship creating an impedance barrier that hides the internal mechanical noise of the ship from distant listening devices. A test target was designed to create a curtain of gas bubbles at the beam window in an attempt to hide the window from the pressure pulses created in the mercury. Note that this approach differs from the bubble mitigation technique, which introduces a population of small bubbles dispersed throughout the mercury volume.

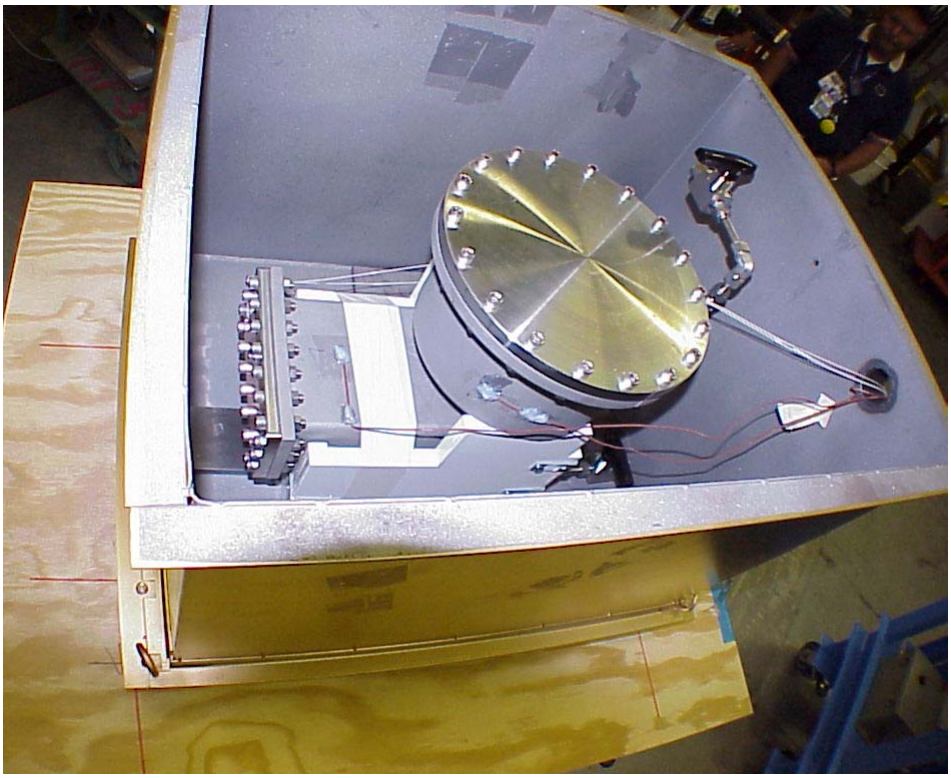

Fig. 2.11 Target “L”, having an angled rear wall.

While nearly all targets were tested with 100 pulses, a single target was tested to 1000 pulses. This target used the basic rectangular cross-section design with a single beam window made of cold worked 316LN stainless steel, taking pulses at a rate of 2 per minute. The progression of damage with the order of magnitude increase in pulses is to be assessed.

Other rectangular target tests included: deliberately using an incomplete fill, thus leaving a gas void; employing a cylindrically curved front beam window; using an electro-polished beam window, as opposed to mechanically polished; using the surface hardening treatment "Kolsterizing" on cold worked, 316LN type stainless steel; and using cold worked Nitronic 60 stainless steel.

A target was also included to test a new type of diagnostic to detect the presence of bubbles and provide information on their lifetimes. This target had fiber optic cables which terminate at the mercury / stainless steel interface. The concept is to detect bubbles by the changes in reflected laser light from the interface. An additional fiber optic sensor was employed to detect the presence of bubbles in the bulk fluid.

Some cylindrical targets (Large Effects type) were also tested during this campaign. They included 3 ASTE targets (AGS Spallation Target Experiments) that were originally planned for tests at BNL, but were included in the WNR test campaign after the 2002 ASTE tests were canceled. Test surface materials included martensitic steels being considered by the ESS project, chrome nitride coated 316-type stainless steel (under consideration by the JNS project), and annealed 316 stainless steel. Also tested was a molten lead-bismuth filled target; this one was uniquely tested with 200 pulses.

It is worth noting that all test targets used stagnant mercury, which is not prototypic of the SNS target. A flowing mercury experiment is under consideration for future tests.

### 2.3 Progress and Plans for Off-Line High Cycle Tests

Using the LANSCE short-pulse beam in the Blue Room at the WNR facility, the pitting for various materials and target shapes has been characterized for up to 200 pulses (1,000 pulses were achieved for one target in the June 2002 tests, but this target remains to be examined). To understand how to extrapolate this data to the SNS lifetime goal of $2.7 \times 10^8$ pulses, off-line devices that accurately simulate the pitting damage are being pursued. The near term goal is to achieve at least one million pulses in a device with a pressure rise time of tens of microseconds and peak pressures in the range of 40 MPa. To achieve one million cycles in a reasonable time, the repetition rate should be 1 Hz or higher. The JAERI Split-Hopkinson Pressure Bar (SHPB) apparatus achieves the correct peak pressure, does a reasonably good job on pressure-rise time, but has a low-repetition rate. An ultrasonic processor, such as that being used by the SNS team

for materials screening, gives an adequate pressure rise time, a high repetition rate (20 kHz may be too high), but does a poor job of matching the pressure (on the order of 0.1 MPa).

Four off-line devices are currently being pursued, three by the SNS team and one by the JNS team. These devices include:

(1) A simple mechanical drop test device set up at ORNL,

(2) A lithotripter (kidney stone blaster) available at Boston University,

(3) A device being built by Southwest Research Institute (SwRI) using a piston and cylinder arrangement driven with a servohydraulic actuator, and

(4) An electromagnetically driven device built by JAERI that drives the deflection of the center of a large plate in contact with mercury.

The status of each of these devices is briefly described below.

A simple mechanical device with dimensions similar to JAERI's SHPB, but using a striker bar that is dropped from heights of 100 to 500 mm, has been fabricated and is undergoing initial tests at ORNL. The pits obtained for a cold-worked 316SS specimen subjected to 100 drops from heights of 500 mm and 130 mm are shown in Fig. 2.12. The pits resulting from the 500 mm drop appear to be twice the size of the largest ones observed in 200 pulse beam tests, whereas the pits for the 130 mm drop are in the range of some of those observed in the beam tests. A comparison of the fraction of area damaged in tests in the SHPB apparatus, this new drop test apparatus, and pulsed beam tests is shown in Fig. 2.13. The damage fraction for drop tests at 130 mm are in general at the low end of the in-beam tests from 2001. Based on the match in pit size and low, but easily observable, damage fraction after only 100 pulses, the 130 mm height has been selected as the nominal position for performing an initial set of tests for the reference 316SS material (cold worked 20%). Microscopy and weight loss measurements will be performed for specimens up to one million cycles. Two cold-worked 316SS specimens, one with a surface hardening treatment (Kolsterizing) and one without, will be tested prior to the October decision date.

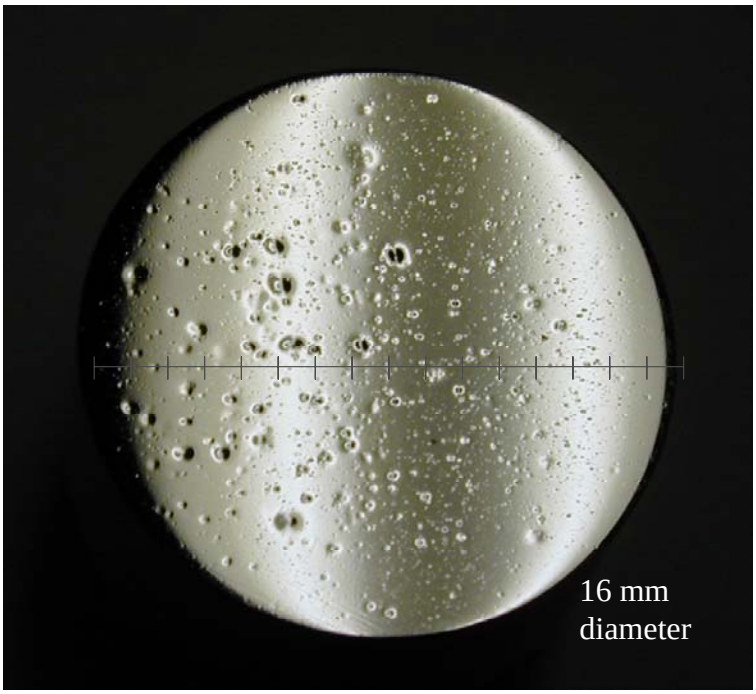


**(a)**

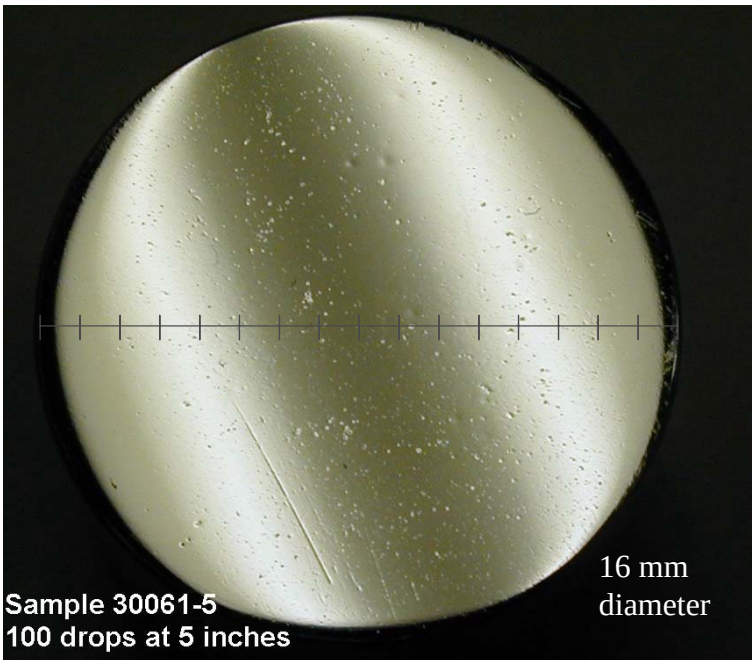


**(b)**

Fig. 2.12 Photos of 3166SS test surfaces exposed to 100 pulses dropped from (a) 500 mm and (b) 130 mm on the ORNL vertical drop test apparatus.

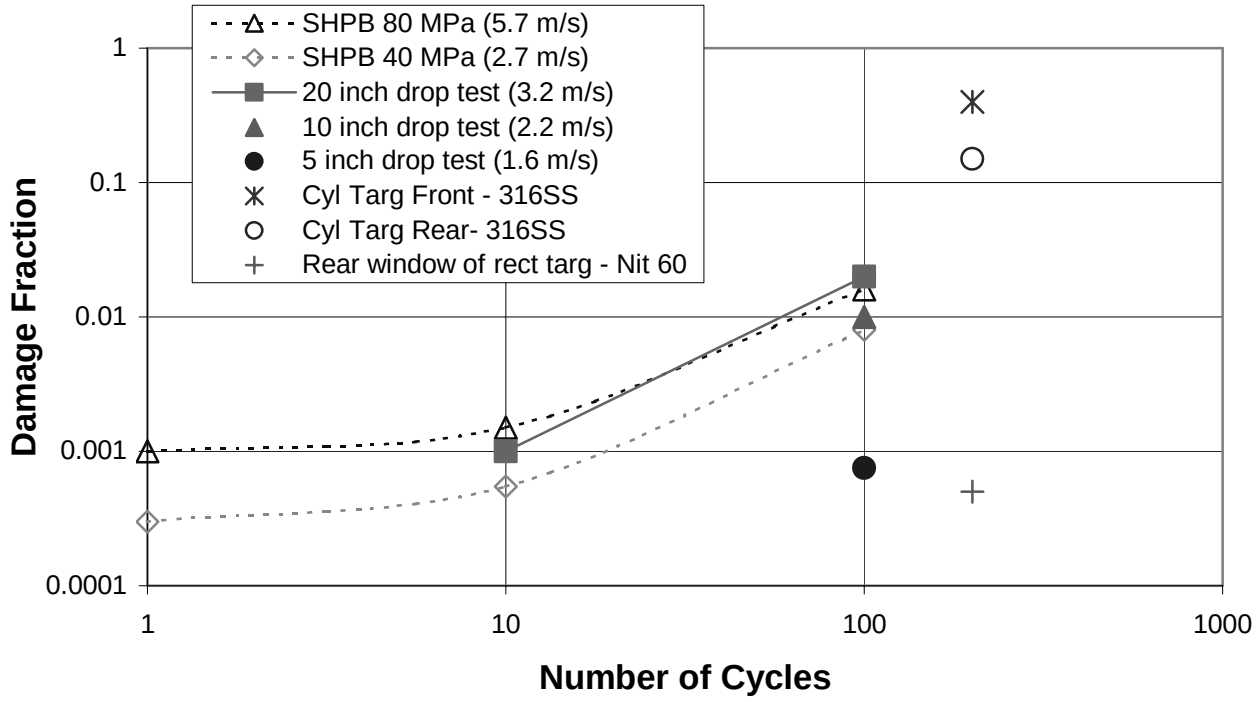


Fig. 2.13 Comparison of pitting damage on JAERI's SHPB apparatus, ORNL's vertical drop test device, and WNR pulsed beam.

Initial tests on a lithotripter apparatus at Boston University have also shown promise for improving the understanding of how pitting damage scales with number of pulses. An SEM micrograph of a specimen subjected to 1,000 pulses applied at a repetition rate of 1 Hz on this device is shown in Fig. 2.14. The damage is judged to be similar to that observed from beam tests. Based on these initial results, the SNS team has contracted with Boston University to conduct a series of tests up to $10^5$ pulses. The $10^5$ pulse limitation for this device is due to the need for replacing its spark igniter after about 2,000 pulses. Use of an electromagnetically driven lithotripter is being pursued to extend the tests to one million or more pulses.

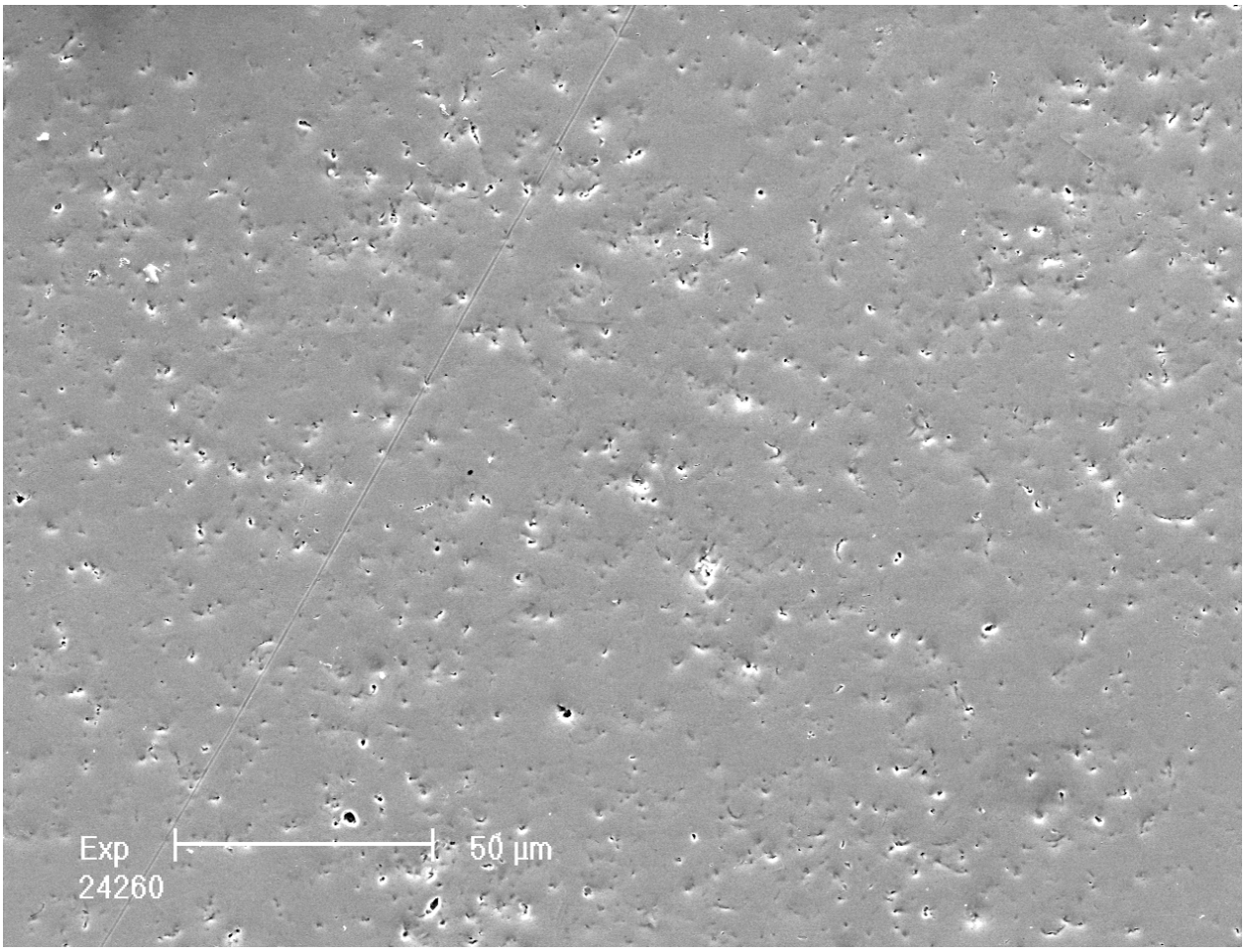


Fig. 2.14 Micrograph of a specimen after being exposed to 1,000 pulses on Boston University's lithotripter.

The SNS team has also contracted with the SwRI to develop a servohydraulically driven device that can provide pressure pulses of the magnitude needed to simulate the beam pitting damage. This device, which should operate at frequencies above 1 Hz, will be tested in August 2002. If this device yields pitting damage of the type observed in beam tests, it will be used to test specimens up to one million or more cycles.

The JNS/JAERI team has developed an eletromagnetic device that drives the deflection of a plate in contact with mercury at frequencies up to 20 Hz. A photograph of this apparatus is shown in Fig. 2.15. The central region of the plate undergoes pitting that appears to simulate that observed in beam tests. Because higher frequencies are possible with this device, tests up to $10^7$ cycles may be attempted. The JAERI team will conduct pre- and post-test examinations of test

specimens that will be fabricated by the SNS team. SNS will also provide manpower to support the testing activities.

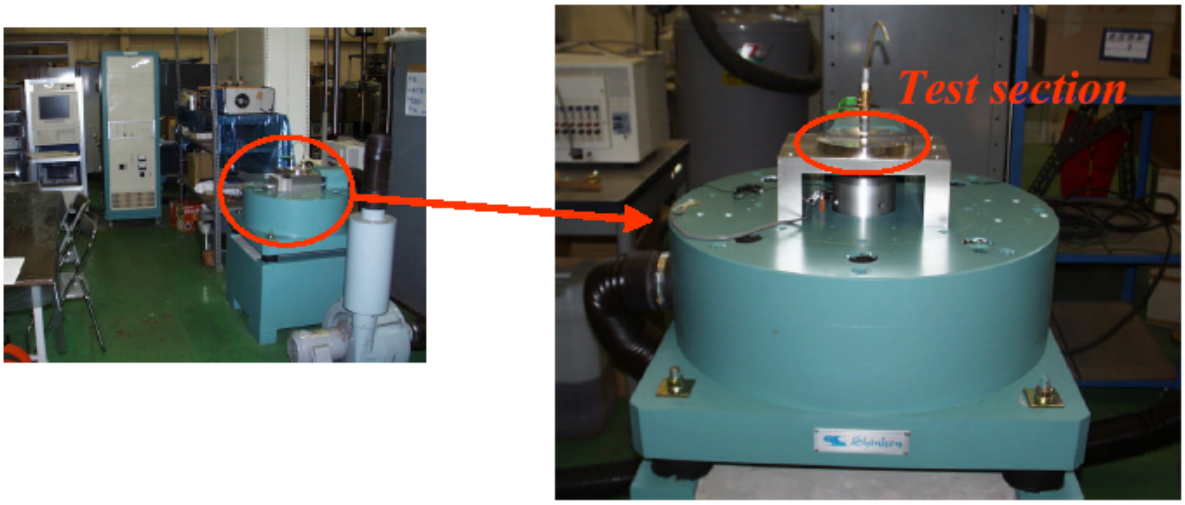


Fig. 2.15 Electromagnetically driven pressure pulse device fabricated by the JNS team to simulate pitting damage.

### 2.4 Mitigation Strategies

Injection of gas bubbles to increase the compressibility of the mercury might be effective at reducing the damage. This approach is being pursued by the ESS team, with some limited support from the SNS team. An initial experiment using bubble injection was included in the June 2002 WNR tests, but results are not yet available.

Injection of a protective gas layer might also offer protection for the mercury container walls. This was suggested as a promising approach by our team of cavitation damage experts (see Appendix B). The gas layer is used primarily as a surface to acoustically reflect the incoming compression wave back to the bulk mercury without interacting with the container wall. An initial experiment using this gas injection concept was also included in the June 2002 WNR tests, but results are not yet available.

A possible inherent mitigation process could be present at a 60 Hz repetition rate. Evidence from lithotripter (kidney stone blaster) research has shown that these cavitation-based devices are capable of breaking up kidney stones when operated at 1 Hz but are ineffective when operated at 60 Hz. This is believed to be due to the persistence of cavitation bubbles from previous pulses that greatly increase the compressibility of the fluid thereby reducing the intensity of the

cavitation bubble formation and collapse processes. This suggests that the cavitation bubbles last somewhere between 17 ms and 1 s in the lithotripter case. The question of whether this same effect is present for our mercury target operating at 60 Hz remains unanswered at this point. It should be noted that the JNS electromagnetic device gives significant pitting damage when operated at 20 Hz.

An option that has yet to be investigated is textured surfaces. There are qualitative arguments to suggest that such an approach might reduce erosion. Textured surfaces can be produced by etching, hammering, shot peening, milling, or rolling, the latter two being reproducible. The size scale of the texturing might have to be of the size of pits, say 100 μm or so. The use of porous sintered layers or “steel wool” or other mesh like material, perhaps with gas flowing through the porous structure of these materials might also be effective in mitigating the damage.

# 3.0 IMPLICATIONS OF CHANGING TARGET TYPE DURING OPERATIONS

## 3.1 Switch From Mercury to Water Cooled Solid Target

### 3.1.1 Assumptions

We have completed an initial assessment of the effort required to convert from a mercury target to a heavy water cooled solid target after initial beam operation has been started with the baseline mercury target system at SNS. This conversion would take place assuming that the beam power has been limited to stay below Hazard Category 3, that no mercury has been released into the core vessel, and that the mercury releases in the hot cell are limited to those associated with normal target operations. Preliminary analysis shows that after one year of operation at 300 KW, Hazard Category 2 is reached. At this power level the impact on changing out the system is expected to be mainly the difficulty of storing and handling the mercury inventory for disposal. A Hazard Category 3 facility would have to be found or constructed for amalgamation of the mercury or the material processed in the SNS hot cell, adding to the time required to complete the changeout.

The solid target concept is based on very preliminary designs and layouts. It assumes an initial low performance heavy water cooled Zircalloy rod target based on technology proven at SINQ. The cooling system design has two separate loops, including the primary loop and an independent auxiliary loop for decay heat removal from the target. They are sized with the capability to later install a tungsten plate target designed to give neutronic performance equivalent to mercury at 1 MW.

There has been no systematic safety evaluation of this system, so there is the possibility that significant design changes will be required when the safety evaluation is performed. One preliminary safety related concern is that the decay heat removal systems may have to function through a PC-2 seismic event. This may require a new system since the conventional facilities secondary loops and systems (cooling towers, electrical power, etc.) are not designed to function after a PC-2 earthquake. A preliminary hazard analysis is to be started in August.

### 3.1.2 Impact on Baseline Design

Some consideration has been given to incorporating design changes to the mercury target system to reduce the difficulty of replacing it with a solid target system. This was done to minimize additional costs prior to a decision to use a solid target.

The design of the target carriage has been changed so that the support plate for the mercury piping at the front of the carriage is now bolted to the carriage base platform instead of being welded. This feature allows the platform, which is the most highly activated part of the carriage, to be removed during the change-out thus significantly reducing the radiation level present when new cooling piping is installed for the solid target.

An option has been proposed to use the water loop that cools the target shroud and proton beam window in the mercury target system for decay heat removal from the solid target. This option is under consideration and may simplify the solid target design and installation. With this approach new pumps and tanks would not be needed for this loop.

As discussed in Section 4.3, a change to increase the thickness of the concrete between the charcoal filter room in the basement and the instrument floor level has already been implemented. This provides the needed additional shielding for filters and ion exchange columns in the solid target cooling water loops.

No changes are expected to the core vessel or reflector/moderator assemblies or their associated water-cooling loops.

### 3.1.3 Schedule

A preliminary schedule has been developed for the activities required to replace the mercury target system with a water-cooled target, and is included as Appendix C. Included in the schedule is the amount of time required to remove the mercury systems, decontaminate the hot cell, modify the facility, and design/procure/fabricate/install the solid target system. In summary this schedule shows that:

- The amount of time the facility will be out of operation for the change (i.e., beam-off to beam-on) is expected to be approximately 23 months including:
  - 4 months to remove the mercury system,
  - 9 months to decontaminate the hot cell, and
  - 10 months to install and test the solid target system.
- Design and procurement activities on the solid target system must start 19 months prior to the shutdown in order to have the necessary tools, facilities, equipment, and solid target components available as needed during the shutdown.

The estimate for the removal of the mercury equipment was derived by developing a detailed disassembly sequence and assigning a time to each by consulting with in-house personnel experienced in performing remote handling operations.

The decontamination work includes two phases - initial decontamination using remote tools (6 months), and final manual decontamination in protective clothing and respirators (3 months). These estimates were developed by reviewing ORNL decontamination experience and developing an algorithm that estimates the time based on the beginning and ending contamination level and the amount of area to be cleaned. However, this estimate contains a large potential for error due to the lack of experience in dealing with contaminated mercury and the unknown degree to which the hot cell will be contaminated.

The estimate for the design, procurement, and installation of the solid target, its cooling loops, and facility and support equipment was also based on a detailed listing of the necessary tasks. The times and sequencing of the tasks was performed by an experienced estimator using project scheduling software and considering the SNS project experience for similar equipment wherever available.

The detailed list of assumptions used in developing this schedule is included in Appendix C. Principal among these are the assumptions that;

- Work will be conducted on a 24 hours a day/7 days a week schedule during the shutdown
- Skilled manpower is available as needed and necessary tools have been procured as necessary to minimize schedule.
- There will be no time lost for administrative actions such as obtaining necessary licenses or permits.

### 3.1.4 Cost

The cost for the conversion to a solid target is still under evaluation and will include all aspects of conversion, including mercury decontamination, waste handling, storage, and transport activities as well as design, fabrication, installation, and startup testing for a water-cooled solid target. It is anticipated that the majority of this cost can be funded from the operating budget during the period.

### 3.2 Replacement of a Water Cooled Solid Target with a Mercury Target

Replacement of a water-cooled solid target with a mercury target has not yet been studied and therefore costs and schedule estimates are not currently available. However, we anticipate that these studies, to be carried out prior to October 15, will result in total cost and times less than those for the mercury-to-solid scenario since the contamination resulting from operation of the water loops will be less than from the operation with mercury.

# 4.0 FUTURE TARGET DEVELOPMENT NEEDS

## 4.1 International Collaboration on High Power Target Development

Because all major Spallation Neutron Source Projects (SNS and JNS under construction; ESS early phases of CDR) have Hg as their target material, a strongly coupled international collaboration has been established to investigate the cavitation erosion issue. Plans for this collaborative effort were outlined by SNS, JNS, and ESS personnel at the recent International Workshop [2] on the Development of High Powered Targets (IWDHPT). Since JNS and SNS have to make decisions soon (mid-October 2002 for SNS and December 2002 for JNS) as to whether to switch to a solid target backup, certain action items have been established which will yield data to assist in making this decision. These action items were chosen to allow the design engineers to get a "realistic" estimate of the lifetime of the target module or to develop a pathway forward such that the lifetime of the target can be substantially increased. These action items include: (1) analysis of the current WNR test samples and (2) out-of-beam tests, which yield similar damage and can yield 1 to 10 million pulses. The out of beam tests will give a good measure of the erosion rate as a function of pulses. The June 2002 WNR tests, which included participants from ESS and JNS, have been carried out on a number of targets.

In the longer term, SNS test facilities may be used to support the ESS bubble injection efforts. Possibilities include using the TTF as a test facility in which bubbles will be introduced to mitigate pressure pulses produced by an electric magnet force driver on the front face of the target. This test would investigate damage with and without the bubbles. The use of smaller loops like the Mercury Thermal Hydraulic Loop (MTHL) are also being considered.

Also, in the longer term, the collaboration is working toward designing, building, and performing in-beam tests on a target with flowing Hg. A preliminary design of this Hg loop will be developed and during January 2003, a meeting will be held to determine who will be responsible for what components. During the near-term, accelerator facilities will be visited to determine if there is any interest in supporting such an experiment. The facilities currently under consideration include ISOLDE/CERN, FNAL, BNL/AGS, and LANSCE. Recently, a group of SNS researchers visited CERN to tour the ISOLDE Facility. This facility can provide $3x10^{13}$ one-GeV protons/pulse at 1 hertz with an acceptable beam size. This beam is comparable to the WNR beam. Visits to the other facilities will occur during the following months.

To keep the collaboration members in close contact with each other, videoconferences will be initiated.

### 4.2 Anticipated Mercury Target Design Changes

The results of the pitting tests to date indicate that changes to the present design of the stainless steel mercury target may be necessary to achieve acceptable target vessel life. These changes can be incorporated in two stages: (1) minor modifications to the initial target(s) and the mercury process loop during the time that additional R&D data is collected, and (2) more significant changes, which could be incorporated at a later date, based on lessons learned in cavitation erosion testing and during early operation.

The target beam window is one of the areas of greatest concern for pitting damage. The present design uses two stainless steel windows each with a thickness of 1.3 mm. Mercury flows in the space between the two stainless steel walls to remove the heat deposited in them from interactions with the proton beam. The wall thickness is limited by thermal stress resulting from the deposited beam energy at proton beam power of 2 MW. Since the first target will be operated at less than full design power levels, it is possible to increase the window thickness significantly. Surface treatment of the beam windows by Kolsterizing could be added to the manufacturing process if it is determined to be desirable. This increased beam window thickness and surface treatment will result in added protection against cavitation erosion and would not require changes to the mercury process loop or any of the target support systems. It is also anticipated that the first target will be outfitted with extra instrumentation to measure key parameters during operation with a low power proton beam. Key information can also be gained from inspections of the target vessel surfaces after the initial target is removed from service, and methods to perform these inspections need to be developed. Preliminary plans for this work are already in place. [3]

Some of the other methods being considered to mitigate the pitting damage will have a larger impact on the mercury target system. The results of the December 2001 testing at LANSCE show that the two surfaces that form the target window flow channel are expected to have a large amount of pitting damage. One potential solution to this problem is to replace the Hg coolant that flows in this channel with water. Tests to identify the effect of this change were included in the June 2002 test program at LANSCE. If the results of these tests show an advantage, changing the

window coolant to water would necessitate a change in the design of the target module as well as configuration of the mercury and water target coolant loops. In the present target system, there are a minimum of two walls separating the mercury from the water used to cool the protective shroud surrounding the mercury vessel. This arrangement allows the majority of the water coolant loop to be located outside of the hot cell since a double failure would be required to introduce activated mercury into the water system. If the target beam windows were to be cooled with water there would be only a single barrier, the inner window, separating the water from the mercury. In order to prevent the possibility of activated mercury leaving the hot cell from failure of this window, it would be necessary to either modify the present water shroud loop to preclude this possibility or add another water loop wholly contained within the hot cell. In addition, the flow channels that are machined into the target module and the mercury supply piping would have to be reconfigured so that mercury flow is removed and water flow added.

Adding gas bubbles to the flowing mercury to eliminate the pitting would add a significant complication to the target system. A significant effort will be required to design and demonstrate a method of introducing the bubbles into the mercury and insuring that the introduced gas does not separate from the flowing mercury and accumulate at undesirable points throughout the loop. Although there has been no work to date, to investigate how a gas bubble system could be added, it is anticipated that the limited space available close to the target module and maintainability requirements of the system will require that the system be added somewhere in the hot cell. This means that the bubbles will have to travel large distances within the flowing mercury both before entering the target module and when leaving it.

### 4.3 Implications of Changing to a Solid Target in October 2002

A conceptual design effort on the solid target was conducted in the first half of this year and has resulted in a definition of a solid target system that could be used in SNS. This study established the principal features of the target, the sizing of the cooling loops necessary for its operation, and a plan for locating the system's components in the space available within SNS target building. This conceptual design was then used as the basis for developing initial estimates of the cost and schedule required for its implementation.

By October of this year, much of the target building will have been built, with the design complete and contracts in place for the construction of the remainder. Many of the rooms within

the building were sized, located, and incorporated features specifically chosen to support the operation of the target mercury system. Consequently, part of the conceptual design effort on the solid target was directed toward identifying how the building could be adapted to the water cooled solid target and what modifications would be necessary. The resulting arrangement, shown in Fig. 4.1, utilizes three of the rooms on two levels of the building, including the hot cell adjacent to the target monolith and the two rooms below the hot cell originally intended for processing mercury and the air that is vented from the hot cell.

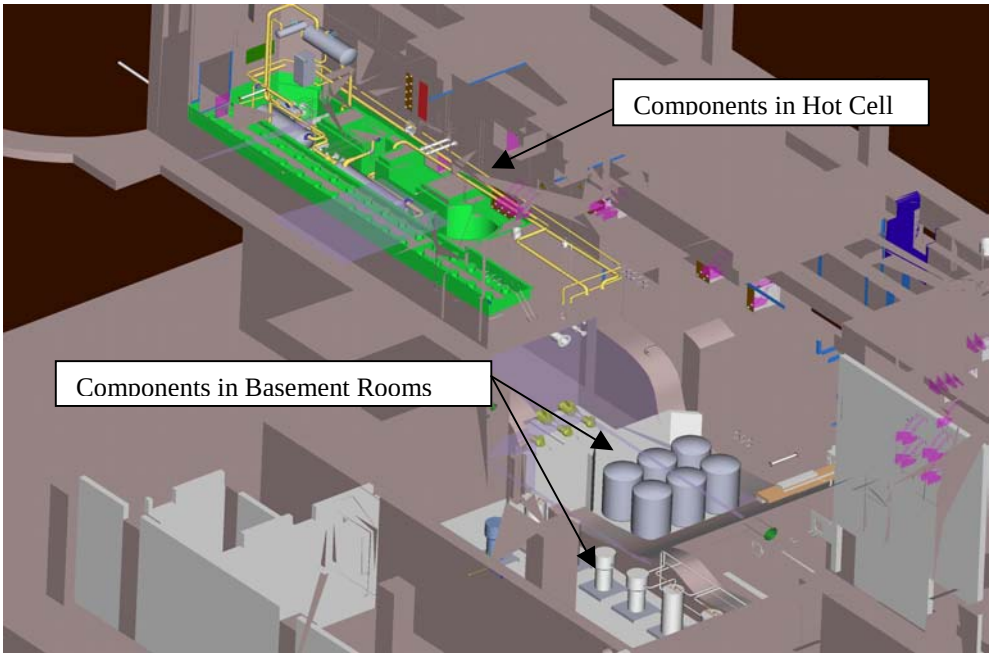


Fig. 4.1 Location of the Solid Target Cooling Loops in the Target Building.

Four changes to the building will be required for the installation of the solid target cooling loops: (1) thickening of the section of the experimental floor that forms the ceiling of the air filter room in order to provide additional shielding for the ion exchange columns that would be located within it, (2) installing additional shielding on the walls of this room, (3) providing an auxiliary floor in the two basement rooms that provides the necessary supports for the water loop components and a volume for collecting water leaks, and (4) providing additional penetrations in the floor of the hot cell for routing pipes to the basement. Only the first of these changes, the thicker floor, needs be provided during the construction of the building while the other three can

be included as part of the installation of the solid target system. This change has been incorporated, and the building will be built with the thicker floor.

The conceptual design effort on the solid target included the generation of a preliminary estimate of the cost and time required for it's design, fabrication, and installation. This estimate was used to show that an October 2002 decision to install the solid target rather than the mercury one would result in a net cost increase of approximately $7 million and require an additional six months to complete its construction. The net cost increase was calculated as the total cost of the system (~ $10 million) less the amount that could be saved by not completing the procurements and installation for the mercury system. Delaying the decision beyond October would increase the net cost of the solid target, since more funds would have to be committed to procurements for the mercury target in order to meet the project schedule, and since the spending rate on these procurements increases significantly after October. Furthermore, it should be noted that these costs would be significantly greater if the switch to a solid target occurs after the start of operations. If a decision to use a solid target is made in mid-October, the projected start of beam operations (CD-4) would be April 2006. This meets the project execution plan milestone for project completion.

## 5.0 CONCLUDING REMARKS

A series of tests were conducted at LANL's WNR facility during July of 2001 to examine whether the pressure pulse phenomenon caused by the interaction of a short-pulse (300 ns), high-energy proton beam with mercury causes pitting damage to the stainless steel container. Results showed that, at least for the materials and target configurations tested, pitting damage occurred. A cluster of large pits, visible to the naked eye, as well as smaller, more randomly distributed pits, were seen on all four-window specimens used in the July 2001 tests.

Subsequent tests at the WNR in December 2001 were dedicated to further examining the pitting phenomenon and looking at an array of possible solutions, or at least reductions, to the pitting problem. Seven targets were tested in the December 2001 campaign. Most notably, a target with a rectangular cross section was used in an attempt to eliminate the postulated radial focusing of the pressure wave and be more prototypical of the actual SNS target shape. Also, windows with increased thickness, intended to reduce the large stresses, were tested. Post-irradiation examination of the targets irradiated in December showed that pitting occurred for all test specimens except for one; a thick end plate on a cylindrical target made from cold-worked 316SS with a Kolsterizing treatment had no observable damage.

The magnitude of the pressure pulse, results of off-line cavitation threshold tests, and post-test examination of damaged surfaces, lead us to conclude with a reasonably large degree of confidence that the mechanism causing the pitting damage is collapse of bubbles created as part of a mercury cavitation process. Because of this, the cavitation damage literature has been studied to help understand the phenomenon and postulate potential solutions or improvements and a review meeting was held with a panel of cavitation damage experts. The major conclusions from this panel of experts were that they: (1) concurred with our interpretation of this damage being caused by cavitation bubble collapse, and (2) endorsed the SNS team's method of attack for resolving this issue. They also suggested the bubble curtain method for possibly mitigating cavitation erosion; this was included in the June 2002 tests.

To date, in-beam tests have not been able to clearly demonstrate a solution to the pitting issue, although some concepts/material combinations may hold promise. Approaches using bubble injection to either increase the compressibility of the mercury/gas target or to provide a protective layer of gas along the solid wall boundaries are being considered. Another concept is

the use of a target with either no double wall structure near its front or using water in this thin slot formed by the double wall. Any of these changes represent a modification to the SNS baseline design and will require careful evaluation before they could be incorporated, and may lead to breakage of engineering design, increased component costs, and greatly reduce or even eliminate all schedule float in SNS target fabrication, installation, and testing. Initial proof-of-principle tests were conducted for each of these concepts in the June 2002 tests at the WNR facility. An attempt was also made to determine whether the WNR test target geometry produced more severe pitting than a prototypic open loop geometry. Results are expected to be available prior to the October 2002 decision date.

Estimating the target lifetime using the data from a few hundred-beam pulses requires an enormous extrapolation, i.e., by more than a factor of one million. To facilitate the extrapolation of the beam test data to lifetimes in the range desired for the SNS target, a series of off-line, high cycle tests are being pursued. These pitting simulation devices will enable us to better understand the dependence of pitting erosion on the number of pulses prior to the October 2002 decision date.

To minimize cost and schedule impacts associated with resolving the so-called pitting issue, the mercury target development activities have recently become more integrated with our international partners in Japan and Europe. In addition to participating in the June 2002 WNR tests, our partners provided test targets, specimens, and measurement equipment. The collaboration will continue in the near term, with the JAERI team examining the high cycle dependence of the pitting erosion using an electromagnetically driven diaphragm that is capable of operation at 20 Hz. The SNS team is planning to provide manpower and test specimen fabrication support for conducting tests on this apparatus. We continue to rely on the ESS team for their expertise in gas injection schemes that are proposed as a means of mitigating the cavitation induced damage. Plans for a more long-term collaborative test that achieves a much greater number of beam pulses (> one million) with a flowing mercury loop are also being formulated.

Besides contemplating the prospects for achieving an acceptable solution to the pitting issue, another factor to be considered in the mercury versus solid target decision is the implication of switching from a mercury to a solid target after some initial period of operation. To support the decision-making process, a study was undertaken to evaluate the impact of implementing such a

target change out. The cost, which includes mercury decontamination, waste handling, storage, and transport activities as well as design, fabrication, installation, and startup testing for a water-cooled solid target, is still under evaluation. Although the total schedule for this activity is estimated to take more than 3 years, by beginning the design, licensing, and long lead time fabrication activities prior to beam shutdown, the total time from beam-off to beam-on can be minimized to about 23 months. A similar study considering switching from a water-cooled solid to mercury target will be conducted prior to the October decision date.

## REFERENCES


[1] J. R. Haines, et al., “Summary of Mercury Target Pitting Issue,” SNS-101060100-TR0004-R00, April 1, 2002.

[2] Workshop on the Development of High Powered Targets, Research Center, Juelich, Germany, July 12-16, 2002.

[3] E. H. Lee and L. K. Mansur, "Surveillance and Post-Mortem Examination Plan for the 1 GeV/2 MW SNS Target," SNS-101060000-TR0002-R00 and SNS-TSR-192, September 30, 1999.

# *APPENDIX A*

# *SUMMARY OF MERCURY TARGET PITTING ISSUE*

# Summary of Mercury Target Pitting Issue

**Date: April 2002**

SNS-101060100-TR0004-R00

# Summary of Mercury Target Pitting Issue

**J. R. Haines, K. Farrell, J. D. Hunn, D. C. Lousteau, L.K. Mansur,
T. J. McManamy, S. J. Pawel, and B. W. Riemer**

**April 1, 2002**

Date Published: April 2002

Prepared for the
U.S. Department of Energy
Office of Science

UT-BATTELLE, LLC
managing the
Spallation Neutron Source Activities at the
Argonne National Laboratory
Brookhaven National Laboratory
Thomas Jefferson National Accelerator Facility
Lawrence Berkeley National Laboratory
Los Alamos National Laboratory
Oak Ridge National Laboratory
under contract DE-AC05-00OR22725
for the
U.S. DEPARTMENT OF ENERGY

## Table of Contents

List of Tables

## *LIST OF FIGURES*

## *EXECUTIVE SUMMARY*

A team of researchers from the Japan Atomic Energy Research Institute (JAERI) reported in the fall of 2000 that they had discovered pitting damage on stainless steel surfaces in contact with mercury that was subjected to mechanically induced pressure pulses of the magnitude expected in short-pulse spallation targets. Because of concerns that pitting damage might also occur in the stainless steel container for the SNS mercury target, the SNS target development team conducted tests at Los Alamos National Laboratory's (LANL) Weapons Neutron Research (WNR) facility during July 2001. Cylindrically shaped, mercury-filled containers with flat end caps were irradiated with 200 pulses of 800 MeV protons at relevant beam intensities. Test results showed that, at least for the materials and target configurations tested, pitting damage occurred for beam intensities comparable to SNS operation at almost 3 MW. A cluster of large pits, visible to the naked eye, as well as smaller, more randomly distributed pits were seen in micrograph images of all four window specimens used in the July 2001 tests. Although a cluster of large pits was also found on the surface hardened (Kolsterising, a carburizing process), annealed 316SS window, dramatically fewer randomly distributed pits could be detected at the resolution used to perform the inspections (~ 5 μm), thus giving some indication that hardening reduces the degree of pitting.

The magnitude of the pressure pulse, results of off-line cavitation threshold tests, and post-test examination of damaged surfaces, lead us to conclude with a reasonably large degree of confidence that the mechanism causing the pitting damage is collapse of bubbles created as part of a mercury cavitation process. Because of this, the cavitation damage literature has been studied to help understand the phenomenon and postulate potential solutions or improvements.

Considering the July 2001 test results, it was concluded that additional testing was needed to further examine the pitting phenomenon and investigate possible solutions, or at least reductions, to the pitting problem. With this in mind, tests on an array of targets were conducted in December 2001 at the WNR facility. Four mercury targets, using different cross-sectional shapes or different window materials, were exposed to 200 beam pulses. Most notably, a target with a rectangular cross section was used in an attempt to eliminate the postulated radial focusing of the pressure wave and to represent a shape that was more prototypical of the actual SNS target shape. This target also included a double wall, forming a thin mercury layer in an attempt to simulate the window cooling geometry used in the baseline SNS target design. Post-irradiation examination of the targets irradiated in December has begun and is scheduled for completion in April 2002. The present version of this report does not incorporate results from the December 2001 tests. When results become available, they will be added.

Estimating the target lifetime using the data from the 200 pulse tests requires an enormous extrapolation, i.e., by more than a factor of one million. Assumptions regarding the nature of the pitting process that have yet to be validated are required to create this erosion lifetime estimate. Nonetheless, linear extrapolations have been performed to give some comparison of projected lifetimes to design goals. These estimates illustrate that the large cluster of pits near the center of the beam interaction region must be eliminated to achieve an adequate target lifetime. If the large pits are eliminated by geometric or other considerations (not fully demonstrated yet), bare 316SS should be adequate for the planned first six months of low power operation with no target replacement. In addition, if we can find a target container material that has an erosion resistance comparable to that of the Kolsterised surface (limited to 33 μm thickness) with an erosion

thickness greater than 500 μm, then lifetimes approaching 1/3 of the goal of 1250 hours at 2 MW operation may be possible. This would give us adequate target lifetime for the first several years of operation, when power levels are being slowly increased. This initial operating period could be used to further understand the problem and examine methods to extend the erosion lifetime. It should be noted that there is risk associated with this approach, that is, if an adequate mercury target lifetime is not ultimately achieved, changing from a mercury target to a water-cooled solid target would require considerable downtime (roughly estimated to be 2 years) for the SNS facility.

Finally, the direct relevance of the off-line and in-beam tests conducted so far is somewhat questionable since many of the variables that could be important for pitting damage cannot be accurately simulated in these tests. Several examples of the discrepancies between tests and the actual SNS conditions include:

- Interactions between subsequent beam pulses could be important if the residence time of cavitation bubbles is comparable to or longer than the 17 ms between pulses in SNS (corresponds to 60 Hz repetition rate),
- Flowing of the mercury may alter the contact condition between the mercury and stainless steel and thereby change the way in which bubbles form and collapse,
- The shapes of targets used in tests have been either different or rather great simplifications of the SNS target shape and do not include the long open-ended Hg supply and return lines, and
- Both off-line and in-beam tests have been limited to a small number of pulses (≤ 200) compared to the baseline target lifetime (based on radiation damage) of $2.7 \times 10^8$ pulses.

Given the uncertainty in erosion lifetime, it is concluded that more in-beam tests should be performed to examine whether the proposed ideas for target shape and materials can be shown to extrapolate to reasonable lifetimes (say $10^8$ pulses, which is equivalent to almost 3 weeks of operation at 60 Hz, for example) at SNS relevant power levels (≥ 1 MW). Tests scheduled for May and June 2002 will examine alternate materials, coatings, target shapes, and power levels, but additional tests may be required. Also, exploring ideas for developing an off-line pitting test apparatus capable of going to a high number of cycles should be pursued since such an apparatus could greatly reduce the uncertainty associated with extrapolating from the 200 in-beam test cycles to the SNS lifetime of $2.7 \times 10^8$ cycles. Finally, developing Hg target design concepts, diagnostics, and post-irradiation examination procedures that emphasize the experimental nature of early SNS operations should be pursued.

## 1.0 PURPOSE

The purpose of this paper is to summarize relevant information on the so-called pitting issue for the mercury target. With this goal in mind, results of in-beam as well as off-line experiments and computer model predictions are reviewed along with a summary of information from related technical literature. Plans for completion of tests in FY 2002, potential implications of this issue on target design and implementation, and speculation on the most likely physical mechanisms that could explain this phenomenon are also summarized.

## 2.0 BACKGROUND/INTRODUCTION

One of the most important issues associated with using liquid metals as targets for pulsed proton beams is withstanding the loads caused by the rapid pressure increase resulting from the intense heating of the liquid metal from a single pulse of protons. This heating occurs essentially instantaneously compared to acoustic wave time scales; therefore, the mercury undergoes a large pressure increase. Most of the previous SNS R&D program efforts on this issue had focused on studying the effects that these pressure spikes have on the structural integrity of the mercury target container. For example, in-beam tests with mercury targets conducted prior to 2001 concentrated on measuring the vessel strain using an array of target shapes, diagnostics, and instruments.

During 2000, a team of researchers at the Japan Atomic Energy Research Institute (JAERI) observed pitting of stainless steel surfaces that were in contact with mercury subjected to large mechanically induced pressure pulses of the same magnitude as those expected for full power (2 MW) pulses in SNS. The question then became; “Do the inner surfaces of liquid mercury target containers with comparable beam-induced pressure pulses also pit?” Post-irradiation examinations of targets previously used in pulsed proton beam tests at LANL’s WNR facility were unable to resolve this question because no pre-test inspections had been performed and the roughness of the surfaces was too great to distinguish between beam-induced pits and other imperfections in the surface of the materials.

Because of the urgency associated with completing the SNS target design, two test campaigns were conducted in 2001 to study the pitting issue; the first in July and the second in

December. Large pits, visible to the naked eye, were found near the center of all four diaphragms tested in July 2001. Microscopy revealed that small, randomly distributed pits were also present on the diaphragms, although there were dramatically fewer of these small pits on the diaphragm that had been treated with a surface hardening process. The December 2001 tests were dedicated to further examining the pitting phenomenon and looking at an array of possible solutions, or at least reductions, to the pitting problem. Post-irradiation examination of the targets irradiated in December will be completed in April 2002.

## 3.0 SUMMARY OF EXPERIMENTAL RESULTS

### 3.1 WNR Tests

#### 3.1.1 Test description

Two test campaigns were conducted at the LANSCE – WNR during 2001 to investigate cavitation damage in mercury spallation targets. Target components from the first of these (tests have been thoroughly examined, while examinations from the second are currently in progress.

The WNR beam parameters are summarized in **Error! Reference source not found.**. Although total energy per pulse is substantially lower than the SNS target, by tailoring the beam size, maximum energy density in test targets is comparable to that in SNS. Using a test target size that is roughly ½ scale of SNS, the proportion of the beam cross-sectional area to the target cross-sectional area is also comparable.

Two targets were tested in the July campaign. Both of these were the so-called "Large Effects" (LE) type, which is a simple cylindrical shape with a 100 mm diameter (4 inch) and 286 mm (11.4 inch) overall length. The end flanges are flat and have been thinned (~ 1 mm thick) to produce large strains in response to the pressure pulse. Note that the SNS target minimum thickness is 1.25 mm. A sketch of the target geometry on its support stand is shown in Fig. 1.

Table 4. WNR Beam Parameters for Cavitation Damage Tests

| | SNS (@ 2 MW) | WNR |
|---|---|---|
| Proton Energy [GeV] | 1 | 0.8 |
| Protons per pulse | $2 \times 10^{14}$ | $2.8 \times 10^{13}$ |
| Beam size [mm] | Elliptic, ~ 70x200 | Circular, $\sigma \sim 10$ |
| Energy deposited in mercury target [kJ] | 20 | 2.2 |
| Maximum energy deposition density [$MJ/m^3$] | 13 | 19 |

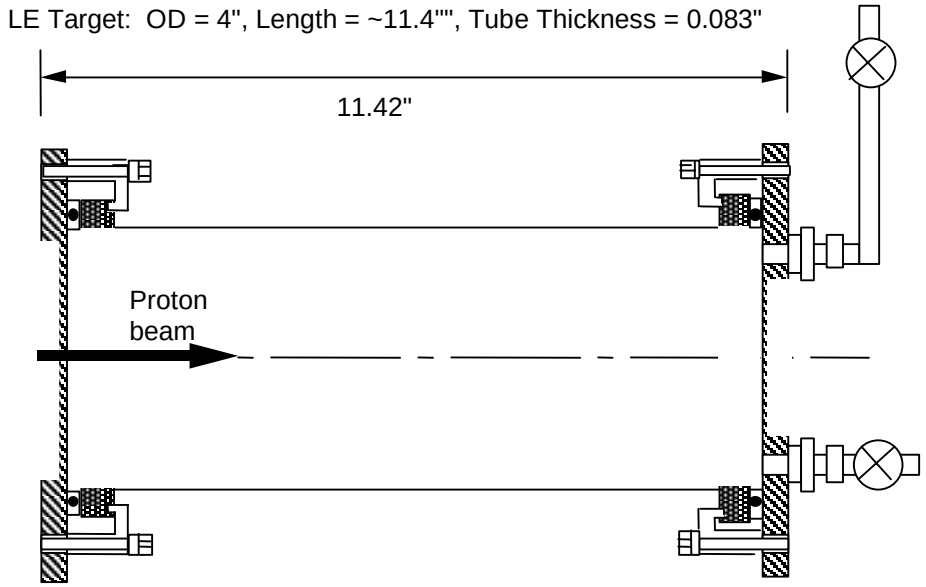


Fig. 1. LE Target Geometry

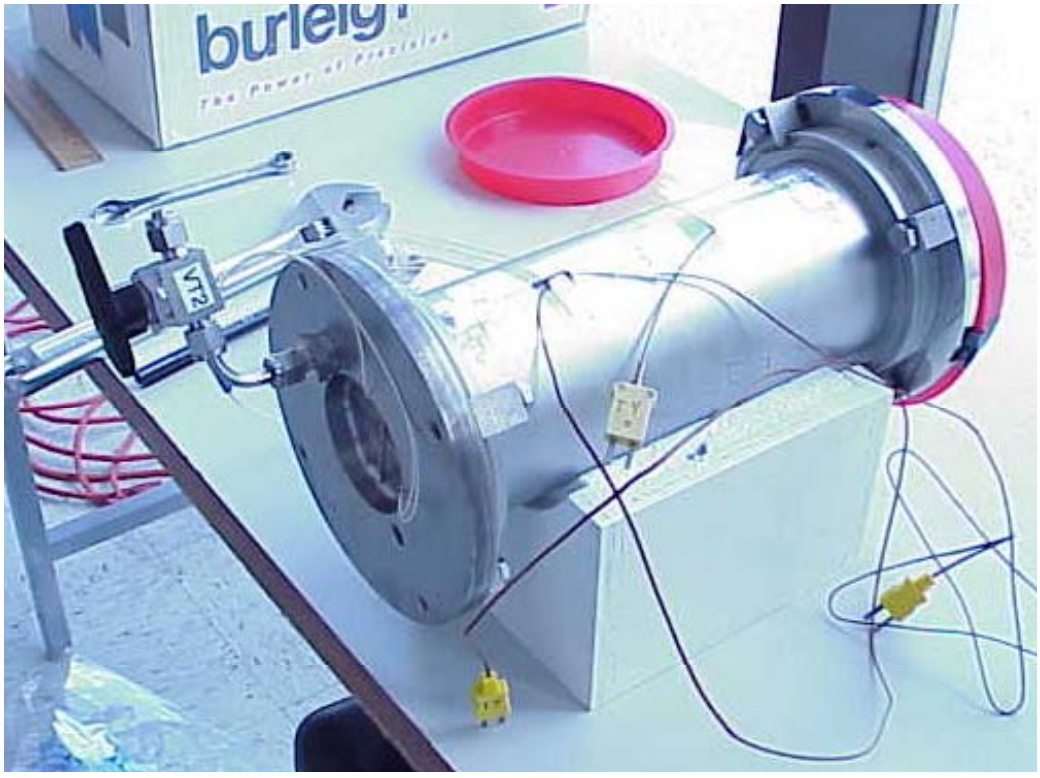


Fig. 2. LE4 Target Before Test

The first of the targets (LE3) used flanges made of 316LN stainless steel. This is the same material to be used in the SNS target; the flanges were also annealed to approximate regions of the target affected by welding that lose cold working. Likewise, the second target (LE4) used annealed 316 LN, but the front flange (up beam) was treated after annealing with a surface hardening process called "Kolsterising," a proprietary low temperature carburizing process. This process increased surface hardness up to 1100 Hv over a depth of roughly 30 μm. Note that the annealed surface hardness was approximately 140 Hv. The only other difference for LE4 was the inclusion of an array of small disk specimens of various materials (10-mm diameter) around the cylinder wall. No pitting was found on any of the specimens, so no further discussion of these specimens is provided in this report. A picture of the LE4 target during pre-test preparation is shown in Fig. 2.

During testing, targets were set in secondary container boxes and positioned to align the axis of the target with the beam. The technique used has limited precision; errors of a few mm are possible. The average location of the beam was determined after testing using activation surveys with a collimating instrument.

In addition to measuring strain on the thinned regions of the flange (membranes), thermocouples monitored the target temperature. Beam pulses were repeated at a maximum rate of one per minute over several sessions until 200 total pulses were achieved. Maximum target temperature was less than 50°C.

### 3.1.2 Photographs of large pits

After irradiation, the targets were stored at the WNR for about one-month for activation to subside. At that time, the mercury was carefully drained from the targets and they were shipped back to ORNL. Disassembly and decontamination work was conducted in a laboratory at ORNL.

It was immediately apparent that there was damage on all flanges. Clusters of pits near the geometric centers were seen unaided, the clusters ranging from a few to nearly 10 mm in size. Images of the front and rear flanges of LE3 are shown in Fig. 3 and Fig. 4. Scribed "X" marks can be seen at the geometric center; the pit clusters were located a few mm from the centers in all cases. The size of these clusters was larger on front flanges, but the size proportion front to rear did not scale with beam intensity. The beam was nearly stopped in these targets and its intensity at the rear was considerably less than 10% compared to the front.

Activation surveys were conducted on the flanges to locate the (average) beam centers relative to the geometric centers and pit clusters. Fig. 5 shows the result for the front flange of LE3. It can be seen that the while the beam was directly above the geometric center, the high damage region was below by twice the distance. This was true for the LE4 front flange as well. This observation has sprouted theories that the axisymmetric target geometry used for these tests unfortunately focuses reflections off the cylindrical walls leading to intense rarefaction near the axis, and hence more aggressive cavitation. Such theories remain unverified.

Fig. 3. Front Flange of LE3

Fig. 4. Rear Flange of LE3

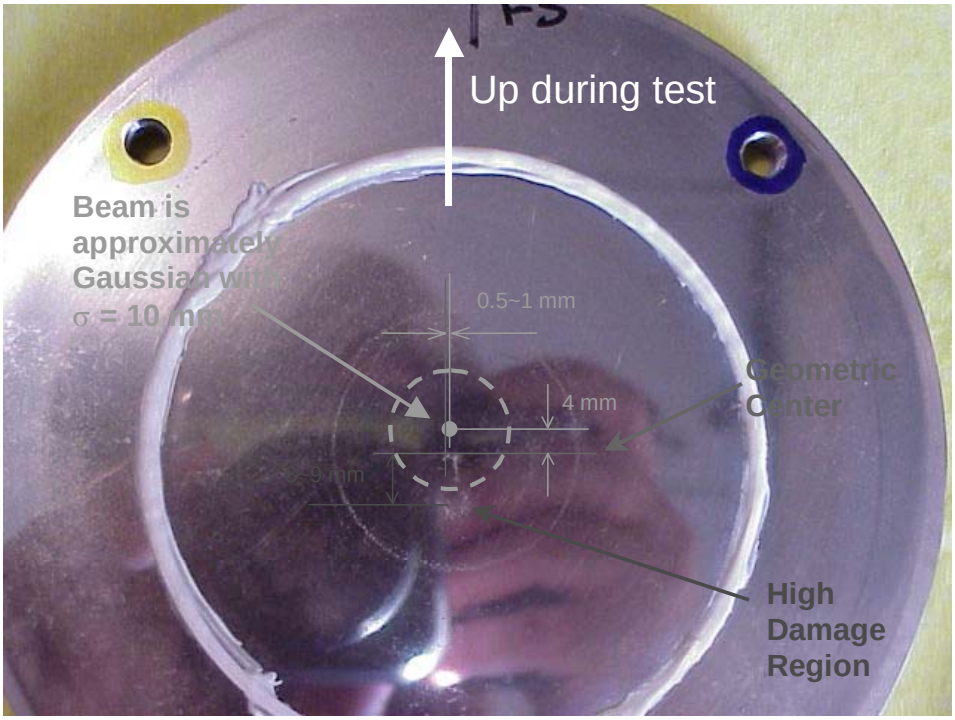


Fig. 5. Average Beam Center on LE3 Front Flange

### 3.1.3 Detailed Examination

Scanning electron microscopy (SEM), optical microscopy, and laser profilometry have all been used to conduct detailed examination of the flange surfaces before and after irradiation. Flanges were machined flat and highly polished to assist in the identification of any features larger than a few microns that may have been introduced by the test. Flanges were then annealed to remove work hardening introduced by the machining and polishing. The annealing also resulted in a visible grain structure on the polished face, which aided in verification of the position on the flange during microscopy. Polishing was difficult due to the large diameter of the flange, so some areas were not as well polished as others; effort was made, however, to achieve a good polish in the center of the flange, where the microscopic analysis was concentrated. Even with careful polishing, some 1-10 μm size features were still evident due to voids or defects in the material, polishing defects, inclusions, etc. For this reason, careful pre-examination was performed by SEM so that any features identified after the irradiation could be verified not to be a pre-existing condition. In order to balance between resolution and areal coverage, a magnification of 105x was chosen for the pre-inspection imaging. With the digital capture resolution available on our SEM, this magnification allowed for the clear identification of surface features larger than 5 μm in diameter. One hundred images were obtained of each flange, moving out 25 mm in four directions from a scribed X in the center of the flange. The total area covered in the pre-inspection consisted of two perpendicular bands 1 mm wide and 50 mm long, centered on each flange.

Fig. 6 shows part of the area of heavy damage on the rear flange of LE3, previously shown in Fig. 4. The arrow identifies the same recognizable grain on the before and after images. Pits in this area were up to 200 μm in diameter. Laser profilometry showed some of these pits to be up to 100 μm deep. Pits typically appeared as roughly hemispherical depressions in the surface, with or without craters due to dislodged material. Fig. 7 shows a cluster of large pits in the heavily damaged region on the front flange of LE3, previously shown in Fig. 3. Shadowing of the electrons collected by the secondary electron detector, which sits at about a 45-degree angle to the surface, produces the light/dark shading that makes the pit topography obvious. The dark spots are relatively deep, sharp walled craters out of which few, if any, secondary electrons reach the detector. Fig. 8 shows some of the pits at higher magnification. The parallel striations within

each single crystal grain are “slip plane” ridges formed by adjacent planes of atoms sliding over one another through the movement of dislocations, evidence that mechanical deformation had occurred. Fig. 9 shows another such pit with an irregular crater at the bottom of the depression.

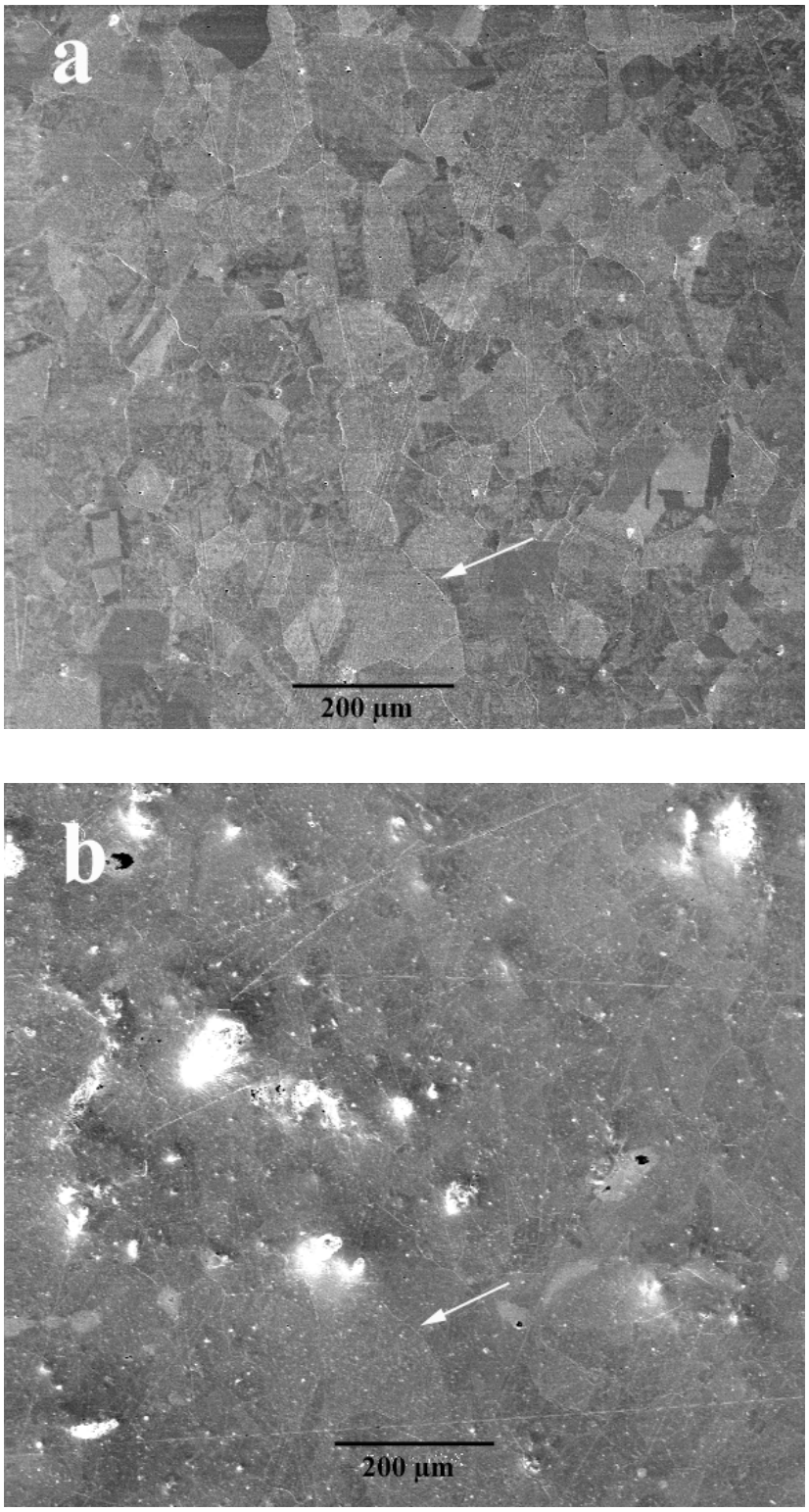


Fig. 6. LE3 rear flange, heavily damaged region (a) before and (b) after irradiation. Arrow identifies the same grain in each image.

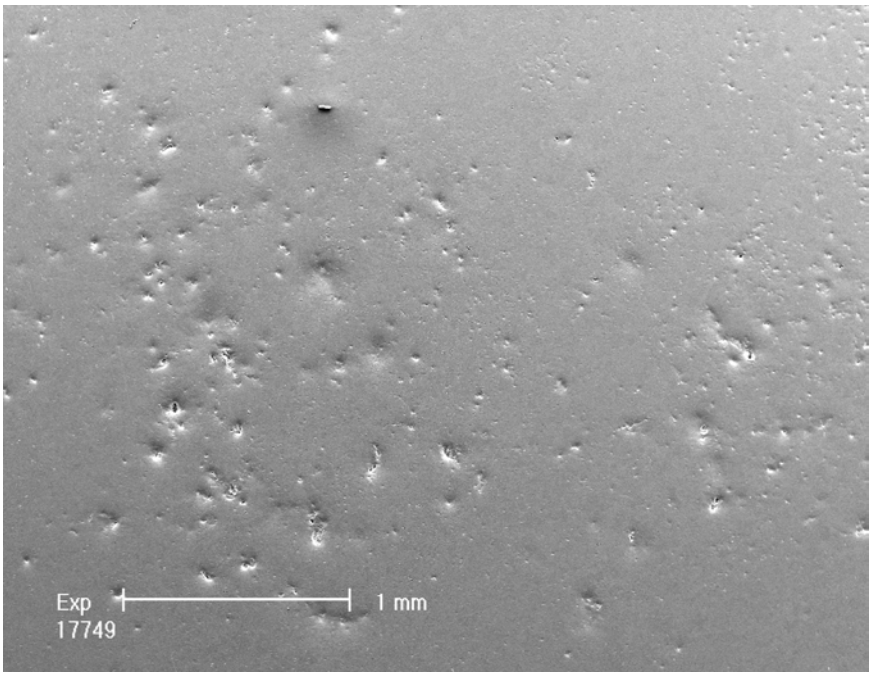


Fig. 7. LE3 front flange, heavily damaged region.

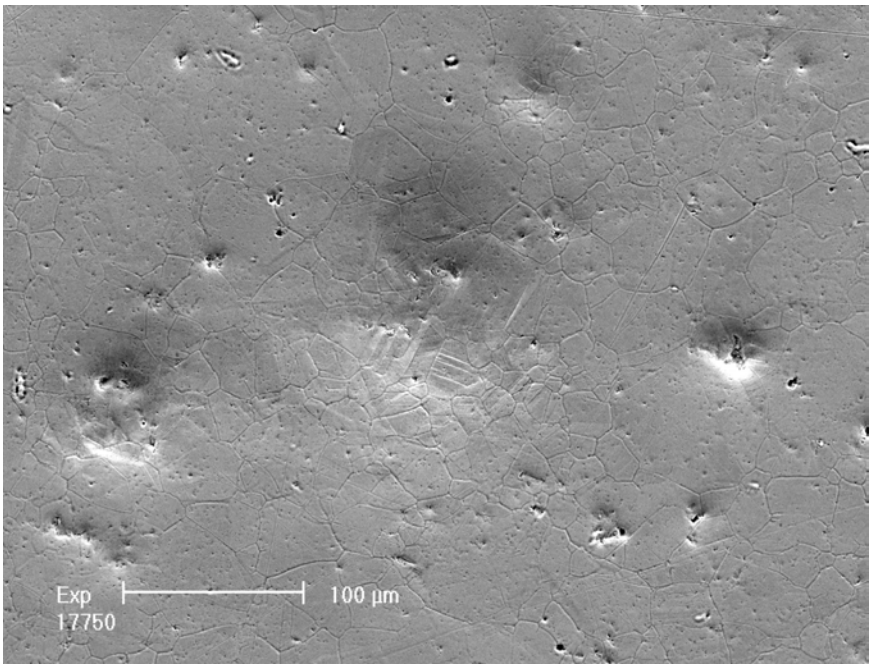


Fig. 8. LE3 front flange, heavily damaged region, slip lines in a large depression.

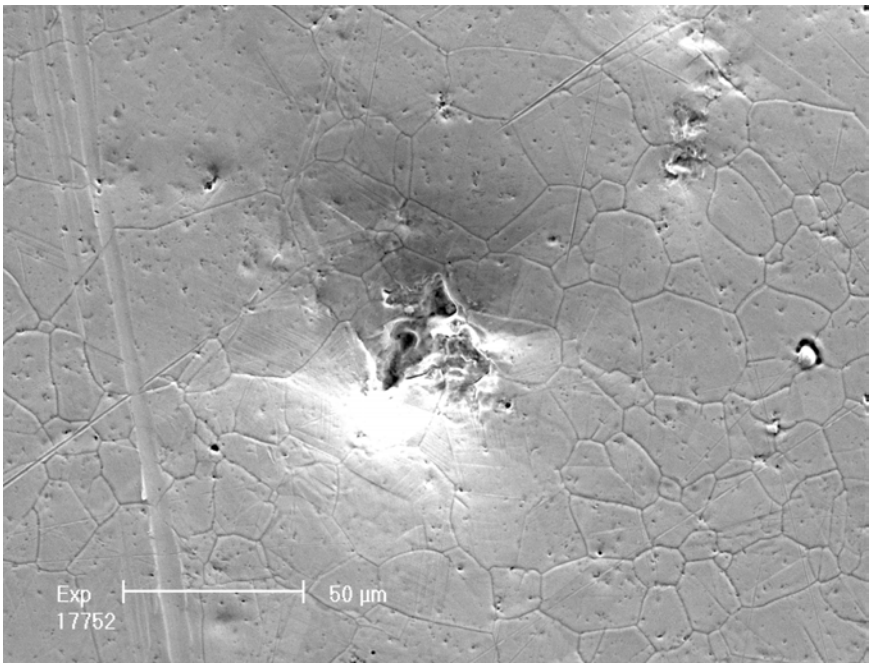


Fig. 9. LE3 front flange, heavily damaged region, crater at the bottom of a pit.

Fig. 10 shows the heavily damaged area from the two rear flanges. The flange from LE4 was not as heavily damaged as its counterpart due to a Kolsterising surface treatment that essentially increases the surface hardness by about a factor of 10. Qualitatively, the pits were the same on the Kolsterised flange, but they appeared smaller and at a lower density. Fig. 11 shows a crater at the bottom of a pit in the Kolsterised flange. Craters like these tended to show strata on the sidewalls. This can also be seen in Fig. 12, which looks down into a large crater in the front flange of LE4.

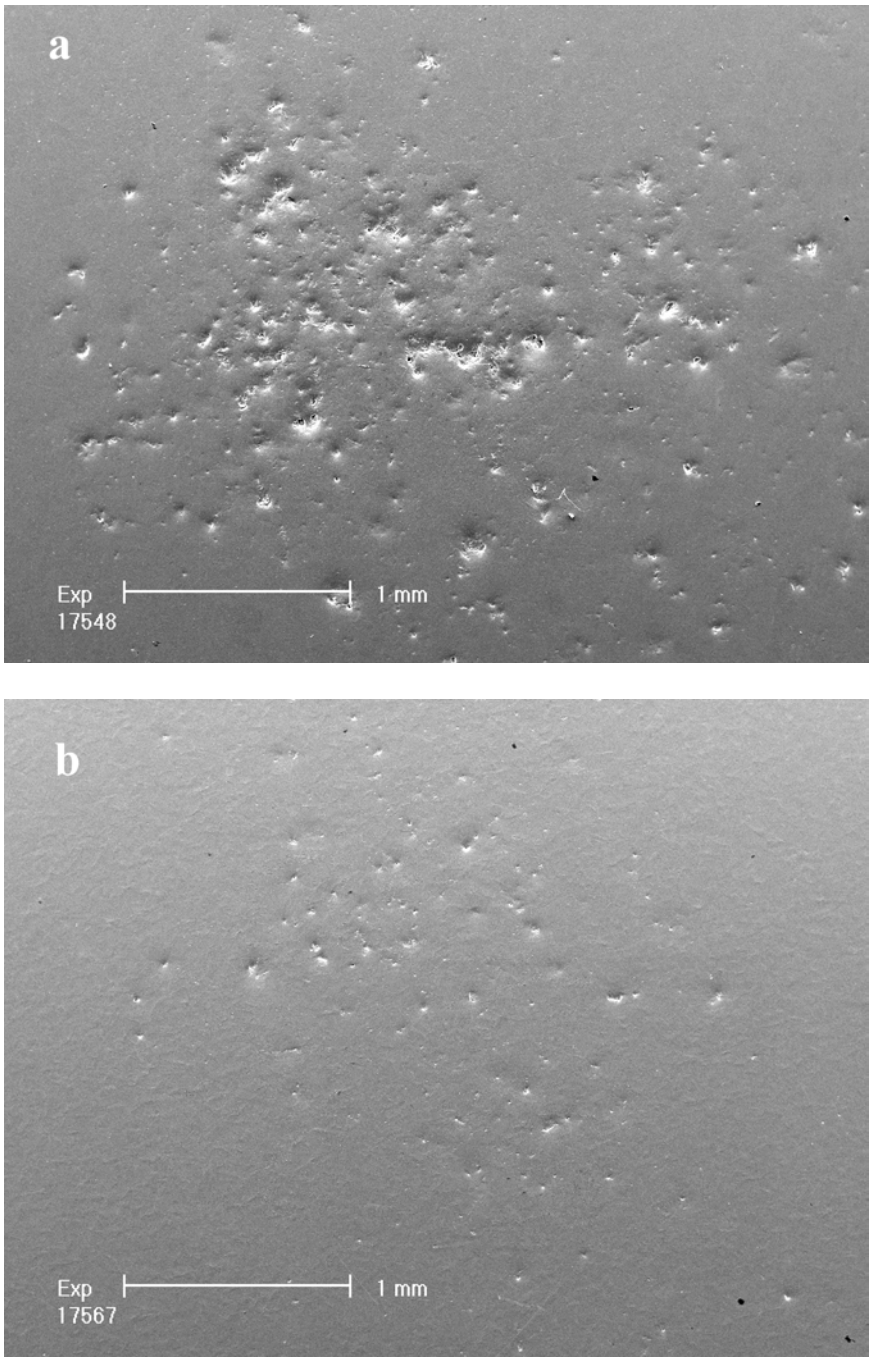


Fig. 10. (a) LE3 rear flange and (b) LE4 rear Kolsterised flange, heavily damaged region.

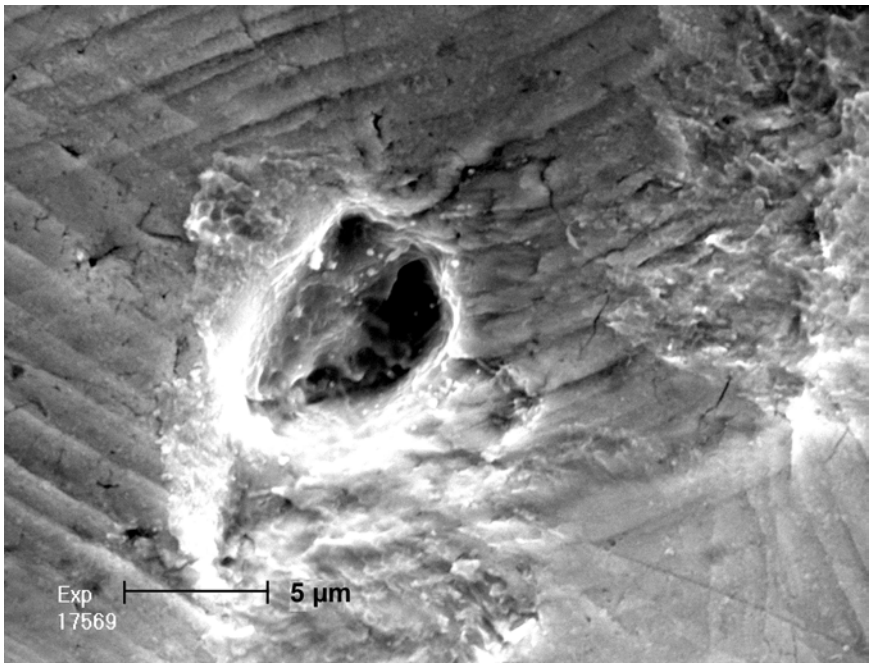


Fig. 11. LE4 rear Kolsterised flange, heavily damaged region, crater.

In addition to the large pits that were obvious upon initial inspection with the naked eye, other smaller 5-20 µm pits were found scattered over the entire surface of the flanges. Fig. 13 shows the center of the front flange from LE3. The surface is pockmarked with small pits that were not there before irradiation. Sometimes these small pits appeared in high-density clusters as in Fig. 14, which shows an area immediately to the right of Fig. 13. The small pits were qualitatively the same as the large pits observed in the heavily damaged region. Fig. 15 shows a crater at the bottom of a small, isolated pit on the front flange of LE4.

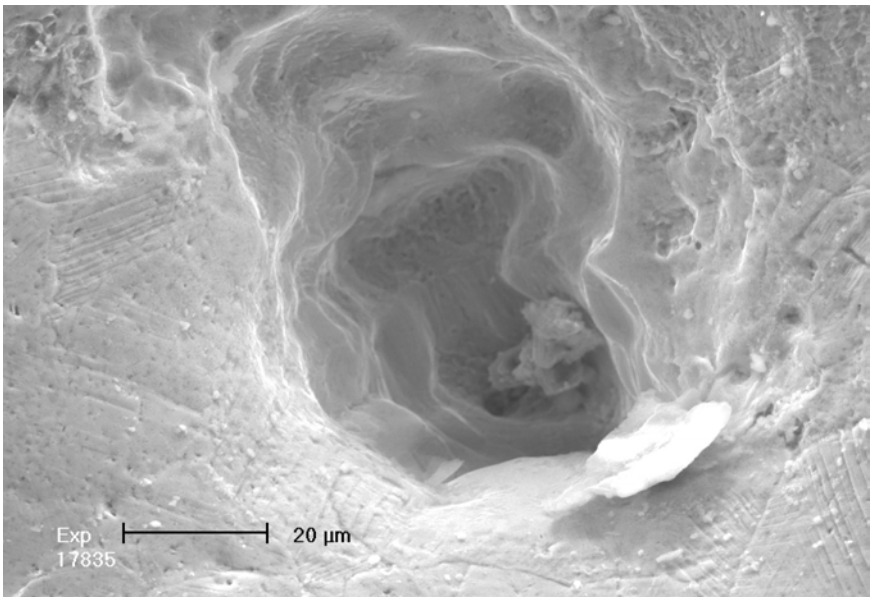


Fig. 12. LE4 front flange, heavily damaged region, crater.

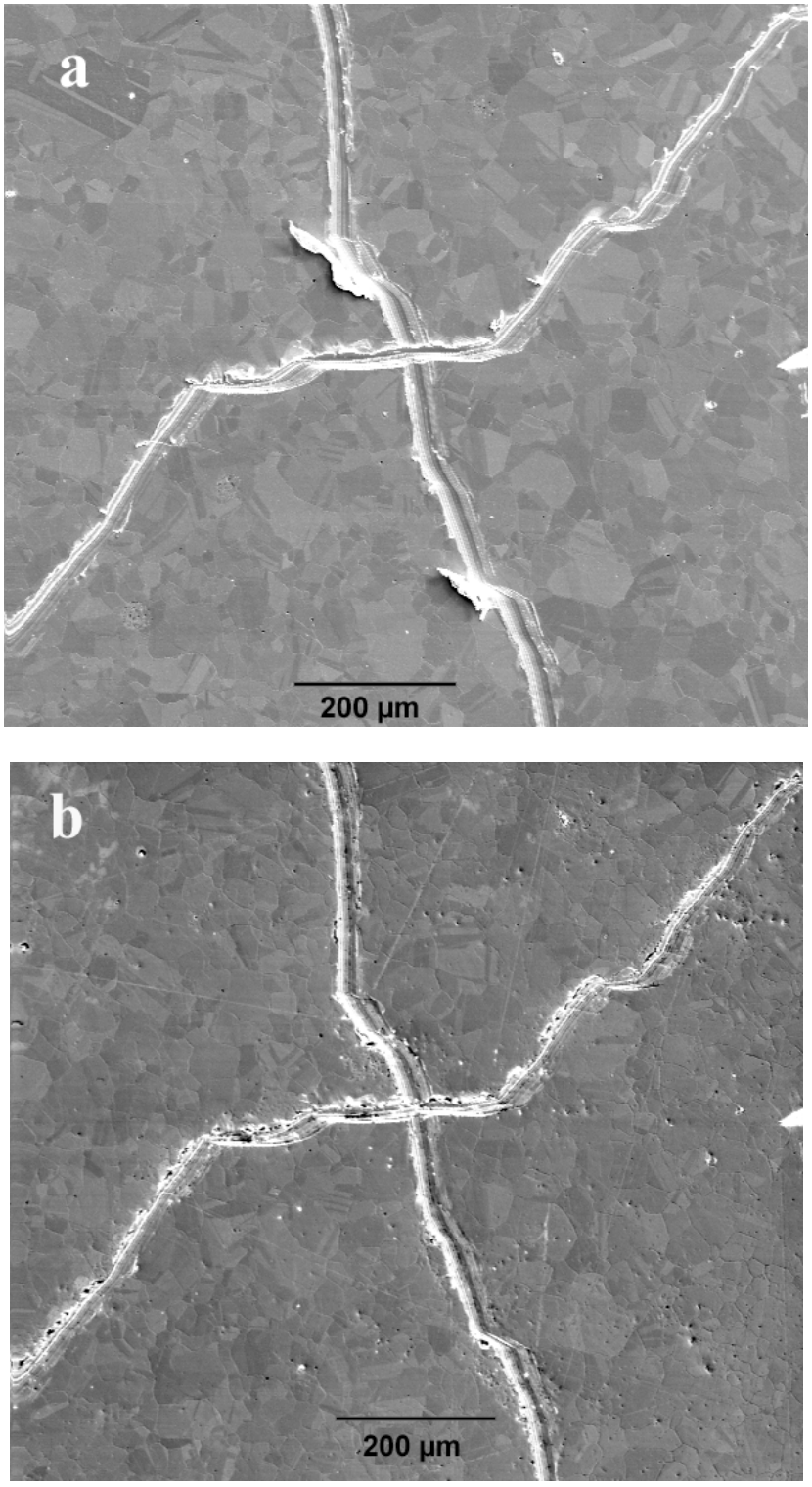


Fig. 13. Center of LE3 front flange, (a) before and (b) after irradiation.

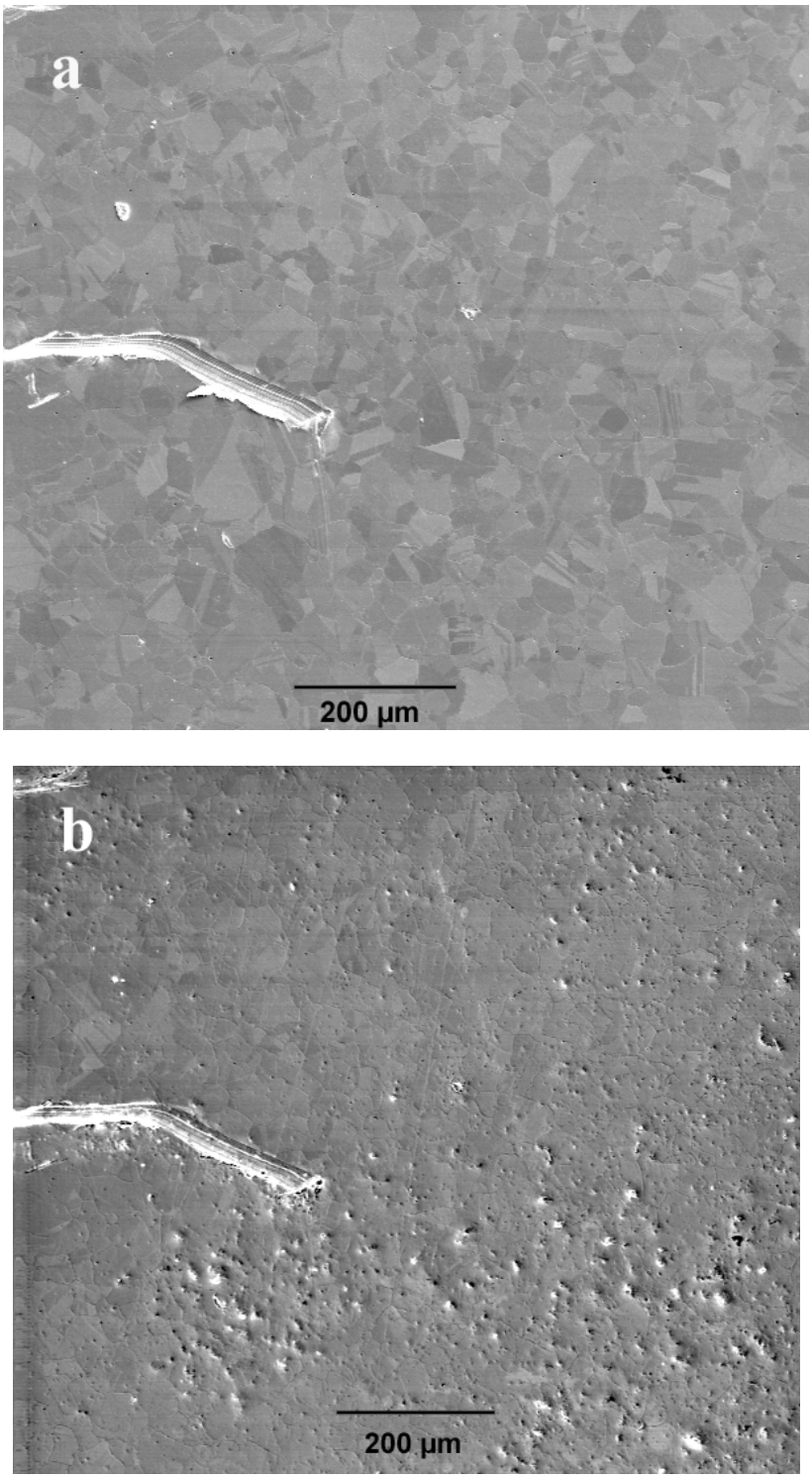


Fig. 14. Just off center of LE3 front flange, (a) before and (b) after irradiation.

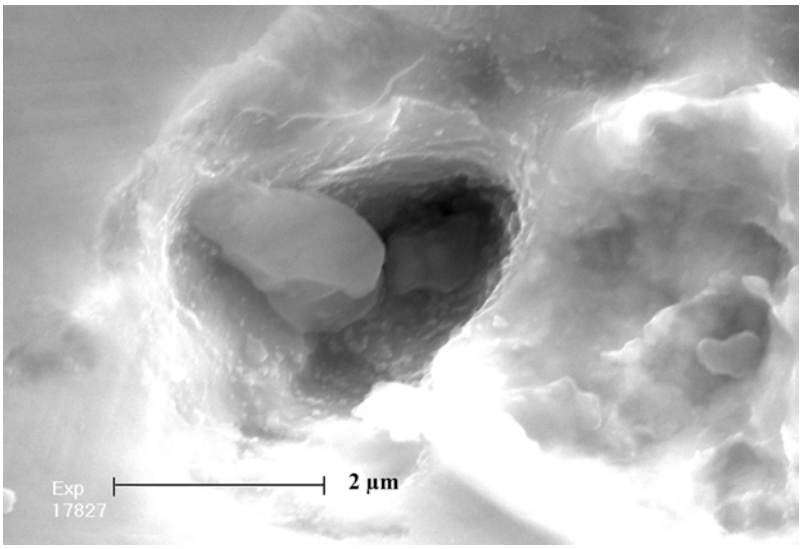


Fig. 15. LE4 front flange, crater in small isolated pit.

Small pits were not as obvious on the Kolsterised surface because there were more than a factor of ten fewer of them (none in clusters), and partly due to the fact that the Kolsterising treatment roughened the polished surface making inspection more difficult. Fig. 16 shows a small, isolated pit on the Kolsterised flange.

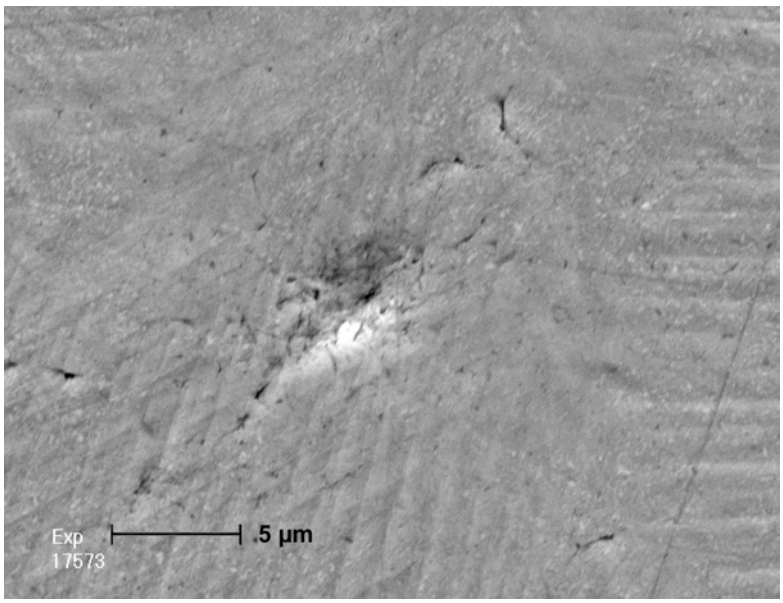


Fig. 16. LE4 rear Kolsterised flange, small isolated pit.

### 3.1.4 Limitations/shortcomings of WNR tests

- The total number of pulses on WNR test targets has been limited to 200. This is six orders of magnitude lower than the recommended SNS dpa limited lifetime. Significantly more test pulses are not feasible because of facility constraints and difficulties handling higher activation levels. Extrapolating the test results to the SNS dpa lifetime is highly uncertain.
- WNR test targets incur no significant radiation damage effects compared to SNS.
- The WNR pulse repetition rate is limited to 0.03 Hz (2 per minute) vs. 60 Hz for SNS.
- WNR test targets are closed volumes without mercury flow. Including flow may be possible but at considerable increase in test complexity and cost. WNR target geometries for cavitation tests are not prototypic of SNS.
- Polished surfaces were used, in lieu of prototypical surface finishes, to facilitate pre- and post-test examinations.
- Flat surfaces were used in lieu of prototypical shapes to facilitate inspection.
- WNR beam size and total energy are smaller than SNS.
- Each test campaign requires approximately 6 months and $0.5M to prepare, perform, and evaluate test specimens**.**

## 3.2 Related tests

### 3.2.1 Mercury Cavitation Threshold Tests

During exposure to short proton beam pulses, mercury will undergo a rapid pressure increase. As the mercury expands, the compression wave eventually reflects as a rarefaction wave from the interface between the walls of its container and the surrounding gas environment (air in our experiments or He in SNS). If low enough pressures are reached in this process, the liquid mercury can break apart (i.e., form cavitation bubbles). It is well known that cavitation bubble collapse can eventually cause severe damage to surfaces. Therefore, it was important to establish whether mercury would cavitate at the pressure levels anticipated for the SNS target, that is, approximately ± 40 MPa. It was also hoped that the presence of cavitation bubbles might act as scattering centers or increase the compressibility of the liquid and bubble mixture, thereby helping to mitigate the stresses in the container wall, but as discussed in the section on WNR testing, no such reduction has been measured. **The tests described below established that**

**cavitation is very likely, if not certain, to occur early in the rarefaction portion of the process following exposure of a mercury target to an intense proton beam**.

Previous research has shown that for extremely high purity, and degassed mercury, the cavitation threshold is a tensile pressure of several hundred atmospheres, but is much lower for mercury that is exposed to gasses and/or has even extremely small amounts of impurities. To study this phenomenon under more realistic conditions, two types of cavitation threshold experiments were conducted. The first experiments were conducted with an apparatus that measured the cavitation threshold under steady conditions, while the second established the threshold for pressures applied in a transient fashion (25 kHz).

The steady state cavitation experiments used a simple spinner apparatus, shown schematically in Fig. 17, that exerted a tensile load on the central region of mercury filled glass tube rotating at high-speed [1] and [2]. By slowly increasing the rotational speed, the value at which the mercury separates can be determined. As shown in Fig. 18, resulting thresholds range from tensile pressures of about 0.2 to 0.5 MPa, depending to some degree on surface treatment. The threshold was relatively insensitive to temperature for the range examined in these tests (up to 250 ºC). It is believed that cavitation at such small tensile pressure levels was gaseous type cavitation, which resulted from release of previously dissolved gasses, as opposed to vaporization of mercury itself.

The transient tests were conducted in a glass sphere with pressures applied through a piezoelectric transducer at the resonant frequency for the chamber of about 25 kHz (Ref. 2). The cavitation threshold was established based on the onset of large, high frequency fluctuations in the pressure signal measured with a piezoelectric disk microphone that was attached to the outside of the sphere. Results of these tests are shown in Fig. 19 for helium or air cover gas pressures up to 0.3 MPa. Treated surface implies that the glass sphere was heated prior to the tests to drive off as much of the interfacial gases as possible. Cavitation occurred in these transient tests at pressures that were about 0.15 to 0.2 MPa below the cover gas pressure. Surface treatment appears to have only a minor impact.

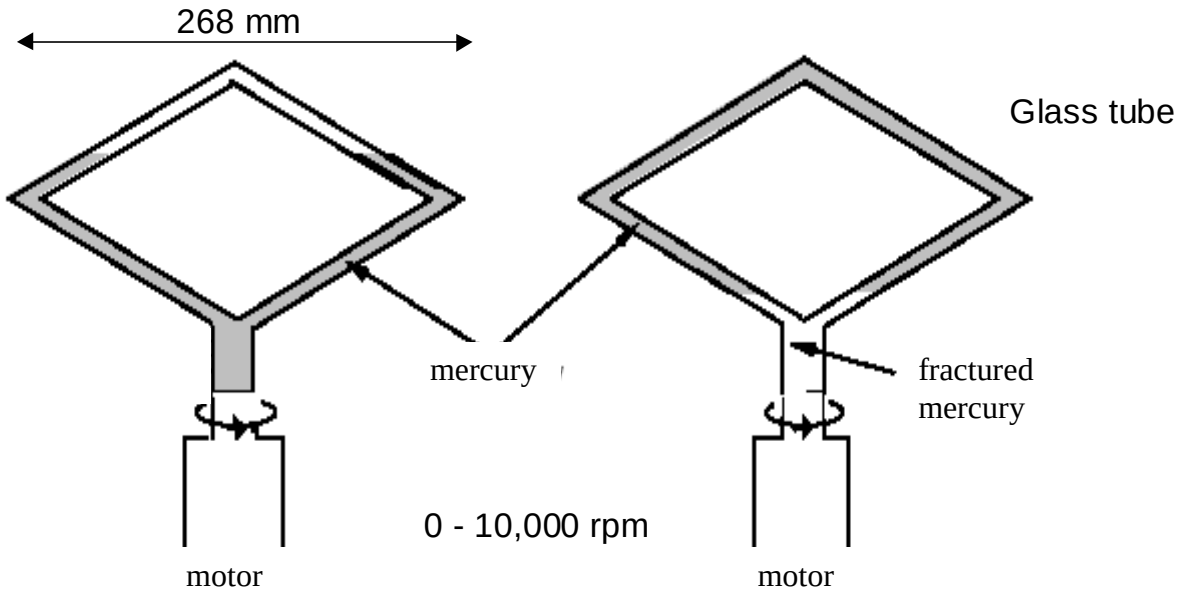


Fig. 17. Schematic of apparatus used to measure the static threshold for mercury cavitation.

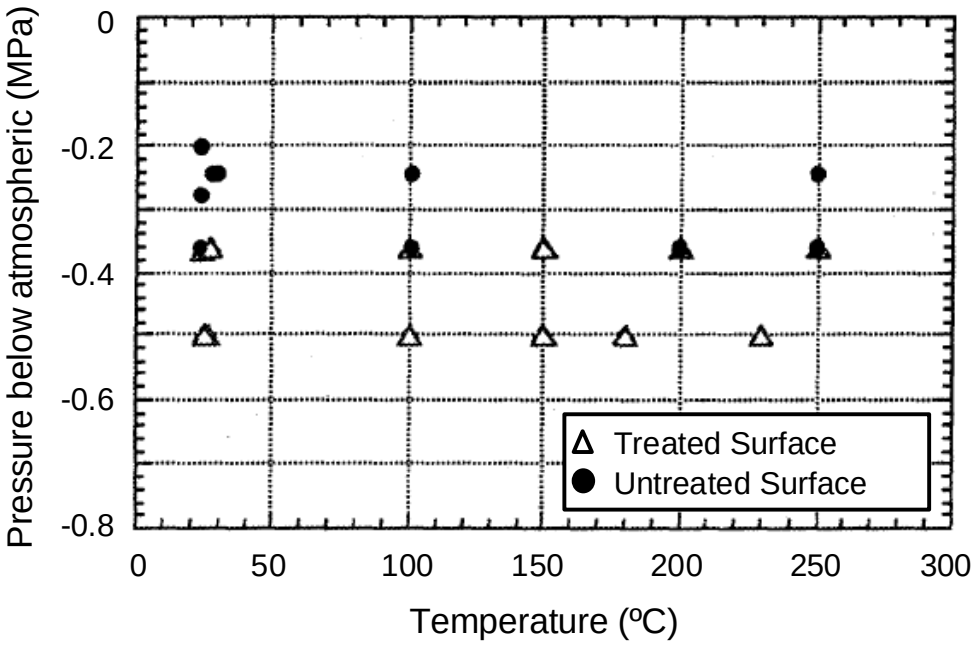


Fig. 18. Static cavitation threshold for mercury.

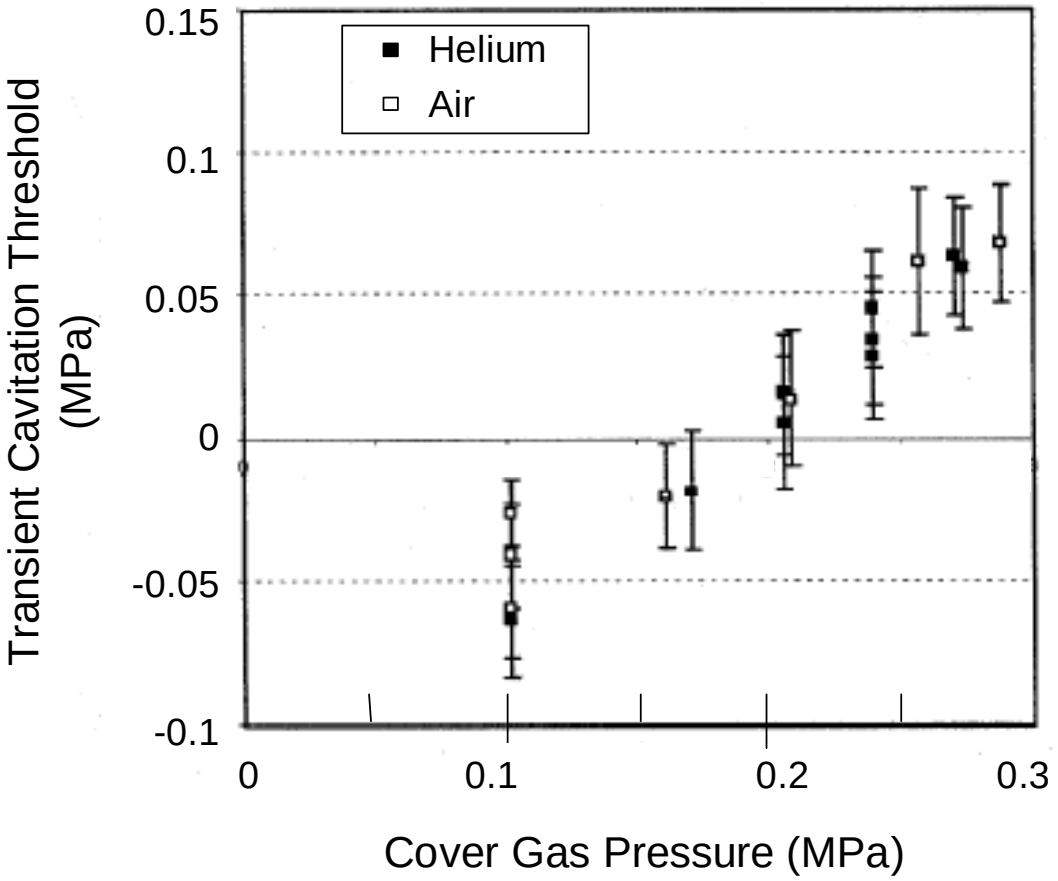


Fig. 19. Cavitation threshold for 25 kHz pressure fluctuation.

### 3.2.2 Split-Hopkinson Pressure Bar (SPHB)

At the 2nd International Workshop on Mercury Target and Cold Moderator Engineering, held in Tokai, Japan in November 2000, JAERI/KEK researchers presented their discovery of cavitation pitting damage inside the test cavity of their Split Hopkinson Pressure Bar apparatus (SHPB). This mechanical device is normally used to determine material properties under impact conditions; the JAERI team had adapted it for measuring the wave speed of mercury. The impact pressures reached in the test cavity during test were comparable to those created with each proton pulse in the SNS target. This discovery was the motivation for conducting cavitation damage tests for a mercury spallation target.

The JAERI team has conducted a number of tests with the SHPB to investigate cavitation damage. Tested materials included A6061-T6 aluminum (129 Hv), SS316L (not annealed, 211 Hv), Inconel 600 (215 Hv) and Maraging steel (310 Hv). Two impact levels have been used corresponding to cavity pressures of 40 and 80 MPa. Key findings from the SHPB tests are:

- Pits are created with only one impact on SS316L for either pressure.
- The number of pits increases (or eroded area increases) with increasing impacts.
- The number of pits increases with higher impact pressure.
- The maximum number of impacts on a set of cavity specimens has been 100.
- The degree of damage of the materials ranks inversely with the material hardness: A6061 > SS316L >Inconel > Maraging steel.

The JAERI team also tested SS316 (not annealed) with Kolsterising surface treatment, at the request of SNS Target Systems. Their test was limited to the case of 80 MPa and 10 impacts, but the result was no clearly observable pits. The same difficulty of inspecting a rough surface was encountered as with the Kolsterised WNR target flange.

Limitation of SHPB tests

- The SHPB test applies pressure to the mercury through a solid material interface. This is in contrast to a spallation target where pressure is generated internally in the mercury via volumetric energy deposition.
- The SHPB test cycle takes considerable time due to alignment checks and other preparations needed for every impact. The apparatus cannot practically be used for more than a few hundred pulses per test specimen, i.e., the number of impacts prototypic of the SNS target are not possible.
- The SHPB is a JAERI apparatus. There are limits to the resources they can provide for future testing for our benefit.
- Only small, flat, and highly polished specimens can be used.

### 3.2.3 Liquid metal target experience at CERN

The CERN–ISOLDE facility produces radioactive ion beams with liquid metal targets. The facility can produce pulses with $3 \times 10^{13}$ protons within 2.4 microseconds. Their initial report of shock type damage is given below for tantalum targets with molten lead:

ISOLDE NEWSLETTER

July 1994

“In the last tests of the molten metal targets the splashing from the surface the metal following the shock wave induced by the proton beam pulse could efficiently be damped and kept out of the ion source by means of a chimney equipped with baffles. This allowed to operate the targets somewhat longer. Unfortunately this only lead to the discovery of a new deleterious effect of the shock wave, which causes the targets to fail. In fact a cavitation like effect which both corrodes and stresses the beam entrance wall of the target container and causes welds to break so that the charge of molten metal is lost through leaks. During the shut down autopsies in the hot cell on a number of failed targets allowed us to document the damage caused by this effect. ….”

The following was documented in 1995 in a paper presented at ICANS XIII:

Target designs were improved by increasing the wall thickness, changing the weld design from TIG to e-beam with the weld located away from the beam and protecting the window with a pyrocarbon disk.

Recently tests have been conducted at CERN and at Brookhaven National Laboratory with mercury in pulsed proton beams, in support of the Muon Collider and Neutrino Factory design development. Tests with mercury in a cup with a free surface confirm high initial pressures by measurement of high surface velocities on the order of 10’s of meters per second.

## 4.0 COMPARISON OF STRAIN PREDICTIONS WITH MEASUREMENTS

This topic is not directly related to the cavitation damage issue, but it is an outstanding problem for the mercury target design. An incomplete physical understanding of the cavitation process during a beam pulse has made structural modeling of the mercury – vessel system, including pressure wave propagation with cavitation effects, a difficult analysis to perform. A hoped for empirical model based on experimental results has not been obtained.

Efforts to simulate the mechanical response of mercury target vessels have been underway for several years. Pressure waves induced by the rapidly deposited energy from each proton pulse propagate through the mercury and interact with the vessel leading to a complex dynamic stress response. The simulations would provide the basis for estimating the fatigue life of the SNS target vessel. While early attempts using simplified target geometry suggested the approach could estimate these dynamic stresses, it was clear that experimental results were vital to calibrate the simulations and gain confidence in the approach The first credible strain measurements made on mercury targets with beam intensities similar to the SNS were performed in August 2000 tests at the WNR facility [3].

Confidence in the simulation approach has not been achieved. Although the predicted response of a graphite target shows excellent agreement with measurements, attempts at simulating mercury test target response have yet to provide a good match to measured strains. The main difficulties are the lack of adequate descriptions of mercury's behavior (bulk modulus, or wave speed) over the expected range of pressures (positive and negative), and of the interaction between the mercury and vessel (i.e., the contact behavior).

Using the nominal wave speed of mercury (about 1460 m/s) in simulations with interface behavior that supports both tension and compression typically gives strain response frequencies that are higher than those measured in experiments. Sometimes the earliest part of a response is reasonably predicted, but soon after, measured strains reveal lower frequency and sometimes larger magnitude response than those predicted.

Some examples of simulation and measured strain data follow from WNR tests on "Large Effects" targets. Fig. 20 and Fig. 21 show strains at sensor locations on the thinned portions of the front and rear flanges. Predicted strain is shown for two cases: (1) nominal mercury wave speed and contact behavior; (2) mercury wave speed reduced to 20% of nominal, softened tensile contact behavior, and applied beam energy scaled by the reduction of wave speed (scaling

chosen to give improved match in predicted strain magnitude). Measured strains from three WNR tests shown in Fig. 20 and Fig. 21 include two from LE1 (tested August 2000) with mercury de-gassed in one case and with a modest overpressure of helium in the other. The LE4 strains (July 2001) also used helium, but had fully annealed flanges.

The nominal simulation significantly under predicts the measured strains at both front and rear locations. During the first 0.5 ms, the prediction roughly follows measured values for the rear flange. Afterwards the actual rear strains grow considerably and oscillate from negative to positive. The reduced wave speed simulation case does a somewhat better job of matching the compressive strain magnitude and oscillation at a low frequency, but it does not predict the large tensile values measured. The reduced wave speed simulation is also better than nominal at the front location. The simulations are not adequate at either location.

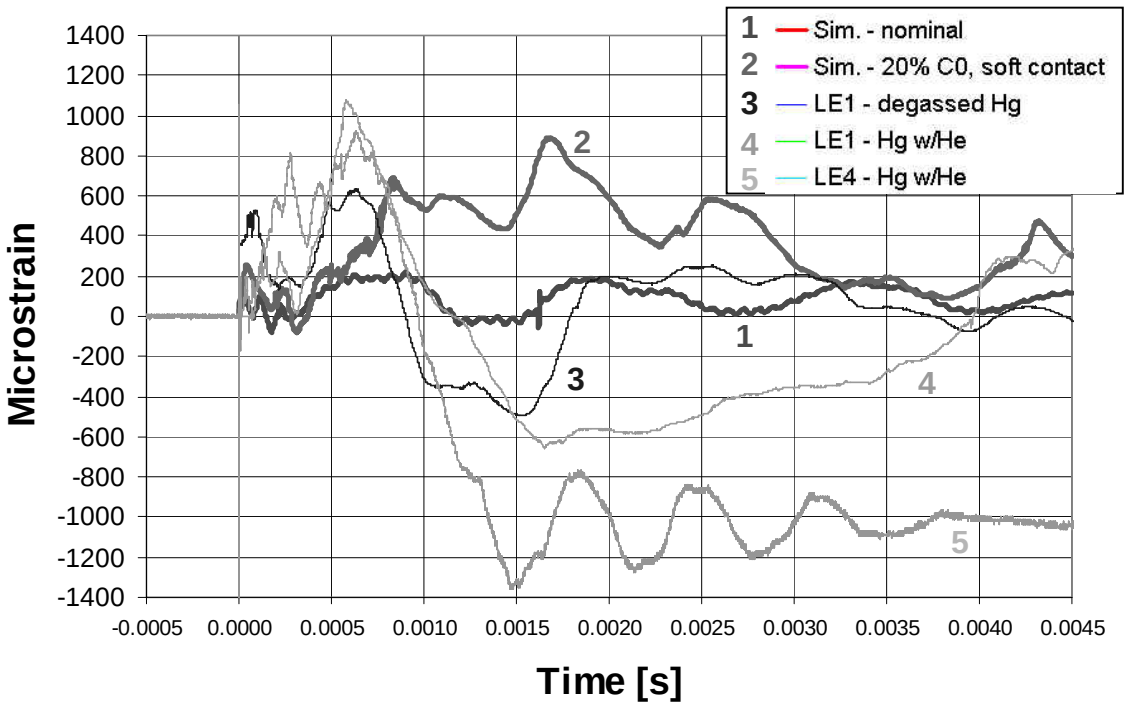


Fig. 20. Simulated and measured data from LE target, front center.

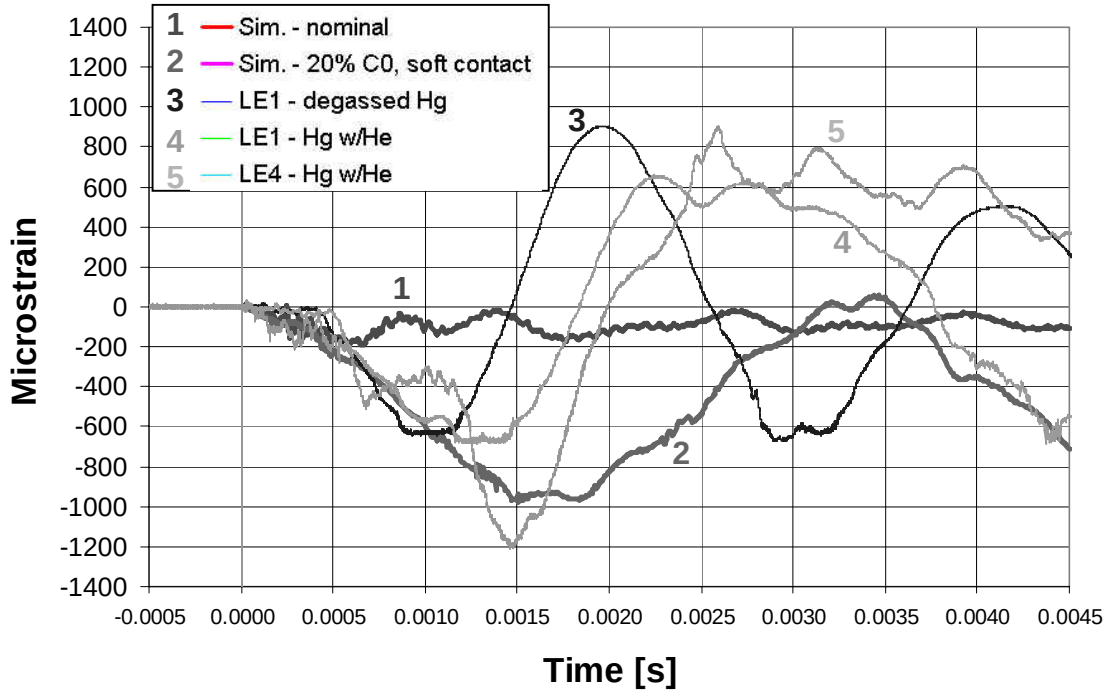


Fig. 21. Simulated and measured data from LE target, rear edge.

Review of mercury pressure evolution from either simulation predicts that very large fluid tensions are produced at various times, on the order of hundreds of atmospheres. Based on bench top experiments, gaseous cavitation is expected at only a few atmospheres tensile pressure. The presence of gas bubbles formed by cavitation will greatly change the effective wave speed in the mercury. No means to predict the spectrum of bubble sizes, their volume fraction, or their lifetime has been found. Wave speed in a bubbly mixture is highly sensitive to these parameters [4].

For any given target and test condition, the experimental data has been repeatable, giving hope that an empirical description of the behavior of mercury could be found. Regretfully this has not yet happened. The current situation is that there is no means to confidently predict the fatigue life of the target.

Strain predictions made for the ASTE target have shown excellent agreement with experimental measurements, however considering this target's geometry and the nature of the energy deposited by the AGS proton beam, the interaction between the mercury and target vessel is weak. The stress wave propagated primarily through the vessel itself. This is not characteristic of the SNS target.

## 5.0 HYPOTHESES ON PITTING MECHANISMS

Although there have been no direct observations of the mechanism responsible for the pits found in post-test inspections, three mechanisms or factors that might have caused or at least contributed to the damage have been seriously considered. These mechanisms are:

(1) Cavitation bubble collapse,

(2) Radial focusing of pressure waves in an axisymmetric target, and

(3) Large mechanical strains, well into the plastic range.

These three mechanisms are not mutually exclusive, i.e., two or possibly all three mechanisms could have worked together to cause the damage observed in the July 2001 mercury target tests at the WNR facility. Item (1) is probably happening; the other two may be making it worse. Each of these three mechanisms is briefly explained below. It should be noted that the combination of mechanisms (2) and (3) above was specifically addressed in the December 2001 tests where thick diaphragms, yielding low strain, were used on a non-axisymmetric (rectangular cross section) target.

Current understanding of cavitation damage mechanisms are summarized in the next section of this report; however, it should be noted that the pitting damage we see in the micrographs of diaphragms irradiated at the WNR facility are typical of the type observed in cavitation bubble collapse. Given this observation along with the indications from our theoretical predictions that we easily achieve tensile pressures that reach the threshold we have measured for cavitation, it seems highly probable that the pits are caused, at least in part, by cavitation bubble collapse.

Radial focusing of the pressure waves in the axisymmetric targets used in the July 2001 tests is the most likely explanation for the location of the large pits. A photograph of the mercury-facing surface of one of the end-plate diaphragms from these tests is shown in Fig. 5. As shown in the photo, large pits, visible to the naked eye, are distributed over a region that is about 5 mm in diameter and centered about 10 mm directly below the center of the diaphragm. Using activation analysis techniques, the beam was found to be centered approximately 5 mm directly above the center of the diaphragm. This 180$^{o}$ shift between the beam center and center of the region with large pits is thought to be due to radial focusing of the pressure wave and its reflection off the side walls of the cylinder. The question remains whether these pits are caused by the collapse of the rarefaction wave as it reflects from the side walls of the cylinder, resulting in intense cavitation near the center of the diaphragm, or are they the result of impingement of an

axial jet of mercury on the diaphragm due to radial focusing of compression waves, or some other mechanism. Although it is unlikely that the December 2001 tests may resolve which of these hypotheses is correct, the question of whether radial focusing is a primary factor in generating the large pits should be answered after inspecting the diaphragms from the rectangular cross-section target.

The very large strains and deflections developed in the central region of the thin windows used in the July 2001 WNR tests may have also contributed to the number and size of the more or less centrally located “large” pits. A typical strain measurement for a sensor located near the center of one of the diaphragms is shown in Fig. 22. The elastic limit for the strain of the annealed 316SS is expected to be about 850 micro-strain. Clearly, this diaphragm underwent plastic deformation. Although it is highly unlikely that this strain by itself caused the pitting, there is some reasonable probability that this was a contributing factor. Furthermore, the reaction of this central region of the window to the initial pressure pulse causes a large, rapid movement of this region, which may lead to separation of the window from the mercury (cavitation). One argument against these mechanisms is that the large pits were not exactly in the center of the diaphragm or the center of the beam (see Fig. 5) and the discussion in the previous paragraph). Whether or not this is an important part of the damage story should be answered soon, since five of the six mercury targets tested in December 2001 at the WNR facility used much thicker diaphragms that had much lower strains.

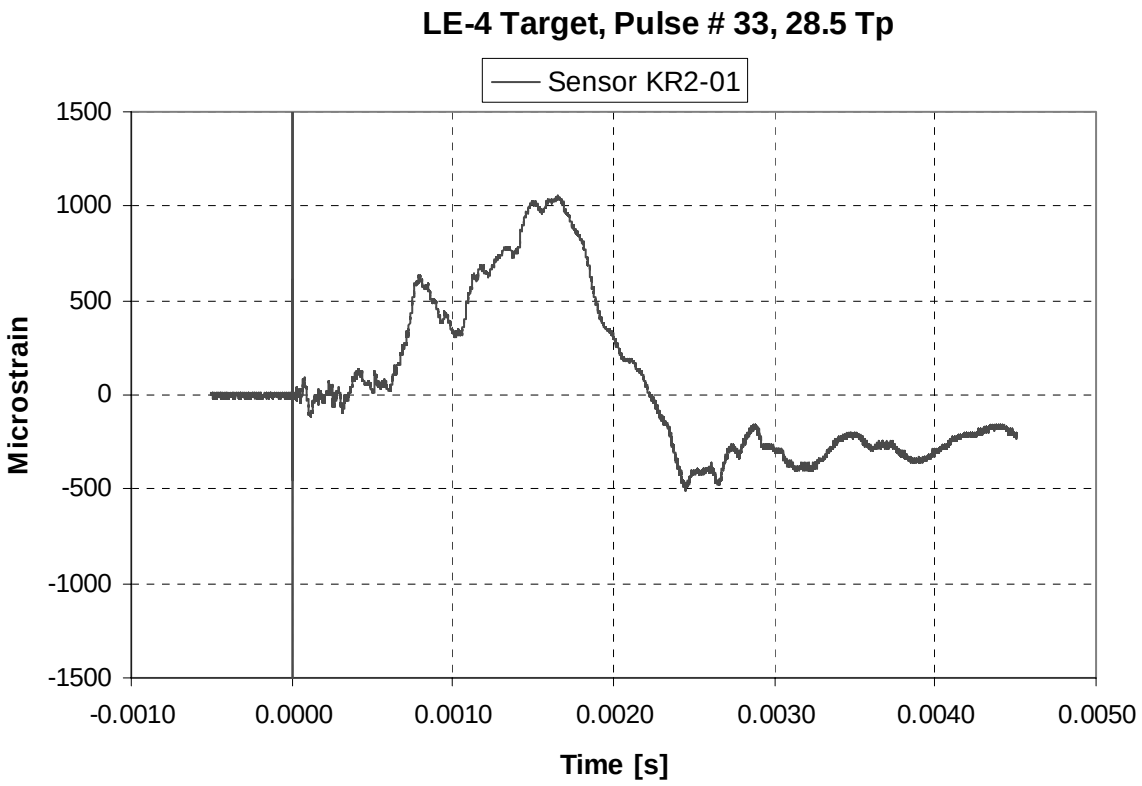


Fig. 22. Typical strain response for a region near the center of an LE target diaphragm following a proton beam pulse from July 2001 WNR tests. Since the elastic limit is approximately 850 micro-strain, this region underwent significant plastic deformation.

# 6.0 IMPACT ON HG TARGET DESIGN AND LIFETIME

## 6.1 Present design basis

The current mercury target vessel design is a result of a five-year optimization process involving a complex set of design requirements and parameters including:

- Neutronic performance
- Material selection
- Structural integrity
- Thermalhydraulic performance
- Spent target handling and disposal
- Affordable costs

Austenitic stainless steel type 316 (grade L / LN) was chosen as the material for the mercury target vessel based on:

- Its chemical and metallurgical compatibility with mercury over an acceptable range of temperatures, and
- The availability of a large database of acceptable structural properties for both the normal and irradiated conditions, supplemented by data on fatigue allowables in mercury from the SNS R&D program.

The derived target design, and cost estimate, is based on available 316 L(N) stock sizes, manufacturing techniques, and welding and weld inspection technology. The target life is limited by changes in material properties due to irradiation, and the remote maintenance and spent target handling techniques being planned are based on after heat and material activation levels applicable to 316.

Extensive, though incomplete, static and dynamic stress analysis has been conducted on the target vessel. Especially critical is the sizing of the proton beam windows and their attachment to the target body. The inner window thickness of 0.050 inches (1.3 mm) is thick enough to withstand the static pressure of the circulating mercury and pressure waves from thermal shock while being sufficiently thin to limit the temperature rise and thermal stress arising from proton beam energy deposition. The 0.13 inch (3.3 mm) gap between the two beam windows is sized to provide mercury flow velocity sufficient to cool the windows. The outer window’s thickness is

also 0.050 inch (1.3 mm), for reasons similar to the inner window. The curvature of the windows not only determines the mercury flow pattern but is also important in establishing the level of stress in both the window and the weld attaching it to the main target vessel body.

### 6.2 Effects of pitting on the target vessel structure

While it is obvious that an accumulation of clusters of large pits seen on the WNR test targets would result in failure of the target vessel's mercury pressure boundary, there are also concerns arising from the presence of the smaller, more distributed pits seen on the test samples. The principal issues are:

- The manner, in which these pits accumulate over the life of the target, could erode the surfaces sufficiently to fail the pressure boundary.
- The effect of the resulting material surface condition, possibly in combination with a reduced effective material thickness, on the fatigue life of the target beam windows is unknown. Furthermore, there is no practical method to produce fatigue test samples with the corresponding surface condition.
- There is a limited ability to predict the areas subject to damage, resulting in a concern about the effects of accumulated damage on components expected to last the lifetime of the SNS facility.

The uncertainty of the testing and results place an increased importance on obtaining additional data during early SNS operation. To do this a method must be developed to perform post-irradiation inspection of spent targets.

If, in the worst case, the pitting results in unacceptable life times for mercury targets, a very difficult, costly, and time consuming effort will be required to remove the mercury cooling loop, decontaminate the hot cell, dispose of mixed wastes, and install a water cooling loop.

### 6.3 Issues with options for eliminating pitting

There are several techniques currently being considered for eliminating, or at least controlling the amount of, pitting on the target vessel. In general, these involve a change of the target vessel material, adding a cavitation resistant coating to the base material, and/or changing the target geometry. Design issues related to these solutions are outlined below.

- Issues with changing materials
  - No or limited data base on irradiated mechanical properties
  - Material availability, manufacturability limitations, cost
  - Spent target after heat, radiation levels, handling
  - Joining of the new material to balance of system - location of transition
  - Properties of weld material and heat affected zone
  - Unknown compatibility with mercury
- Issues with coatings
  - How & where they can be applied, control of quality
  - Effect of process temperatures on base material properties
  - Coverage of weld joints
  - Required thickness - life
  - Unknown compatibility with mercury
  - Unknown irradiation properties
- Issues with changing target geometry
  - Limits on space and shape of target zone in reflectors, moderators, inner plug, etc
  - Changing of the flow pattern
  - Cooling of window
  - Recirculation zone on baffles

# 7.0 REVIEW OF CAVITATION DAMAGE LITERATURE

## 7.1 Definitions

The term ‘cavitation erosion’ refers to loss of material from a solid surface by exposure to a cavitating liquid. The liquid can be stationary or flowing. Cavitation erosion is not a corrosion phenomenon. It is mechanical damage. If cavitation erosion and chemical corrosion occur together, they can be strongly self-reinforcing. The impacts in cavitation erosion are pressure-related and may be initiated by fluctuations in flow or by imposed vibrations. In fluid dynamics, a cavity is a void or bubble in the liquid medium. To avoid confusing this cavity with the cavities or indentations produced at the solid surface, the latter will hereafter be referred to as surface craters or pits. Going further, a pit without a break in its surface will be defined as a dish or depression. A pit from which material has been removed will be called a crater.

## 7.2 Information sources

The information on cavitation erosion is abundant; most of it devoted to cavitation in water. Our understanding of cavity formation and collapse in liquids begins with the seminal studies of Lord Rayleigh [5] on an imploding spherical cavity. Two good literature reviews of cavitation erosion are by Hammit [6] and Hansson and Hansson [7]. A third review by Karimi and Martin [8] emphasizes the materials aspects. A review of liquid droplet erosion, which is related by similar physical processes to cavitation erosion, is given by Heymann [9]. Two outstanding papers on the basics of damage mechanisms are Tomita and Shima [10] and Philipp and Lauterborn [11]. Two books on cavitation are by Knapp et al [12] and Brennen [13]. The information on cavitation in mercury is sparse. Early papers on the topic are by Garcia et al. [14] and Young and Johnson [15]. More recently, work in connection with liquid metal spallation targets has been carried out by West [16], Kass et al. [17], Pawel et al. [18] and Futakawa et al. [19].

Standardized methods have been devised for conducting cavitation erosion tests. The most common method, particularly for comparative screening of the erosion resistance of different materials, is high frequency sonic vibration [20]. Bar charts of materials rankings compiled from such tests are available in Ref. [6](p. 190). Bar charts of erosion rate rankings for liquid droplet erosion are available in Ref. [9] (p. 229), and are very similar to those for cavitation erosion.

### 7.3 Summary of information

Cavitation erosion of a solid surface is caused only by those cavities that collapse at, or very close to, the surface. Shock waves and high-speed liquid jets from the collapse strike the surface with sufficient force to deform and gouge it. Many materials, such as metals, rocks, concrete, polymers, etc., have been investigated for cavitation erosion responses in water under many conditions, and it seems that all materials can be made to pit under the right conditions. It is important to note that no exceptions have been reported. From the literature, it is clear that although a great deal is known about the phenomenological aspects of pitting and the basic processes that are in operation, no permanent cure has been found. However, some materials are more resistant to pitting than others, under similar circumstances. Some coatings and surface hardening treatments afford improved resistance but they may be effective, or not, depending on the intended service life compared to the time interval for the erosion of the protective surface region. Materials that undergo progressive work hardening or phase changes as a result of the surface impacts offer more persistent resistance. Cavitation erosion rates in liquid mercury are up to 20 times higher than in water. Pitting mitigation strategies must use a combination of materials improvements and cavitation abatements.

#### 7.3.1 Cavity formation and collapse

Cavities are formed by local fluctuations of pressure in the liquid. Tensile pressures can open cavities in the liquid. Such pressures can be found in turbulent flow regions and in rarefaction pressure waves caused by vibration or impact. If a cavity migrates to a region of higher pressure, or if it encounters a compressive pressure wave, it collapses. The driving forces for the collapse are the difference in pressure between the local hydrostatic pressure and the vapor pressure in the cavity, and the capillary force due to surface tension that increases as the cavity size decreases. Ignoring the increase in collapse velocity from surface tension, the collapse velocity, v, varies as $[(P-P_v)/\rho]^{1/2}$, where P is the hydrostatic pressure, $P_v$ is the vapor pressure, and $\rho$ is the density of the liquid. For a cavity with an original radius of one mm, collapsing under one atmosphere overpressure in water, the collapse velocity is approximately 100 m/s [7]. The collapse time typically is about 10 μs in water. The collapse entails a sudden inflow of liquid, generating a high pressure near the center of collapse and emitting an associated shock wave. Some of the energy of the collapse is dissipated as heat so intense as to emit visible light. Analyses of the light

flashes indicate temperatures of 5,000 – 10,000 K. The duration's of the flashes are only tens of picoseconds. It is not known whether the heat of cavity collapse is involved in pitting.

Collapses in cavities located away from a solid surface occur symmetrically inward and are non-damaging to the surface. Surface erosion is caused by collapse of cavities that are located on the solid surface or very close to it. The presence of the solid boundary induces pressure gradients that distort nearby cavities; collapse is asymmetrical and is directed towards the solid surface. A consequence of this interaction is that fluid flow in the region between the collapsing cavity wall and the boundary is reduced and the pressure becomes higher at the opposite cavity wall, forcing the cavity center towards the boundary. This motion towards the boundary is accelerated in the final stages of collapse and it ensures that all cavities whose centers are within a distance of one cavity diameter from the surface will collapse on the surface.

Another consequence of distorted cavities and their asymmetrical collapse is that the influx of liquid is non-symmetrical. A liquid cone, or jet, is formed that passes through the center of the collapsing cavity immediately before complete closure, thus changing the shape of the cavity from spherical to toroidal. There are two types of impact on the surface, a shock wave from the violent collapse and a liquid hammer from the jet. In detail there are at least two shock waves, one from the compressive collapse and one initiated when the liquid jet descends from the top of the cavity and hits the internal surface of the cavity closest to the boundary [11]. The impacts occur in time scales of microseconds and the impact stresses may have magnitudes as large as 1,000 MPa [8], which exceeds the yield strength of most metallic materials. They plastically deform the solid surface, resulting in dished or cratered pits.

### 7.3.2 Pit formation and erosion progression

It is well demonstrated that the pits formed in cavitation erosion are developed by local plastic deformation and fracture under the impact forces of cavity collapse. Strain rates are very high, of order $10^4$ to $10^6$/s. In contrast, a common strain rate for a tensile test is $10^{-3}$/s. Thus, all other things being equal, strain rate sensitive materials have been reported to experience worse cavitation erosion than those that have lower strain rate sensitivity. The relative contributions of the jets and the collapse shock waves in the formation of pits are a matter of disagreement in the literature. The relative contributions are found to depend on the original size of the cavity and its location with respect to the boundary at the moment of implosion. The strength of the shock

wave is attenuated in proportion to the inverse of the square of its distance from the collapse center, whereas the jet exerts it largest force at its tip. It is believed that material is lost from the surface by a variety of mechanisms including impact fracture, shearing of protruding crater rims, and fatigue crack propagation.

Pit formation in response to these impacts is generally acknowledged to be a complex process. The shape, depth, and appearance of pits will depend on the nature of the forces acting on the pit region, which depend on the technique used to generate the cavity. Pit formation mechanisms are not well understood. It is assumed that forces dominated by the collapse shock wave should give simple compressive stresses that should favor dishing. Repeated impacts of this type can lead to impact fractures, fatigue crack propagation and loss of material. Forces dominated by the jet will entail a strong shear component that could gouge out material. Tests made with single cavity collapses produced by a vortex cavitation generator or a Francis turbine show pits that are deeply gouged, are irregular in cross section, and have raised rims. Tests in a vibratory device show that the surface first becomes undulated and marked with deformation bands before pits are formed [8]. Of course, brittle materials will crack and chip off under such shock loading. It is known, too, that cavities tend to gather in clusters. The collapse of one cavity can produce pressure transients that may trigger the collapse of nearby cavities. If clusters collapse in concert, the damage will be more concentrated.

It is recognized that chemical corrosion can exacerbate removal of material to form craters. Protective films on the surface tend to be much less ductile than the substrate metal, and under repeated blows they can spall off, exposing the bare substrate to chemical attack. In aqueous media, absorption of hydrogen may cause embrittlement. Even in the absence of chemical dissolution and hydrogen embrittlement, spalling of an oxide film will encourage self-renewal of the film, and the spallation/renewal cycle will accelerate removal of the substrate.

Establishment and measurement of erosion rates requires sampling of many pits in reasonable time periods, and simple techniques for gauging the erosion. The most convenient and rapid method is a standardized procedure of acoustic vibration using coupons of the test material on which erosion is measured by weight loss at intervals [20]. Despite the standardization of this technique, the erosion rate depends very strongly on the particular test conditions, and is not especially reproducible or controllable. In general, though, it follows a nucleation and growth route, whereby there is an incubation phase (in terms of time or number of

impacts), where the erosion rate is small, followed by a rapid growth regime which then settles down to a slower growth phase. A schematic depiction of the stages of erosion progression is shown in Fig. 23.

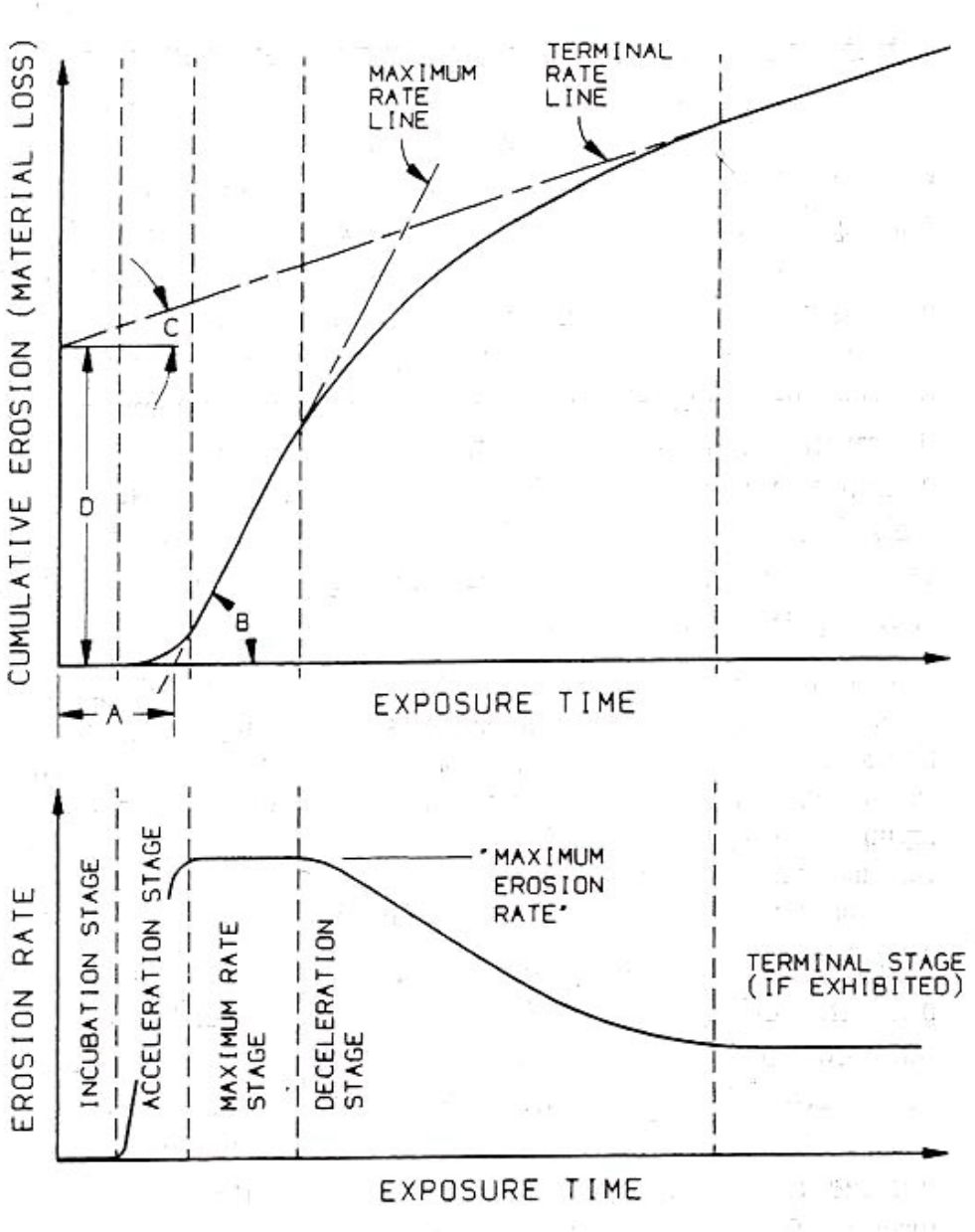


Fig. 23. Characteristic stages of erosion-time patterns in cavitation [20].

This pattern is derived from weight loss measurements and involves many pits at different stages of development. Growth of individual pits seems to be sporadic and unpredictable Interpretations of the various stages are:

- Incubation; surface hardening and initiation of first pits.
- Acceleration; expansion of damage over the whole area of the specimen.
- Maximum rate; steady state rate on uniformly damaged surface.
- Terminal; reduced rate of damage due to cushioning effects of liquid trapped in pits and crevices; deflection of jets by slopes on roughened surfaces.

The incubation period means that laboratory tests for screening materials for pitting resistance should be conducted to a high enough number of impacts to ensure that the rapid rate of pitting has been reached. It is important to remember that this pattern is for acoustic vibration and may not be applicable to other cavitation routes.

### 7.4 Materials rankings

Development of the acoustical testing technique allowed rapid comparative testing of materials for erosion resistance under standardized conditions and resulted in bar charts as shown in Fig. 24.

The data are normalized to annealed 300 series austenitic stainless steel, which is given an erosion rating of one. Compared to it, aluminum alloys have ratings <0.1. The most resistant materials, with ratings of 10 or more, are the cobalt-base Stellite alloys, tool steels, maraging steels, and ausformed steels that have been strain-transformed to martensite.

There is no well-defined correlation of pitting proclivity with physical or mechanical properties of the pitted material. In general, the greatest resistance to pitting is shown by those alloys that offer a combination of corrosion resistance, high strength (hardness), and toughness (but not hardness and brittleness). High strength for protection against pitting can be achieved throughout the bulk by cold working it or by heat treating prior to service. Or strength can be improved in just the surface layers before service by a surface hardening treatment such as carburizing, shot peening, or laser treatment, or by a surface coating treatment such as spraying, cladding (weld deposits), and plating. Effects of surface treatments are not included in Fig. 24. Surface hardening treatments generally affect only shallow depths of tens of microns. Surface coatings can be tens of millimeters thick, and are particularly useful for rebuilding eroded

surfaces. A shortcoming with shallow, one-time surface treatments, is that they can give a false sense of security. They may seem to offer satisfactory resistance in the short term, but once they are broken through, pitting might suddenly accelerate. Better alternatives to the one-time surface treatments are surface hardening treatments that are self-renewed during service by the hammering action of the pitting process. Such continuously renewed hardening depends on plastic strain caused in the surface layers by the impacts; the strain either work hardens the layers or causes them to transform to another, tougher phase, usually to a martensite phase. Alloys with low stacking fault energy, such as Stellite and prestrained stainless steels, are found to be suitable for these treatments [21]. From these considerations, it seems that maximum resistance to pitting in the long term will be offered either by bulk treatments or by surface hardening treatments that are continuously renewed by the cavitation action.

For many years there has been a search to find the best parameter or combination of parameters describing a material, which could serve as a reliable figure of merit for resistance to cavitation erosion. In general, there has been found no reliable parameter that can fully describe cavitation erosion resistance. One suggested metric is derived from examinations of the dependence upon the material hardness of the volume of individual particles eroded from the surface. This dependence is combined with dependence of the particle removal rate, which is taken to be proportional to the fatigue crack growth rate. The resulting erosion volume loss rate in the maximum rate stage (Fig. 23) is found to be proportional to $H^{-3/2}E^{-2}$, where H is Vickers hardness and E is Young's modulus [22]. This parameter gives a good correlation for Al, Cu, and carbon steel, in both annealed and hardened and tempered conditions over three orders of magnitude in erosion volume loss rate.

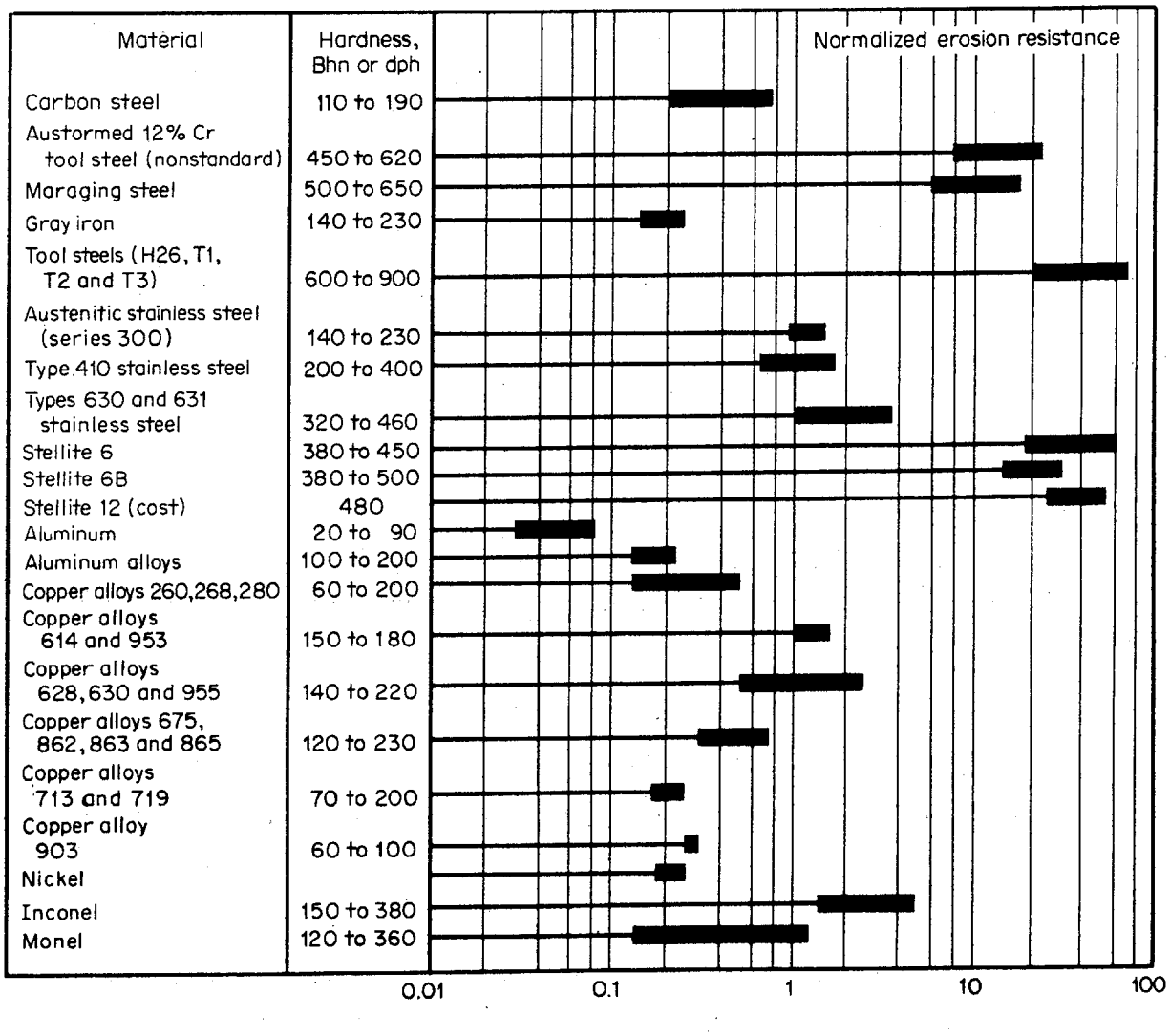


Fig. 24. Erosion resistances of various alloys relative to 18Cr-8Ni austenitic stainless steel [6].

### 7.5 Cavitation erosion in mercury

Cavitation in a liquid mercury target was broached as a likely possibility in the context of the SNS target based on an examination of design parameters and cavitation thresholds [16]. It was pointed out that cavitation erosion might or might not be a problem, depending upon whether cavitation bubbles formed close to the surface of the target container or in more distant regions.

Relatively little is known about cavitation erosion in liquid mercury, but several features are established. One is that pitting does occur in various types of tests [14][15][17][19]. Another is that the degree of pitting is decidedly worse, 3 to 20 times, than in water under similar test

conditions [14][15][17]. In examining the parameters relevant to the possibility of cavitation erosion in the SNS target it was found that a type 316 stainless steel exposed in water and mercury differed in its erosion response to increasing input power level in acoustic horn experiments [17]. In water the erosion depth exhibited a linear response to input power, while in mercury it exhibited a greater than linear response that could be approximated as a quadratic function. In later experiments for the SNS, an ultrasonic transducer was used to generate cavitation damage on specimens of annealed 316L stainless steel immersed in mercury [18]. In a 24 h exposure, tenacious mercury wetting of the stainless steel was developed and, after cleaning, the specimen was found to be significantly roughened in uniform fashion over all exposed surfaces (no isolated pits). SEM profile analysis indicated peak-to-valley surface roughness of at least 15 μm on the eroded specimen compared to 0.5 μm on the virgin specimen.

At the present time experiments are ongoing using an acoustic horn technique similar to that described in [20]. Initial testing has focused on the cavitation erosion of annealed 316LN in mercury at 25 °C to establish the specimen and test conditions required to generate reproducible results. It is evident from the preliminary information that the ultrasonic processor can be used to develop significant cavitation that results in relatively uniform surface roughening across the exposed specimen surface. To date, isolated pits have been observed infrequently, only for the longest exposure times and always accompanied by uniform erosion. Future tests will compare annealed 316LN with 316LN in other conditions, which include cold-worked, surface-modified or coated, and welded. Other alloys will be examined for comparison, as well as the effects of modifying test conditions over a limited range relevant to the SNS target, such as by varying test temperature. Results from this program will be used to rank the erosion resistance for materials of interest, to assess materials for potential inclusion in future in-beam tests, to interpret related test data, and to evaluate potential design modifications for the target container.

From the sparse data, it also seems that the erosion resistance rankings of materials in mercury at room temperature are similar to those in water at room temperature [14]. It was presumed [14] that the greater damage in mercury was due to the greater density of mercury, which is 13.5 times larger than water. But other differences in physical properties for mercury at room temperature are surface tension (6 times larger than water), bulk modulus (13x), viscosity (0.1x), specific heat (0.03x), thermal conductivity (15x), heat of vaporization (0.1x), thermal expansion (9x), compressibility (0.09x), and vapor pressure (0.0001x to 0.001x for temperatures

of interest). These properties will affect the formation and collapse parameters of cavities, and the pitting forces. For example, for a given amplitude pressure pulse in water and mercury, the damage would be expected to be worse for mercury because the compressibility is much lower and the surface tension is much larger. Lower compressibility means less cushioning of a blow to the boundary surface and higher surface tension means a more violent collapse of small bubbles.

### 7.6 Cavitation in Target Test Facility (TTF) Feed lines

The SNS Target team accumulated some additional firsthand experience on the cavitation phenomenon during the final development tests on the full-scale hydraulic test loop referred to as the Target Test Facility (TTF). Cavitation occurred in the feedlines to the prototypical target just downstream of the second of two 90-degree bends spaced closely together. The onset of cavitation occurred at flow rates that were about 20% of the nominal value. When operated at the nominal flow rate, the system was extremely noisy, making audio communication outside the TTF enclosure difficult and causing significant vibration of the concrete floor in the building housing the experiment.

Prior to redesigning and replacing this section of feed line piping, the TTF loop was operated for several hours at nominal and one-half nominal flow rates to gather data on the velocity field in the prototypical target. It is worth noting that the ultrasonic Doppler velocimeter measurements were greatly facilitated by the presence of cavitation bubbles. Measurements could not be made on the previous TTF configuration because inadequate scattering surfaces existed in the flow.

Despite operating under these extremely noisy conditions for hours, it is remarkable that no significant damage to the feedline piping could be detected in the post-mortem examination of the section of piping where the noise originated. However, it should be noted that no pre-inspection of the piping surface was performed, so that minor changes of the surface would not have been detectable. These results lead one to speculate that flow induced cavitation of the type experienced in TTF is a very different phenomenon than the cavitation that is occurring in targets exposed to short pulse proton beams where significant damage occurred in a very short period of exposure to the cavitation environment.

## 8.0 MITIGATION STRATEGIES

It should be pointed out that there might be an automatic mitigation process operating for the SNS target. It is known that displacement-inducing irradiation causes substantial hardening in structural materials. Typically, for irradiation of solution annealed austenitic stainless steels the yield strength increases by a factor of two to three after irradiation to doses of only 0.01 to 0.1 dpa, i.e., 0.1 to 1 day at the front center of the target at full power. Hardening is generally found to be beneficial in reducing cavitation erosion. In this respect cold-worked materials, which provide some qualitative similarities in hardening to irradiated materials, will be tested in the ongoing experiments described in section 7.5.

An option that has yet to be investigated is textured surfaces. There are qualitative arguments to suggest that such an approach might result in reducing erosion. Textured surfaces can be produced by etching, hammering, shot peening, milling, or rolling, the latter two being reproducible. The size scale of the texturing might have to be of the size of pits, say 100 μm or so. A suggestion that this approach might be effective can be gleaned from Fig. 23. There the deceleration and lower steady-state terminal stage of erosion are associated with highly textured surfaces (where the processing route for obtaining the textured surface is cavitation erosion.)

Other concepts for potentially mitigating cavitation erosion in mercury include:

- Entrain gas bubbles to reduce the formation of vapor bubbles and increase macroscopic compressibility.
- Reduce surface energy of mercury (Composition or thermodynamic external variable change required to alter a physical property).
- Insert “steel wool” or other mesh-like material in Hg to break up/scatter pressure waves.

All of these concepts would require considerable experimental verification.

## 9.0 PLANS FOR NEAR-TERM TESTING

Five testing activities that could contribute to our understanding of the pitting phenomenon will be undertaken before the end of FY 2002, including:

- Additional rounds of in-beam tests at LANL's Weapons Neutron Research (WNR) facility,
- Another round of in-beam tests at BNL's Alternating Gradient Synchrotron (AGS) facility under the auspices of the AGS Spallation Target Experiment (ASTE) collaboration,
- Off-line mechanical load tests on cylindrical (LE) targets to benchmark computer simulation models,
- Off-line tests using JAERI's split Hopkinson pressure bar (SHPB) apparatus to determine the pressure threshold for pitting damage, and
- Cavitation damage tests using an ultrasonic processor to perform screening/comparison tests of target container material candidates.

The test program for each element listed above is briefly described below.

### 9.1 WNR

We plan to conduct one more round of mercury target tests at LANL's WNR facility. A proposal for five days of beam time was recently submitted, and the proposal review committee will meet in April to select those projects that will be given beam time during this year's LANSCE operating schedule that runs from July 1 to December 24. We have requested that our tests be scheduled as early as possible. Although a WNR pulse contains less energy than a pulse for the 2 MW SNS, by focusing the WNR beam down to a size of about 20 mm diameter, the beam intensity, and therefore pressure increase, expected for the SNS can be reasonably simulated. Tests conducted during 2001 are discussed in a previous section of this paper.

Having determined in last year's tests that pitting can occur under pulsed beam conditions, the main purpose of the new tests is to address the following four issues:

(1) Does a small void at the top of the target eliminate or greatly reduce pitting,

(2) Is there a threshold for pitting that is a significant fraction of the full-power intensity of SNS, say 25% or more,

(3) Can the use of more prototypical shaped targets reduce or eliminate pitting,

(4) Can the use of more cavitation damage resistant materials reduce or eliminate pitting?

Item (1) is motivated by the results obtained in the December 2001 tests with Pb-Bi. The strains were anomalously low for this target, and post-test examination of the target indicates that a small void, approximately 1% by volume, likely existed. Item (2) could establish whether a mercury target in SNS might not experience significant pitting damage during the initial few years of operation where low powers are expected. This would allow significant time to develop solutions to the pitting problem in the real SNS environment. Item (3) is motivated by conjecture that the large pits formed in previous tests were primarily due to the radial focusing of pressure waves in an axi-symmetric target. Item (4) is based on the potential for improvements already demonstrated in hardened samples used in previous WNR tests. Since both items (3) and (4) were studied in December 2001, specification of detailed designs and material specimens will await inspection of these test samples.

The surface of the flanges exposed to the mercury will be carefully characterized and micrographed prior to and following tests. A series of single-pulse tests will be conducted on these targets with the total number of pulses limited by the activation and operational limits for experiments in the WNR Blue Room.

### 9.2 ASTE

A series of tests will be conducted at BNL's AGS facility in May on four LE targets being built by our collaborators from FzJ. The ESS team will use the four front diaphragms on these cylindrical targets to test their baseline ferritic steel material, while the SNS team will use the rear diaphragms to study methods to mitigate pitting damage. The heating conditions, and therefore magnitude of the pressure pulse, are essentially the same on the front and rear of these 300 mm long targets. The two pitting mitigation methods to be examined in these tests are the use of hard, cavitation damage resistant coatings and the use of a small void at the top of the target. A bare 316SS diaphragm will be used on one target as a control sample to demonstrate that pitting damage conditions are achieved under the planned beam conditions of $3 \times 10^{12}$ protons per pulse, 24 GeV protons, and 200 pulses for each target. Another bare stainless steel diaphragm will be used for the target with a small void at the top. The two other diaphragms will be coated with either CrN or a non-crystalline metallic glass coating that was recently developed

at the Idaho National Engineering and Environmental Laboratory (INEEL) [23]. The JAERI team is providing the CrN coating, while the SNS team is arranging for the metallic glass coating.

### 9.3 Mechanical testing of LE targets

To improve our understanding of the response of the test targets and benchmark our computer models being used to predict the response of the SNS target to pressure pulses, we plan to conduct a series of simple mechanical load tests on an LE target. The LE target, which will be struck with a "calibrated" hammer to impose a dynamic load, will be instrumented with fiber-optic strain gauges. Tests will be conducted with the target empty, filled with water, and filled with mercury. In each case, predictions from ABAQUS computer models of the target will be compared with the measurements. Given that the level of the mechanical load may not be highly repeatable, achieving the correct frequency response is of primary importance in this comparison between predictions and measurements. Models will be adjusted, if necessary, to achieve the desired level of agreement.

### 9.4 SHPB

Previous tests on JAERI's split Hopkinson pressure bar were conducted at two pressure levels that are consistent with proton beam power levels of about 2 MW and 4 MW on SNS. Researchers at JAERI have agreed to conduct additional tests at pressure pulse levels that are lower than this range to investigate whether the threshold for pitting damage might allow us to operate at significant, but reduced, power levels, without encountering this phenomenon. For example, the JAERI team will perform their tests at the equivalent of 1 MW operation (pressure pulse of 20 MPa). If damage still occurs at this level, they will reduce the pressure level again, say to 10 MPa, and conduct more tests.

### 9.5 Ultrasonic processor

An ultrasonic processor (e.g., a vibratory horn) produces cavitation damage on the face of a test specimen being vibrated at high frequency (20 kHz) while immersed in the test fluid (mercury or water). The rapid reciprocating displacement of the specimen surface induces the formation and collapse of cavities in the liquid, and the collapsing cavities are capable of

producing damage on the specimen surface that can be quantified by weight loss and/or penetration depth as a function of exposure time. The basic test protocol and equipment is described by ASTM Standard G-32 and, provided critical parameters are controlled from test-to-test, this procedure permits qualitative or semi-quantitative comparison of damage rates for a wide variety of materials/treatments.

Presently, there is no specific correlation between the damage intensity/rate produced at the surface of the specimen in the vibratory horn and potential cavitation damage in the SNS mercury target containment resulting from proton pulses. As a result, data from the vibratory horn tests cannot be used to quantitatively predict target life. However, testing can assess relative cavitation resistance of annealed 316LN (the reference material) compared to 316LN in other conditions (e.g., cold worked, surface treated) and other alloys with potentially superior cavitation resistance. Temperature, displacement amplitude, and exposure time are expected to be significant variables for consideration in the test exposures and should be fixed in order to provide valid comparisons. Ultimately, results from this screening test will be used to select appropriate materials for the next round of examinations at the WNR.

## 10.0 PITTING EROSION LIFETIME ESTIMATES

Estimating the target lifetime using the data from the 200 pulse tests requires an enormous extrapolation. The nominal target lifetime based on embrittlement due to irradiation damage is set at 1250 hours for a pulse repetition rate of 60 Hz and time averaged power of 2 MW (corresponds to 5 dpa in 316SS). This goal represents 2.7 x $10^8$ pulses, or more than a factor of a million more pulses than obtained in the tests. Nonetheless, extrapolation is judged to be worthwhile to give some comparison of projected lifetimes with design goals.

The images showing pits from the July 2001 tests were used to estimate the fraction of area that was damaged and the depth of the damage. Estimates were made for both types of pits observed in these tests, i.e. large pits clustered near the center and smaller pits distributed randomly in clusters at a few locations on the surface of the flange. In all cases, we used data from the worst regions of pits and assumed this damage occurred everywhere on the surface. This could be significantly conservative for the small pits, but is likely more realistic for the large pits, which appear to collect near the beam interaction zone (perhaps rotated 180 degrees around the center of the diaphragm).

Key assumptions used for this extrapolation include:

- Damage from WNR pulses with stagnant Hg target is the same as SNS damage, i.e. assumes energy density and ratio of beam to target cross-section are the critical parameters,
- Pitting damage remains constant (same amount of material is removed even after the surface is heavily pitted) at the value measured in the small number of test pulses,
- The thickness of material available for erosion is 500 μm.

By examining the SEM images in the damaged regions, we estimated the pit density ($n_p$ = pits per unit area) and the characteristic diameter of the pits ($d_p$). Using this data, the fraction of the surface area that is damaged ($f$) is given by:

$$f = n_p \frac{\pi}{4} d_p^2$$

The number of pulses that would be required to remove one layer of material is:

$$\frac{N_T}{f} = \frac{4\, N_T}{\pi\, n_p\, d_p^2}$$

where $N_T$ is the number of pulses in the test (200 for the July 2001 tests). The number of layers until end-of-life is reached is simply the thickness ($t_L$) of material available for erosion (assumed to be 0.5 mm for our case) divided by the characteristic depth ($h_p$) of the pits. Assuming that the characteristic pit depth is equal to one-half the characteristic diameter, then the number of pulses in the lifetime ($N_L$) is estimated to be:

$$N_L = \frac{8\ N_T\ t_L}{\pi\ n_p\ d_p^3}$$

The target lifetimes estimated using this linear extrapolation from the test data are shown parametrically in Fig. 25 for pit diameters ranging from 4 to 100 μm. Four data points, corresponding to large and small pits for the bare annealed and treated (Kolsterised) diaphragms, are displayed in this figure.

It is obvious from these extrapolations that the large pits will lead to unacceptably short lifetimes on either bare or Kolsterised 316SS surfaces. Therefore, it is clear that some means must be found to eliminate the large pits.

The estimated lifetimes due to erosion from randomly distributed clusters of small pits are roughly three orders of magnitude greater than those for large pits. The bare 316SS would be expected to last about 6 x $10^6$ pulses, or about 30 hours at full power with a repetition rate of 60 Hz. For purposes of estimating the potential lifetime that might be possible, the Kolsterised surface is assumed to extend to 500 microns, whereas it is actually only 33 microns thick. The lifetime of such a material would be estimated to be about $10^8$ cycles or within roughly a factor of three of the desired value.

Lifetime goals for early phases of SNS operation are also indicated on Fig. 25 to illustrate that the lifetime goal for the first several years of operations are significantly relaxed compared to the ultimate goal of 1250 hours at 2 MW. If the extrapolation performed here applies and large pits are eliminated by geometric or other considerations, bare 316SS should be adequate for the first six months of operations with no target replacement.

It must be emphasized that results from this extrapolation exercise have huge uncertainty bands. Important questions that have yet to be answered include

- Is there an incubation period, i.e. does the erosion actually increase after some initial period of cycles?
- Does hardening of the surface by pitting damage or irradiation slow down the pitting?

- Should the damage fraction be averaged over the entire diaphragm surface?

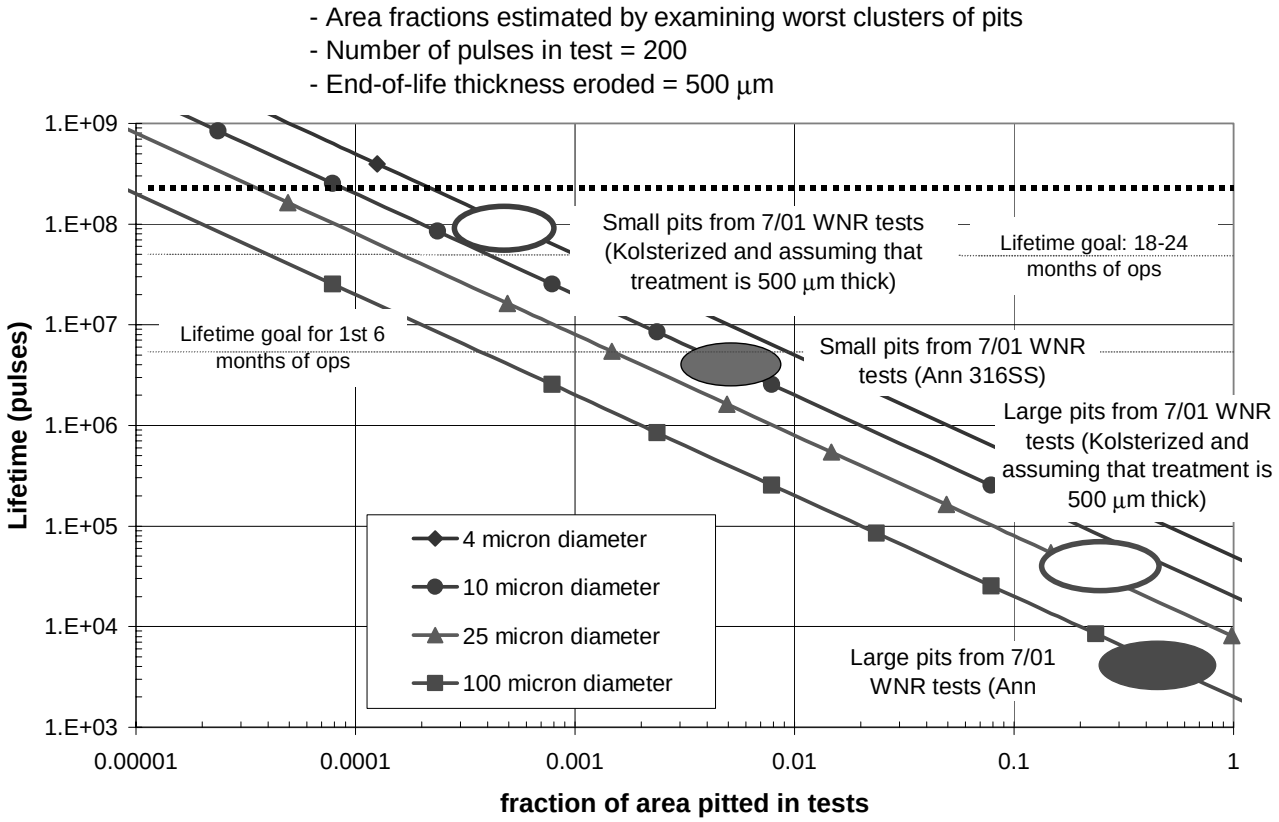


Fig. 25. Target lifetime estimates extrapolated from WNR test results.

## 11.0 CONCLUDING REMARKS

A series of tests were conducted at LANL's WNR facility during 2001 to examine whether the pressure pulse phenomenon caused by the interaction of a short-pulse (300 ns), high-energy proton beam with mercury causes pitting damage to the stainless steel container. Results showed that, at least for the materials and target configurations tested, pitting damage occurred. A cluster of large pits, visible to the naked eye, as well as smaller, more randomly distributed pits were seen in micrograph images of all four window specimens used in the July 2001 tests.

Subsequent tests at the WNR in December 2001 were dedicated to further examining the pitting phenomenon and looking at an array of possible solutions, or at least reductions, to the pitting problem. Seven targets were tested in the December 2001 campaign. Most notably, a target with a rectangular cross section was used in an attempt to eliminate the postulated radial focusing of the pressure wave and be more prototypical of the actual SNS target shape. Also, windows with increased thickness, intended to reduce the large stresses, were tested. Post-irradiation examination of the targets irradiated in December has begun and is scheduled for completion in April 2002.

The magnitude of the pressure pulse, results of off-line cavitation threshold tests, and post-test examination of damaged surfaces, lead us to conclude with a reasonably large degree of confidence that the mechanism causing the pitting damage is collapse of bubbles created as part of a mercury cavitation process. Because of this, the cavitation damage literature has been studied to help understand the phenomenon and postulate potential solutions or improvements.

To date, in-beam tests have not been able to clearly demonstrate a solution to the pitting issue, although a couple of concepts/material combinations may hold promise. One concept is the use of a non-axisymmetric shaped target, which is more prototypical of the SNS target shape, with either no double wall structure near its front or using water in this thin slot formed by the double wall. Either of these changes represent a modification to the SNS baseline design and will require careful evaluation before they could be incorporated, and may lead to breakage of engineering design, increased component costs, and greatly reduce or even eliminate all schedule float in SNS target fabrication, installation, and testing.

The use of more cavitation damage resistant materials may also offer improved erosion lifetime performance, but will certainly increase the unknowns relative to behavior under irradiation. The irradiation database developed for 316SS under relevant spallation target

conditions has given us great confidence in projecting minimum lifetimes and minimizing risk of premature target failure during SNS target operation. This increased uncertainty must be given consideration in making a decision to switch to a different target container material.

Estimating the target lifetime using the data from the 200 pulse tests requires an enormous extrapolation, i.e., by more than a factor of one million. Assumptions regarding the nature of the pitting process that have yet to be validated are required to create this erosion lifetime estimate. Nonetheless, extrapolation is judged to be worthwhile to give some comparison of projected lifetimes with design goals. These estimates illustrate that the large cluster of pits near the center of the beam interaction region must be eliminated to achieve adequate lifetimes. If the large pits are eliminated by geometric or other considerations (not fully demonstrated yet), bare 316SS should be adequate for the first six months of operations with no target replacement. If we can find a target container material that has an erosion resistance comparable to that of the Kolsterised surface (limited to 33 μm thickness) over an erosion thickness greater than 500 μm, then lifetimes approaching 1/3 of the goal at 2 MW operation may be possible. This would give us adequate target lifetimes for several years of operation, which could presumably be used to examine methods to further extend the erosion lifetime.

Finally, the direct relevance of the off-line and in-beam tests conducted so far is somewhat questionable since many of the conditions/variables that could be important for pitting damage cannot be accurately simulated in these tests. Several examples of the discrepancies between tests and the actual SNS conditions include:

- Interactions between subsequent beam pulses could be important if the residence time of cavitation bubbles is comparable to or longer than the 17 ms between pulses in SNS (corresponds to 60 Hz repetition rate),
- Flowing of the mercury may alter the contact condition between the mercury and stainless steel and thereby change the way in which bubbles form and collapse,
- The geometries used in tests have been either different or rather great simplifications of the SNS target shape, lacking structural details, and the long open-ended supply and return lines that flow the Hg, and
- Both off-line and in-beam tests have been limited to a small number of pulses (≤ 200) compared to the baseline target lifetime (based on radiation damage) of $3 \times 10^8$ pulses.

Given the uncertainty in erosion lifetime it is concluded that more in-beam tests be performed to examine whether the proposed ideas for target shape and materials can be shown to extrapolate to reasonable lifetimes (say $10^8$ pulses for example) at SNS relevant power levels (≥ 1 MW). Tests are scheduled for June 2002, but additional tests may be required. Also, developing Hg target design concepts, diagnostics, and post-irradiation examination procedures that emphasize the experimental nature of early SNS operations should be pursued.

## REFERENCES:


[1] L. Briggs, "The Limiting Negative Pressure of Mercury in Pyrex Glass," Journal of Applied Physics, Vol. 24 (1), April 1953.

[2] F. Moraga and R. P. Taleyarkhan, "Static and Transient Cavitation Threshold Measurements for Mercury, Proc. of AccApp'99, November 1999.

[3] M. R. Cates, B. W. Riemer, D. D. Earl, C. C. Tsai, S. W. Allison, D. L. Beshears, J. R. Haines, "Strain Measurements on Targets Tested at the LANSCE WNR Facility," August 2000, SNS-101050200-TR0009-R00, July 12, 2001 (SNS/TSR-0215).

[4] Brennen, C. E., CAVITATION AND BUBBLE DYNAMICS, Oxford University Press, 1995.

[5] Lord Rayleigh, Phil. Mag. 34 (1917) 94-98.

[6] G. Hammitt, "Cavitation and Liquid Impact Erosion," pp. 161-230 in ASME Wear Control Handbook, pub. Amer. Soc. Mech. Eng. (1980).

[7] C. M. Hansson and I.L.H. Hansson, "Cavitation Erosion," pp 214-220 in ASM Handbook Vol 18, Friction, Lubrication, and Wear Technology, pub ASM International (1992).

[8] Karimi and J. L. Martin, Int. Metals Rev. 31 1-26 (1986).

[9] F. J. Heymann, "Liquid Impingement Erosion," pp 221-232 in ASM Handbook Vol 18, Friction, Lubrication, and Wear Technology, pub ASM International (1992).

[10] Y. Tomito and A. Shima, J. Fluid Mech. 169 535-564 (1986).

[11] Philipp and W. Lauterborn, J. Fluid Mech. 361 75-116 (1998).

[12] R. T. Knapp, J. W. Daily, F. G. Hammitt, *Cavitation*, McGraw-Hill, New York, New York, 1970.

[13] C.E. Brennen, *Cavitation and Bubble Dynamics*, Oxford University Press, Oxford, England (1995).

[14] R. Garcia, F. G. Hammitt, and R. E. Nystrom, pp 239-283 in Erosion by Cavitation or Impingement, ASTM STP 408, Am. Soc. Testing Mats. (1967).

[15] S. G. Young and J. R. Johnson, pp 186-219 in Erosion by Cavitation or Impingement, ASTM STP 408, Am. Soc. Testing Mats, (1967).

[16] D. West, pp 645-649 in AccApp '98, Proceedings of 2nd International Topical Meeting on Nuclear Applications in Accelerator Technology, Gatlinburg, TN, Sept. 20-23, Pub. Amer. Nucl. Soc. (1998).

[17] M. D. Kass, J. H. Whealton, N. E. Clapp Jr., J. R. Distefano, J. H. Devan, J. R. Haines, M. A. Akerman, and T. A. Gabriel, Tribology Letters 5 231-234 (1998).

[18] S. J. Pawel, E. T. Manneschmidt, R. P. Taleyarkhan, S. H. Kim, and J. R. DiStefano, "Cavitation as a Mechanism to Enhance Wetting in a Mercury Thermal Convection Loop," ORNL/TM-2001/086 (May 2001).

[19] M. Futakawa, H. Kogawa, Y. Midorikawa, R. Hino, H. Date, and H. Takeishi, "Impact Erosion on Interface Between Solid and Liquid Metals", presented at the International Symposium on Impact Engineering, Kumamoto, Japan (ISIE/4), July 2001. To be published in symposium proceedings.

[20] ASTM Standard Test Method for Cavitation Erosion Using Vibratory Apparatus, Designation G32-98. Annual Book of ASTM Standards (1998).

[21] R.Simoneau, P. Lambert, M. Simoneau, J.I. Dickson, and G. L'Esperance, pp 32-1 to 32-8 in Proceedings of the Seventh International Conference on Erosion by Liquid and Solid Impact, Cambridge, 7-10 Sept. 1987, pub. Cavendish Laboratory, Cambridge University, United Kingdom.

[22] S. Hattori and E. Nakao, Wear 249 839-845 (2002).

[23] D. J. Branagan, W. D. Swank, D. C. Haggard, and J. R. Fincke, "Wear-Resistant Amorphous and Nanocomposite Steel Coatings," Metallurgical and Materials Transactions A – Physical Metallurgy and Materials Science, 32 (10): 2615-2621 (October 2001).

# *APPENDIX B*

# *REPORT FROM CAVITATION DAMAGE EXPERTS REVIEW MEETING*

# Report by the Cavitation Damage Experts Review Committee

## Meeting May 9-10, 2002
## SNS Office Building, Oak Ridge, TN

## "Cavitation Damage Experts Review of SNS Target Pitting Issue"
## by

Roger E. A. Arndt (University of Minnesota)
Steven L. Ceccio (University of Michigan)
Robert J. Etter (Naval Surface Warfare Center, Carderock Division)
Arthur E. Ruggles (University of Tennessee)
David L. Stinebring (Applied Research Laboratory/Pennsylvania State University)

The following is a brief overview of the May 9-10, 2002 meeting at the SNS Office Building, Oak Ridge TN. Notes from the meeting are presented in the Appendix. The objectives of the meeting were to evaluate the current information regarding the target pitting, make recommendations for meeting the October decision deadline, and make recommendations addressing the pitting issue in the long term.

## Statement of the Problem(s)

Cavitation erosion was first observed in tests in Japan with the Split-Hopkinson Pressure Bar (SPHB) using liquid mercury. Similar tests at the Weapons Neutron Research (WNR) facility of a mercury filled target irradiated with 200 pulses of 800 MeV protons at relevant beam intensities. There are concerns, based on damage observed for these tests, that damage might also occur in the stainless steel container for the SNS mercury target and that the damage could significantly limit the life of the container. Furthermore, the current limited tests do not permit scaling/ calculations of the target container lifetime.

## Evaluation of the Progress to Date

The cavitation damage panel evaluated the information presented during the meeting and presented in Haines et al (2002) available on the SNS web site. There was a consensus that the erosion of the SNS mercury target container was due to cavitation and was of serious concern. The problem is exacerbated by the paucity of information n the literature concerning erosion mechanics in mercury and the difficulties in making observations. Target tests are limited to about 200 events, whereas approximately $10^8$ events would occur over the design lifetime of the target. Screening tests using the ASTM G32 vibratory apparatus cannot provide sufficient information concerning the lifetime of the target.

## Requirements to Meet the October Deadline

The primary objective of the meeting was to provide recommendations to meet the October decision deadline on whether the erosion issue can be resolved sufficiently to meet the target lifetime goal, or if an alternative target is required.
June LANSCE-WNR Tests- Recommendations were made to the test matrix for addition of a test to include a bubble generator to "mask"/attenuate the pressure pulse.

Vertical Drop Test Apparatus- These tests should provide the best indication as to the anticipated erosion for large numbers of cycles using mechanically induced pressure pulses of the same magnitude as those expected at full power in SNS. The test surface should be inspected often and the damage documented, especially during the initial impact stages. This can then be used to help scale the WRR data, with few cycles, to anticipated damage with large numbers of cycles.

Vibratory Apparatus- It was recommended to continue tests with the ASTM vibratory apparatus for materials screening because of the low cost. These tests are to be used in conjunction with the vertical drop tests. A modified ASTM G32 test was proposed, where the sample is held at a small distance from the vibrating horn, Fig. 1. The standoff distance is adjusted to where high erosion rates start. A clear sample can be used to view the cavitation bubbles in mercury. A short duration strobe light, i.e., General Radio 1538, operated at 60 Hz to synchronize with a video camera can be used to record the bubble patterns.

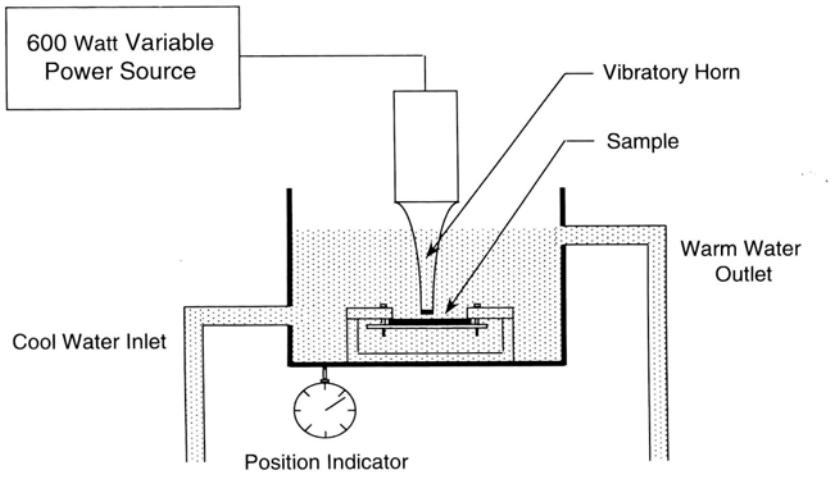


Figure 1: ARL Penn State modified ASTM standard G32-85 cavitation damage screening test apparatus

## Other Near-Term Recommendations

Near term investigations should focus on following guidelines similar to recommendations for meeting the October deadline. Keep testing alternative materials and coatings using the vibratory device(s) and the bar apparatus. Because of the limited sample size to date, do not eliminate a material until further tests are run. Tests should be run and instrumentation developed, for WNR

test for example, to better understand the mechanism for the cavity generation and resulting damage. This will provide input into development of the computational models. The effects of test geometry could start to be investigated with instrumented target containers in the Target Test Facility (TTF). This could be done using acoustic projectors to simulate scaled pressure pulses.

The so-called ductile probe technique could be adopted, where softer materials are inserted in key areas to rapidly focus on areas where changes in geometry would be the most beneficial. An even more rapid assessment can be made with paint tests where damage prone areas are rapidly visualized by paint removal. Pressure sensitive film, which changes color under exposure to damaging blows has also been successfully used.

## Long-Term Recommendations

Long-term recommendations include obtaining a better understanding of the physics associated with the pressure/tension pulse generation, cavitation dynamics, interaction of the cavity collapse with the surface, and resulting damage. Computational models would be used in conjunction with testing. Alternative erosion resistant materials and coatings should also be investigated long term.

## Final Comments

It is the opinion of the committee that the investigations made prior to our meeting are very thorough and provide an accurate assessment of the problem. The SNS target pitting issue will most likely not be resolved using erosion resistant materials alone. It will require a combination of materials, target container geometry, and cavitation mitigation techniques to solve the problem.

# Notes from Cavitation Experts Meetings

# May 9-10, 2002

## List of Important Variables

- Material
- Energy Density
- Total Energy
- Geometry
- Time History
- Mercury Properties/History

## List of Items That Can Be Controlled

- Material/Coatings
- Interior geometry – Longer
- Hg "mixture"
- Hg flow

## Remediation Concepts

- Distributed bubbles
- Compressibility
- Gas layer/Air Slab
- Acoustic mismatch

## Recommended Activities to Be Completed By October

- Enough bar test samples and cycles to give confidence on erosion rate extrapolation
- Scale to beam pulse tests
- Erosion measurement standard
- Sparger effect
- Stand-off vibration test with clear sample

# Observations

| | | |
|---|---|---|
| A.R. | LT | • Pressure history at surface important |
| | ST | • Bar test is important; want to examine pitting as function of time |
| | ST | • Eliminate differences in Hg |
| | | • Saturation w/ gas |
| | | • Temperature |
| | | • Filter |
| R.E. | O | • Stainless steel is likely material given other constraints |
| | ST | • Bubble shielding important to try |
| | LT | • Could use other fluid for shield? Water? |
| | O | • How important is rounded nose on target? This will make bubble layer concept more difficult |
| R.A. | ST | • Study scaling for Hg vs. water |
| | ST | • Between now and October 2002 must evaluate technology |
| | | • Selective materials screening |
| | | • Scaling study/demonstration |
| | | • Geometry is important |
| D.S. | ST | • Sample size and test conditions are limited, so do not drop any materials yet |
| | ST | • Must reduce uncertainty for scaling |
| | | • Materials |
| | ST | • Base |
| | ST | • Coating |
| | LT | • Tough |
| | ST | • Focus on bar apparatus |
| S.C. | O | • Armor won't work |
| | O | • Do things that will give Go-No Go guidance for remediation |
| | O | • Follow \\ Design track |
| All | R | • Add bubble target to test matrix. |

O = Observation
ST = Short term consideration (before October 2002)
LT = Long term consideration (after October 2002)
R = Recommendation

# *APPENDIX C*

# *SCHEDULE FOR CONVERSION FROM MERCURY TO SOLID TARGET*

Appendix C contains the schedule for replacement of a mercury target with a water-cooled solid target. The schedule assumes that all Title I and II design will be completed and all necessary approvals and/or permits will be obtained from state and federal regulatory agencies prior to beam shutdown. The schedule includes necessary procurement activities for materials and equipment associated with the hot cell decontamination and solid target systems. Some of these procurements are long lead-time items such as the solid target. All procurements are scheduled to commence early enough such that they do not prolong the beam downtime. A major impact to the schedule is the limited number of manipulators that can be used during the remote handled hot cell decontamination phase. To help with this problem, a second crane-mounted telemanipulator is included. In addition, to help accelerate the schedule, it is assumed that large items such as the mercury pump, tanks, shield blocks, large bore piping, etc. will be removed from the hot cell in as large of pieces as possible. They will either be reduced in size or placed directly in storage containers in a special enclosure located directly above the hot cell. Also, the schedule assumes that the mercury will be removed from the storage tank, placed in transport bottles and removed from the hot cell for amalgamation elsewhere. The primary focus of the schedule is to reduce the beam downtime to as short a period as possible by finding ways to accelerate the hot cell decontamination and solid target installation.

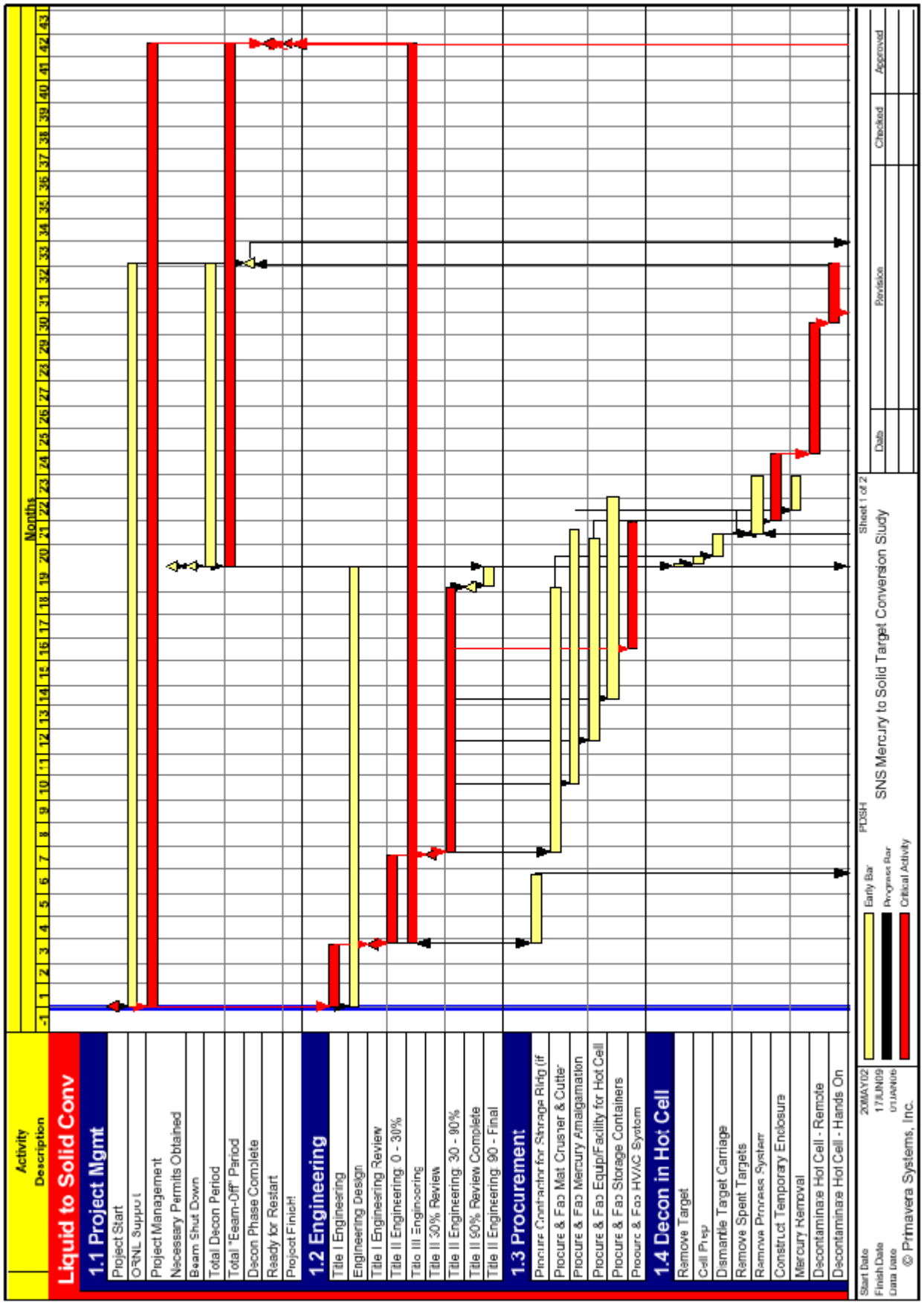
Activity Description
Months
-1 1 2 3 4 5 6 7 8 9 10 11 12 13 14 15 16 17 18 19 20 21 22 23 24 25 26 27 28 29 30 31 32 33 34 35 36 37 38 39 40 41 42 43
Liquid to Solid Conv
1.1 Project Mgmt
Project Start
ORNL Support
Project Management
Necessary Permits Obtained
Beam Shut Down
Total Decon Period
Total "Beam-Off" Period
Decon Phase Complete
Ready for Restart
Project Finish
1.2 Engineering
Title I Engineering
Engineering Design
Title I Engineering Review
Title II Engineering: 0 - 30%
Title III Engineering
Title II 30% Review
Title II Engineering: 30 - 90%
Title II 90% Review Complete
Title II Engineering: 90 - Final
1.3 Procurement
Procure Contractor for Storage Ring (if
Procure & Fab Mat Crusher & Cutter
Procure & Fab Mercury Amalgamation
Procure & Fab Equip/Facility for Hot Cell
Procure & Fab Storage Containers
Procure & Fab HVAC System
1.4 Decon in Hot Cell
Remove Target
Cell Prep
Dismantle Target Carriage
Remove Spent Targets
Remove Process System
Construct Temporary Enclosure
Mercury Removal
Decontaminate Hot Cell - Remote
Decontaminate Hot Cell - Hands On
Start Date 20MAY02
Finish Date 17JUN09
Data Date 01JAN06
© Primavera Systems, Inc.
Early Bar
Progress Bar
Critical Activity
PDSH
SNS Mercury to Solid Target Conversion Study
Sheet 1 of 2
Date
Revision
Checked
Approved

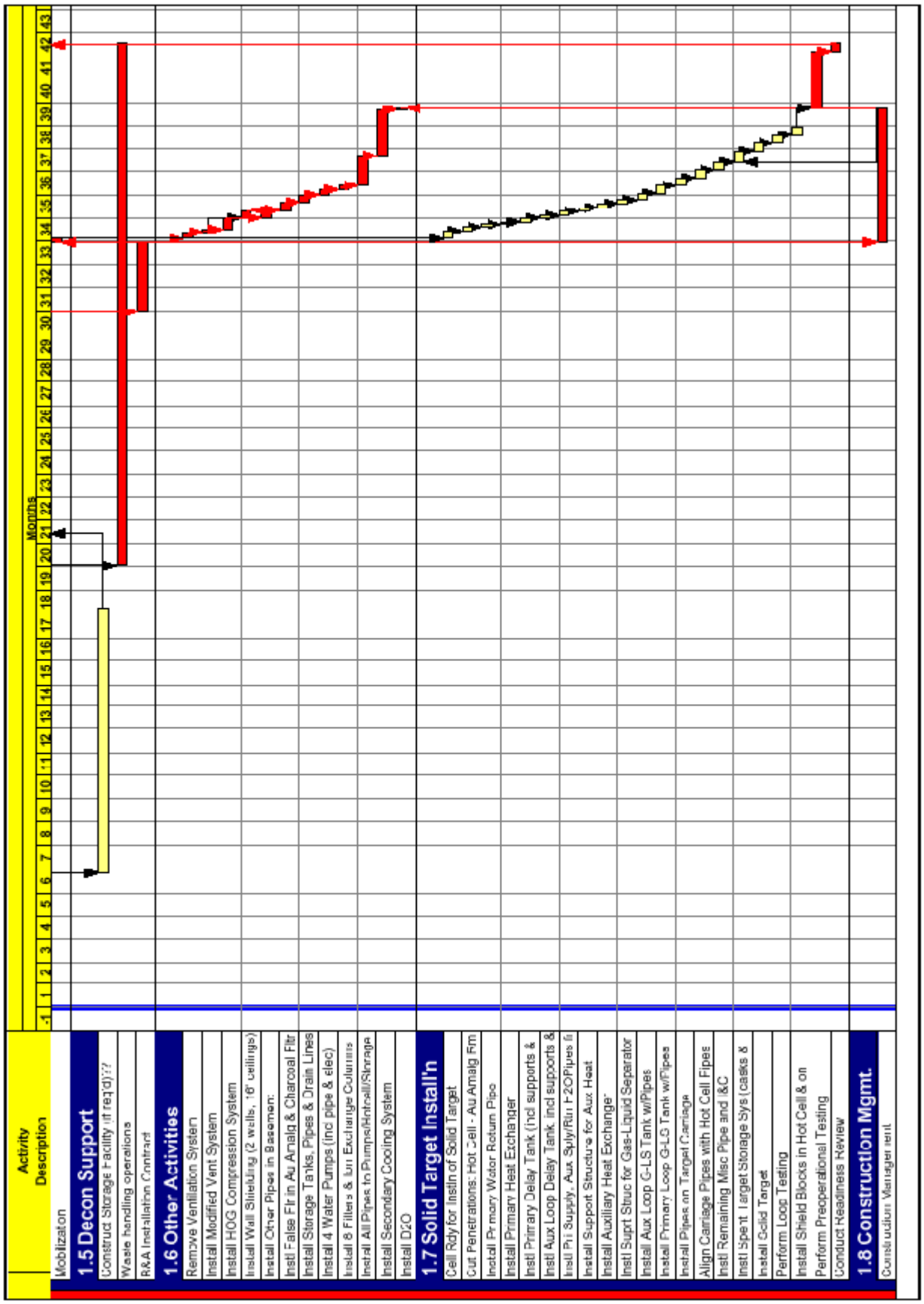
Activity Description
Months
-1 1 2 3 4 5 6 7 8 9 10 11 12 13 14 15 16 17 18 19 20 21 22 23 24 25 26 27 28 29 30 31 32 33 34 35 36 37 38 39 40 41 42 43
Mobilizaton
1.5 Decon Support
Construct Storage Facility (if reqd)???
Waste handling operations
R&A Installation Contract
1.6 Other Activities
Remove Ventilation System
Install Modified Vent System
Install HOG Compression System
Install Wall Shielding (2 walls, 16' ceilings)
Install Other Pipes in Basemen
Instl False Flr in Au Amalg & Charcoal Fltr
Install Storage Tanks, Pipes & Drain Lines
Install 4 Water Pumps (inc pipe & elec)
Install 8 Fillers & Turi Exchange Columns
Install All Pipes to Pumps/Hotcell/Storage
Install Secondary Cooling System
Install D2O
1.7 Solid Target Install'n
Cell Rdy for Instln of Solid Target
Cut Penetrations: Hot Cell - Au Amalg Rm
Install Primary Water Return Pipe
Install Primary Heat Exchanger
Instl Primary Delay Tank (incl supports &
Instl Aux Loop Delay Tank incl supports &
Inst Pri Supply, Aux Sply/Rtn P-2O Pipes fr
Install Support Structure for Aux Heat
Install Auxiliary Heat Exchange
Instl Suprt Struc for Gas-Liquid Separator
Install Aux Loop G-LS Tank w/Pipes
Install Primary Loop G-LS Tank w/Pipes
Install Pipes on Target Carriage
Align Carriage Pipes with Hot Cell Pipes
Instl Remaining Misc Pipe and I&C
Instl Spent Target Storage Sys (casks &
Install Solid Target
Perform Loop Testing
Install Shield Blocks in Hot Cell & on
Perform Preoperational Testing
Conduct Readiness Review
1.8 Construction Mgmt.
Construction Management
Sheet 2 of 2